

2001

# Characterization of sol-gel silica glass and its composites through study of physical and chemical properties of entrapped molecules

Jovica Dimitrije Badjić  
Iowa State University

Follow this and additional works at: <https://lib.dr.iastate.edu/rtd>

 Part of the [Organic Chemistry Commons](#)

## Recommended Citation

Badjić, Jovica Dimitrije, "Characterization of sol-gel silica glass and its composites through study of physical and chemical properties of entrapped molecules " (2001). *Retrospective Theses and Dissertations*. 475.  
<https://lib.dr.iastate.edu/rtd/475>

This Dissertation is brought to you for free and open access by the Iowa State University Capstones, Theses and Dissertations at Iowa State University Digital Repository. It has been accepted for inclusion in Retrospective Theses and Dissertations by an authorized administrator of Iowa State University Digital Repository. For more information, please contact [digirep@iastate.edu](mailto:digirep@iastate.edu).

## **INFORMATION TO USERS**

This manuscript has been reproduced from the microfilm master. UMI films the text directly from the original or copy submitted. Thus, some thesis and dissertation copies are in typewriter face, while others may be from any type of computer printer.

**The quality of this reproduction is dependent upon the quality of the copy submitted.** Broken or indistinct print, colored or poor quality illustrations and photographs, print bleedthrough, substandard margins, and improper alignment can adversely affect reproduction.

In the unlikely event that the author did not send UMI a complete manuscript and there are missing pages, these will be noted. Also, if unauthorized copyright material had to be removed, a note will indicate the deletion.

Oversize materials (e.g., maps, drawings, charts) are reproduced by sectioning the original, beginning at the upper left-hand corner and continuing from left to right in equal sections with small overlaps.

Photographs included in the original manuscript have been reproduced xerographically in this copy. Higher quality 6" x 9" black and white photographic prints are available for any photographs or illustrations appearing in this copy for an additional charge. Contact UMI directly to order.

ProQuest Information and Learning  
300 North Zeeb Road, Ann Arbor, MI 48106-1346 USA  
800-521-0600

**UMI<sup>®</sup>**



**Characterization of sol-gel silica glass and its composites through study of physical and  
chemical properties of entrapped molecules**

by

**Jovica Dimitrije Badjić**

**A dissertation submitted to the graduate faculty  
in partial fulfillment of the requirements for the degree of  
DOCTOR OF PHILOSOPHY**

**Major: Organic Chemistry**

**Major Professor: Nenad M. Kostić**

**Iowa State University**

**Ames, Iowa**

**2001**

**UMI Number: 3016689**

**UMI<sup>®</sup>**

---

**UMI Microform 3016689**

**Copyright 2001 by Bell & Howell Information and Learning Company.**

**All rights reserved. This microform edition is protected against  
unauthorized copying under Title 17, United States Code.**

---

**Bell & Howell Information and Learning Company**

**300 North Zeeb Road**

**P.O. Box 1346**

**Ann Arbor, MI 48106-1346**

**Graduate College  
Iowa State University**

**This is to certify that the Doctoral dissertation of  
Jovica Dimitrije Badjić  
has met the dissertation requirements of Iowa State University**

Signature was redacted for privacy.

**Major Professor**

Signature was redacted for privacy.

**For the Major Program**

Signature was redacted for privacy.

**For the Graduate College**

*To my wife Ana and to my family*

## TABLE OF CONTENTS

<b>CHAPTER 1. GENERAL INTRODUCTION</b>		1
General Overview		1
Dissertation Organization		2
<b>CHAPTER 2. EFFECTS OF ENCAPSULATION IN SOL-GEL SILICA GLASS ON ESTERASE ACTIVITY, CONFORMATIONAL STABILITY, AND UNFOLDING OF BOVINE CARBONIC ANHYDRASE II</b>		4
Abstract		5
Introduction		5
Experimental Procedures		8
Results and Discussion		16
Conclusion		25
References		26
Appendix 1		40
<b>CHAPTER 3. BEHAVIOUR OF ORGANIC COMPOUNDS CONFINED IN MONOLITHS OF SOL-GEL SILICA GLASS. EFFECTS OF GUEST-HOST HYDROGEN BONDING ON UPTAKE, RELEASE, AND ISOMERIZATION OF THE GUEST COMPOUNDS</b>		44
Abstract		44
Introduction		46
Experimental Procedures		47
Results and Discussion		57
Conclusion		68
References		69
Appendix 2		87
<b>CHAPTER 4. UNEXPECTED INTERACTIONS BETWEEN SOL-GEL SILICA GLASS AND GUEST MOLECULES. EXTRACTION OF AROMATIC HYDROCARBONS INTO POLAR SILICA FROM HYDROPHOBIC SOLVENTS</b>		98
Abstract		98
Introduction		100
Experimental Procedures		101
Results and Discussion		108
Conclusion		113
References		114



<b>CHAPTER 5. EFFECTS OF CTAB AND SDS SILICA COMPOSITE GLASS ON REACTIVITY OF DOPANT ORGANIC MOLECULES. CONTROL OF PARTITIONING OF AZO-COMPOUNDS BETWEEN MICELLE/SILICA MONOLITH AND EXTERNAL SOLUTION</b>	<b>127</b>
Abstract	127
Introduction	128
Experimental Procedures	130
Results and Discussion	135
Conclusion	143
References	143
<b>CHAPTER 6. CONCLUSIONS</b>	<b>157</b>
<b>ACKNOWLEDGMENT</b>	<b>159</b>

## CHAPTER 1. GENERAL INTRODUCTION

### *General Overview*

The sol-gel process is a chemical synthesis technique for preparation of oxide gels, glasses, and ceramics at low temperature. The approach is based on controlled hydrolysis of alkoxide precursors followed by their condensation. Chemically modified precursors, surface-active agents, and the compounds of interest may be used in the preparation to expand the range of various materials produced by this technique. As opposed to traditional methods for silicate glass preparation that involves extremely high temperatures, moderate conditions of the sol-gel method enables encapsulation of various organic, inorganic and biological molecules. The porous silica material can be fabricated as monoliths, thin films, powders, and fibers, which opens many possibilities for research and application in all branches of chemistry, catalysis, chemical technology, and engineering.

Thoughtful understanding of local environment around the dopant molecules and interactions at molecular level between dopants and silica glass matrix are essential in achieving desired properties of these materials. Recently, several methods such as solid-state NMR, IR, and Raman spectroscopy have been used in the study of doped sol-gel materials, but due to certain limitations, the details about low-concentrated dopant molecules were scarce.

In our work we take advantage of silica glass transparency as well as high sensitivity of electronic spectroscopy techniques to study physico-chemical behavior of low-

concentrated organic and biological dopant molecules under the controlled various conditions. Throughout our systematic studies of various doped and undoped sol-gel materials and composites, we chose well-characterized and defined systems in solution to examine and understand chemistry within sol-gel glasses. This dissertation represents what we have discovered about interactions, stability, and reactivity of organic and biological molecules inside these materials.

### ***Dissertation Organization***

This dissertation consists of three published papers and one that has been submitted for publication. It is generally divided into two parts: first, effects of sol-gel silica glasses on physical and chemical properties of encapsulated biomolecule bovine carbonic anhydrase (Chapter 2), and second, systematic and thorough examination and characterization of behavior of various organic molecules inside sol-gel silica and its composites (Chapter 3-5). Chapter 2 represents the first report where circular dichroism spectroscopy is used to determine conformational stability of an encapsulated biomolecule. In addition, kinetic studies of ester hydrolysis by encapsulated bovine carbonic anhydrase demonstrate some major limitations in use of sol-gel encapsulated biomolecules for preparation of biosensors and catalysts. Chapter 3 represents systematic study of hydrogen bonding interactions between sol-gel silica glasses and organic molecules diffused into these glasses. In this study we show unexpectedly large effects that hydrogen bonding between organic compounds and sol-gel silica has on equilibria and reactions involving these guest compounds. Moreover, by varying experimental conditions we are able to achieve control over these interactions. In

Chapter 4 we find that hydrophobic aromatic molecules accumulate into hydrophilic polar sol-gel silica from their solution. In systematic and thorough study of this effect, we show that excessive extraction of aromatics into porous sol-gel silica from hexane but not from solvents capable of hydrogen bonding is a general property of aromatic compounds. Our findings are consistent with hydrogen bonding between aromatic  $\pi$  system in the solutes and the hydroxyl groups on the silica surface. Chapter 5 represents study of micelle/silica composite material prepared by the sol-gel method, the interplay of silica and differently charged micelles and their joint effect on the reactivity of co-entrapped compounds. In this study we discovered that the properties of the composite material (including the dopant reactivity) can be controlled by the ionic strength of the solution in which the material is prepared or immersed. Chapter 6 provides general conclusion of studies described in previous sections.

**CHAPTER 2. EFFECTS OF ENCAPSULATION IN SOL-GEL SILICA  
GLASS ON ESTERASE ACTIVITY, CONFORMATIONAL  
STABILITY, AND UNFOLDING OF BOVINE CARBONIC  
ANHYDRASE II**

A paper published in and reprinted from  
*Chemistry of Materials* **1999**, *11*, 3671-3679  
Copyright 1999 American Chemical Society  
Jovica D. Badjić and Nenad M. Kostić

***Abstract***

Bovine carbonic anhydrase II retains its overall conformation when encapsulated in silica monoliths by the sol-gel method. Upon gradual heating the enzyme in solution precipitates at 64 °C, whereas the encapsulated enzyme does not; it unfolds, with the nominal melting temperature of  $51 \pm 3$  °C. Even at 74.0 °C, the encapsulated enzyme is only ca. 77 % unfolded, but it does not refold upon cooling. Upon treatment with guanidinium chloride, the degree of enzyme unfolding is 100 % in solution but only ca. 83 % within the silica matrix. Again, the enzyme does not refold upon removal of the denaturing agent from the glass. The glass matrix constrains the motions of the encapsulated protein molecules and prevents both their full unfolding and refolding. The former may be taken for “stabilization,” the later for

“destabilization” of the native conformation. Evidently, the effect of the glass on the encapsulated protein cannot be described in these general terms.

The encapsulated enzyme obeys the Michaelis-Menten kinetic law as it catalyzes hydrolysis of *p*-nitrophenyl acetate. The apparent Michaelis constant ( $K'_M$ ) is practically the same in the glass and in solution, but the apparent turnover number ( $k'_{cat}$ ) and specific activity for the encapsulated enzyme are only 1-2 % of these values for the enzyme in solution. Because the substrate diffuses slowly into silica pores, most of the catalysis is due to the enzyme embedded near the surfaces of the glass monolith. Effect of encapsulation on structure and activity of proteins should be studied in quantitative detail before protein-doped glasses can be used as reliable biosensors, heterogeneous catalysts, and composite biomaterials.

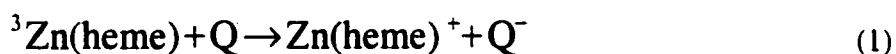
### ***Introduction***

Controlled hydrolysis of alkoxides and polymerization of the resulting oxyacids, the sol-gel method, is very useful in many branches of chemistry and materials science. This method is used for the fabrication of sensors, catalyst supports, optical elements, coatings, and special polymers.<sup>1-4</sup> Enzymes, catalytic antibodies, and other proteins may be entrapped in robust silica glasses under mild conditions and that they retain their chemical activity. Because the resulting bioceramics can be fabricated as monoliths, thin films, powders, and fibers, these recent achievements open many possibilities for research and application in bioanalytical chemistry, biocatalysis, biotechnology, and environmental technology.<sup>5-12</sup>

Hydrogels and xerogels are often referred to simply as sol-gel glasses and, colloquially, as sol-gels.

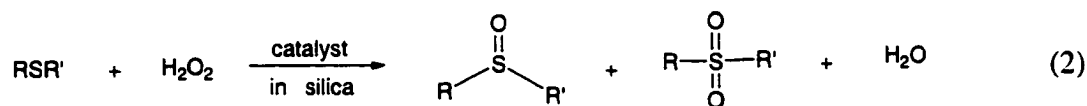
Despite widespread interest in various applications of protein-doped glasses, relatively little is known about their fundamental properties and, especially, about interactions between the protein molecules and the matrix in which they are embedded. These interactions govern the reactivity of the embedded protein, and they must be understood before useful devices can be made. Particularly important are the possible effects of encapsulation on conformation of enzymes, their interactions with substrates, and their catalytic ability.

Research in our laboratory showed that proteins and also small molecules may behave quite differently in traditional solutions and in the pores of a hydrogel.<sup>13,14</sup> We took advantage of transparency of silica monoliths to study photoinduced chemical reactions. The triplet state of zinc-substituted heme proteins cytochrome *c* and myoglobin, designated Zn(heme), is oxidatively quenched by charged metal complexes and neutral organic compounds, designated Q, as in eq 1.



Because the protein was encapsulated and the quenchers were dialyzed in, both reactants were already inside the glass. Therefore the problem of macroscopic diffusion was avoided, and precise kinetic experiments were possible. They revealed interesting electrostatic and structural properties of the glass interior, which make silica matrix quite different from pure solvent as a reaction medium. The same pair of reactants behaves differently when confined in the matrix pores and when free in solution. We also examined

the ability of peroxidases encapsulated in silica and in alkylated silica to catalyze selective oxidation of various sulfide compounds, as in eq 2.

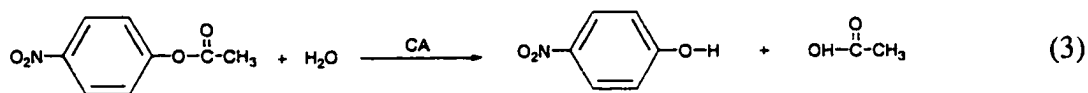


Our studies<sup>13,14</sup> of the first kind disproved the popular notion that, because the pores in silica are relatively large, small molecules diffuse freely in and out of the glass matrix. In fact, even prolonged soaking of silica monoliths in electrolyte solutions may not ensure equal partitioning of a given ion between the monolith and solution. At pH value at which the pore walls are negatively by charged, anions, such as  $[\text{Fe}(\text{CN})_6]^{3-}$ , are only partially taken up, whereas cations, such as  $[\text{Ru}(\text{NH}_3)_6]^{3+}$ , are preferentially taken up. In either case, internal and external concentrations will remain unequal after the equilibrium is reached. Since many analytes are ions, such interactions must be understood before reliable biosensors for these analytes may be designed.

Several elegant, recent studies found that proteins are stabilized by encapsulation in silica.<sup>15-17</sup> But the notion of “stability” has various meanings. We decided to examine one aspect of protein stability, namely propensity for controlled unfolding and refolding. The few kinetic studies of encapsulated enzymes to date all have been done with powdered glasses, to minimize the problem of substrate diffusion.<sup>18-21</sup> We decided to study this diffusion in glass monoliths. An advantage of monoliths over powders is transparency, which permits the use of spectrophotometry.

We chose a well-characterized enzyme, isozyme II of bovine carbonic anhydrase, and a simple reaction, hydrolysis of *p*-nitrophenyl acetate;<sup>22-25</sup> see eq 3.





By comparing the protein unfolding, behavior, and also the kinetics of the reaction in eq 3 inside the glass and in solution, one can learn about the unexpected and important differences between the glass matrix and solvent as reaction media.

### ***Experimental Procedures***

**Chemicals.** Bovine carbonic anhydrase II, ultrapure guanidinium chloride, 3-(N-morpholino)propanesulfonic acid (MOPS), and its sodium salt were obtained from Sigma Chemical Co. Tetramethylorthosilicate (also called tetramethoxysilane and designated TMOS), *p*-nitrophenyl acetate, *p*-nitroanisole, and acetonitrile were obtained from Aldrich Chemical Co. The salts  $\text{NaH}_2\text{PO}_4 \cdot \text{H}_2\text{O}$  and  $\text{Na}_2\text{HPO}_4 \cdot 7\text{H}_2\text{O}$  were obtained from Fischer Chemical Co. The salt  $[\text{Ru}(\text{NH}_3)_5\text{Cl}]\text{Cl}_2$  was obtained from Strem Chemical Co. Distilled water was demineralized to electrical resistivity greater than 17 M $\Omega$  cm. A MOPS buffer having the ionic strength 11.6 mM was prepared by dissolving 1.70 g of the acid and 0.97 g of its sodium salt in 400 mL of water and adjusting the pH to 7.00 with a 0.100 M solution of NaOH. Phosphate buffer with ionic strength of 10.0 mM was prepared by dissolving 0.050g of  $\text{NaH}_2\text{PO}_4 \cdot \text{H}_2\text{O}$  and 0.86 g of  $\text{Na}_2\text{HPO}_4 \cdot 7 \text{H}_2\text{O}$  in 1.000 L of water and adjusting the pH to 8.00 with a 0.100 M solution of NaOH. Ionic strength, not concentration, is specified in this article. The Accumet<sup>®</sup> 925 pH meter was equipped with a glass electrode. Glass monoliths (monoliths) intended for different experiments were prepared with, and finally kept in, different buffers. For monoliths intended for studies of carbonic anhydrase conformation and unfolding, 11.6 mM MOPS buffer at pH 7.00 was used; for the monoliths

intended for enzymatic catalysis and diffusion of substrate analogs, 10.0 mM phosphate buffer at pH 8.00 was used.

**The Sol-gel Process.** Silica sol was prepared by a published procedure.<sup>18</sup> A mixture of 15.25 g  $\text{Si}(\text{OCH}_3)_4$ , 3.38 g water, and 0.300 g 0.040 M HCl was ultrasonicated in an ice bath for 30 min. A 4.64-mL portion of the resulting sol was mixed with 5.64 mL of the appropriate buffer (see above) and kept in an ice bath. A stock solution of carbonic anhydrase II containing a variable amount (2.0-14 mg) of the enzyme in 3.4 mL of the appropriate buffer (see above) was added to the sol, and the clear liquid was transferred to polystyrene cuvettes sized 10 x 10 x 40 mm. The cuvettes were sealed with parafilm and kept at 4 °C. During the 14 days of aging the monoliths were washed twice a day with the same buffer with which they had been made. Then the parafilm was removed for partial drying, still at 4 °C, and in additional 14 days the monoliths shrunk to 8 x 8 x 27 mm. The final volume was ca. 50 % of that of the aged monoliths. The partially dried monoliths were stored in the same buffer with which they had been prepared, depending on the purpose.

**Determining the Enzyme Concentration.** Concentration of bovine carbonic anhydrase II in free solution and in solution confined in the pores of silica monoliths was determined on the basis of absorbance at 280 nm and the plot of that absorbance versus the enzyme concentration in a 11.6 mM MOPS buffer at pH 7.00. For accuracy, liquids were measured by weight rather than volume; because the buffer solutions were dilute, their density was taken to be unity. This approximation did not introduce a significant error in subsequent experiments. The enzyme concentration in the stock solution was 3.84 mg/mL; from it, by dilution, were made

six more solutions, and their absorbances were measured. The slope of the plot gave the conversion factor of 1.48 mL/mg. Monolith doped with the enzyme was soaked in the buffer appropriate for the subsequent experiments, as explained in the preceding subsection. Both the doped monolith (in the sample beam) and the undoped monolith of the same dimensions (in the reference beam) were held in standard cuvettes, filled with the buffer. Ultraviolet absorption spectrum was recorded, and concentration was calculated with the conversion factor, taking into account the path length of 0.80 cm. Concentration so determined always equaled that calculated from the amount of the enzyme encapsulated, considering the increase in concentration caused by shrinkage of the partially-dried monolith.

**Circular Dichroism Spectra.** These spectra were recorded with the instrument J-710 by JASCO, equipped with a peltier thermoelectric cell. When the samples were solutions, the sensor was placed inside the cuvette, and temperature was kept within  $\pm 0.05$  °C; when the samples were silica monoliths immersed in solution, the sensor had to be placed next to the cuvette, and temperature was kept within  $\pm 0.10$  °C. In experiments not concerning thermal unfolding and refolding, temperature was 20.0 °C, and monoliths were kept at it for 30 min before the measurements were started. Far-UV CD spectra, in the region 200-240 nm, were recorded in 1-mm cuvettes, with silica monoliths (1 mm thickness) and free solutions that were both 12  $\mu\text{M}$  in carbonic anhydrase. Near-UV CD spectra, in the region 240-340 nm, were recorded in 10-mm cuvettes; the enzyme concentration was 28  $\mu\text{M}$  in silica and 25  $\mu\text{M}$  in free solution. The soaking buffer was always 11.6 mM MOPS at pH 7.00. In calculation of molar residue ellipticity<sup>26</sup> the molecular mass of the enzyme was

28,900 Da; the path length was 0.80 cm in the case of doped silica monoliths (because of their shrinkage); and the enzyme concentration was determined as explained above.

**Unfolding of Carbonic Anhydrase in Free Solution.** In studies of thermal denaturation, the solution of the enzyme in 11.6 mM MOPS buffer at pH 7.00 had a concentration of 0.761 mg/mL. Ellipticity at 245 nm in a 10-mm cuvette was recorded continuously, during slow heating at the rate of 0.50 °C/min. In addition, the full CD spectrum in the range 240-340 nm was recorded at 20.0, 40.0, 55.0, and 75.0 °C. A stock solution of guanidinium chloride (GdmCl) was prepared carefully, by dissolving 15.1591 g of this denaturant in 25.0251 g of the 11.6 mM MOPS buffer at pH 7.00.<sup>26</sup> Concentration was also checked by measuring the refraction index of the solution. A stock solution of bovine carbonic anhydrase II was prepared by adding 1.0704 g of NaCl to 6.0227 g of the solution containing 3.84 mg of this enzyme per mL of 11.6 mM MOPS buffer at pH 7.00. The protein concentration was checked by measuring absorbance at 280 nm. To 0.5000 g of the stock solution of the protein (and NaCl) were added required weights of the GdmCl stock solution and of the MOPS buffer, to obtain a solution that was 0.600 M in NaCl and between 0 and 3.488 M in GdmCl. A series of these solutions differing only in the denaturant concentration was equilibrated at room temperature for 12 h before their near-UV CD spectra were recorded. The denaturation was reversed (i.e., the protein was refolded) by exhaustive dialysis with Slyde-A-Lyzer<sup>®</sup> 10K cassettes, obtained from Pierce Chemical Co. A 3.00-mL sample of the solution after the CD spectroscopic measurements was dialyzed against 400 mL of the 11.6 mM MOPS buffer at pH 7.00 that was 0.100 M in NaCl.<sup>27</sup> Then the near-UV CD spectrum was recorded again.

**Unfolding of Encapsulated Carbonic Anhydrase by Heating.** A transparent silica monolith sized 8 x 8 x 27 mm containing 28  $\mu\text{M}$  bovine carbonic anhydrase II was soaked in a 11.6 mM MOPS buffer at pH 7.00 inside a quartz cuvette sized 10 x 10 mm. The temperature of the cell holder was raised from 20.0 to 74.0  $^{\circ}\text{C}$  in 3.0-degree steps. After a 30-minute period of equilibration, the near-UV CD spectrum was recorded (for an additional 20 min). The mean residue ellipticities at 245 and 269 nm were plotted against temperature. In control experiments performance of the CD instrument was verified by recording near-UV spectra of the monolith not doped with the protein at 20.0 and 74.0  $^{\circ}\text{C}$ ; the heating was done gradually, with the doped monolith. The doped monolith was then cooled, at a rate of 3.0  $^{\circ}\text{C}/\text{h}$ , back to 20.0  $^{\circ}\text{C}$ , and the CD spectrum was recorded again. The apparent melting (denaturation) temperature of the protein,  $T_m$ , was obtained by fitting the plots at 245 and 269 nm to the simple model of direct conversion of the folded state into an unfolded state.<sup>28,29</sup>

**Unfolding of Encapsulated Carbonic Anhydrase with Guanidinium Chloride.** Because the denaturing agent in this salt is the cation, we first determined the conditions under which cations can be introduced into sol-gel silica glass. In these preliminary experiments we used the salt  $[\text{Ru}(\text{NH}_3)_5\text{Cl}]\text{Cl}_2$  because its cation is colored and because its charge is higher than that of the  $\text{Gdm}^+$  ion. A silica monolith sized 8 x 8 x 27 mm was soaked, for 24 h at 25  $^{\circ}\text{C}$ , in a  $5.2 \cdot 10^{-4}$  M solution of the complex salt in a 11.6 mM MOPS buffer at pH 7.00 that was 0.600 M in NaCl. Diffusion was assisted by gentle shaking. The UV-vis spectrum of the monolith infused with  $[\text{Ru}(\text{NH}_3)_5\text{Cl}]^{2+}$  cations was recorded against an “empty” monolith in the reference beam and compared with the spectrum of the fresh

soaking solution. Concentration of the complex cation was determined on the basis of the absorptivity  $\epsilon_{326} = 1850 \text{ M}^{-1}\text{cm}^{-1}$  and the optical path length of the monolith of 0.80 cm. Transparent silica monoliths sized 8 x 8 x 27 mm containing 28  $\mu\text{M}$  bovine carbonic anhydrase II were each soaked in 10.0 mL of 11.6 mM MOPS buffer at pH 7.00 that was 0.600 M in NaCl and between 0 and 4.35 M in GdmCl. Diffusion of the denaturant and NaCl into the doped glass was assisted by gentle shaking for 24 h at 25 °C. Circular dichroism spectra at 240-340 nm of all the monoliths were recorded, and molar residue ellipticity at 269 nm was plotted against the GdmCl concentration. The monolith containing 4.35 M GdmCl was soaked in 400 mL of the 11.6 mM MOPS buffer at pH 7.00 that was 0.600 M in NaCl, for 24 h at 4 °C. This same procedure was repeated with a fresh buffer. Near-UV CD spectra were recorded at 24 and 48 h, after each soaking.

**Degree of Unfolding of Carbonic Anhydrase.** This degree, designated  $f_u$ , varies from 0.0 to 1.0 and is proportional to the molar residue ellipticity at 269 nm. The limiting values correspond to the protein dissolved in a 11.6 mM MOPS buffer containing no GdmCl and 3.488 M GdmCl.

This denaturant completely unfolds bovine carbonic anhydrase.<sup>30</sup> The same  $f_u$  scale was used for the enzyme in free solution and encapsulated in silica.

**Diffusion of Small Molecules into Silica Glass.** The substrate for carbonic anhydrase (acting as an esterase) is *p*-nitrophenyl acetate; an unreactive analog of it is *p*-nitroanisole. The solvent was a 9 : 1 mixture by volume of a 10 mM phosphate buffer at pH 8.00 and acetonitrile. Solutions were made in volumetric flasks. Their concentrations were 1.00 mM in the substrate and 0.14 mM in its analog. Silica monolith were sized 8 x 8 x 27

mm. Three monoliths doped with 28  $\mu\text{M}$  carbonic anhydrase II were each soaked in 30.0 mL of the substrate solution. The yellow color of *p*-nitrophenoxide anion advanced into the monoliths for 10, 60, and 600 min. From each soaked monolith a 8 x 8 x 7 mm slice was obtained by cutting off 10-mm pieces from both ends, and this slice was photographed with a Canon T-60 camera equipped with a macro lens having FD of 50 mm and 1 : 3 : 5 ratio and with an extension tube having FD of 25 mm. An undoped (enzyme-free) monolith sized 8 x 8 x 27 mm was soaked first in the solvent (the aforementioned 9 : 1 mixture) and then in 20.0 mL of the *p*-nitroanisoole solution for 18 h. Occasionally the monolith was removed from the solution, and its absorbance at 316 nm was recorded against an unsoaked monolith in the reference beam. Absorbance at 316 nm was plotted versus the soaking time.

**Kinetics of Catalysis by the Encapsulated Carbonic Anhydrase.** These experiments were done with 32 very similar silica monoliths sized 8 x 8 x 27 mm, chosen from a set of 64 of monoliths prepared under identical conditions. These 32 were divided into four sets of 8; members of each set were doped with the same concentration of carbonic anhydrase II: 10, 31, 56, and 79  $\mu\text{M}$ . Each monolith was first soaked in 100 mL of a 10 mM phosphate buffer at pH 8.00 to establish the pH value of the interior. After this equilibration, each monolith was soaked in 2.0 mL of the solvent in which the hydrolysis was to be done; a 9 : 1 mixture by volume of this buffer and acetonitrile; the containers polystyrene spectrophotometric cuvettes sized 10 x 10 x 40 mm, were thermally equilibrated in a water bath at 25 °C for 15 min. The reaction was started by addition to each cuvette of a small volume of a solution of *p*-nitrophenyl acetate in the aforementioned solvent. The substrate concentrations in the reaction mixture spanned the range 1.0 to 10.0 mM. Absorbance at 400

nm of *p*-nitrophenoxide anion, a sum of contributions from the monolith and the surrounding solution, was measured over time. Absorptivity of this product,  $\epsilon_{400} = 16,840 \text{ M}^{-1}\text{cm}^{-1}$ , was determined by measuring absorbances of a series of solutions in the same solvent having concentrations in the relevant range, 1.0 to 10.0 mM. After the incubation period of 50 s, dependencies of absorbance at 400 nm (*A*) on time (*t*) were fitted to eq 4

$$A = V_0 t + c \quad (4)$$

with the linear least-squares method embodied in the program SigmaPlot 1.0. In similar experiments with undoped silica monoliths, initial rates for “background” hydrolysis at the same concentration of *p*-nitrophenyl acetate were found to be less than 10 % of the rates of hydrolysis catalyzed by the enzyme-doped monoliths. After the subtraction of the “background” rates, the initial rates (slopes  $V_0$  in eq 4) for the enzymatic hydrolysis of the substrate at concentration *S* were fitted to the Lineweaver-Burk expression (eq 5), and the following kinetic parameters were obtained: apparent Michaelis constant,  $K'_M$ ; maximum velocity,  $V_{\max}$ ; and apparent turnover number,  $k'_{\text{cat}}$ .<sup>31</sup> The primed quantities are termed apparent because the concentration of the enzyme doing catalysis is not known exactly.

$$\frac{1}{V_0} = \frac{K'_M}{V_{\max} S} + \frac{1}{V_{\max}} \quad (5)$$

Specific activity of carbonic anhydrase is  $10^{-3}$  times the number of mg of the substrate (*p*-nitrophenyl acetate) hydrolyzed by 1.0 mg of the enzyme per 1.0 min.



## ***Results and Discussion***

**Encapsulation of Carbonic Anhydrase.** The bovine isozyme II is a well-characterized protein, with the molecular mass of 28,900 Da and the isoelectric point  $pI = 5.9$ . Because none of its 259 amino-acid residues is cysteine, chemical and spectroscopic studies are not complicated by oxidation and formation of disulfide bridges.<sup>27,30,32-34</sup> Because the sol-gel method yields silica glass that is transparent at wavelengths as low as 250 nm, concentration of the encapsulated protein was accurately determined on the basis of the absorbance at 280 nm; shrinkage upon partial drying of the glass monoliths was taken into account in determining the optical path length. Concentration of the enzyme in the monolith was 0.80 mg/mL on the basis of the UV absorption spectrum and 0.79 mg/mL on the basis of the amount of the enzyme used in the encapsulation experiments. Equality of these values within the error margins, seen in Figure S1 in the Supporting Information, proves that frequent rinsings of the monoliths over two weeks during the aging of silica does not leach the trapped enzyme. Indeed, the enzyme was not detected by UV absorption in the rinsing buffer.

**Monitoring of Carbonic Anhydrase Unfolding.** Although diffusion of relatively small molecules through the porous sol-gel silica glass has been studied before,<sup>35,36</sup> subtler kinds of motions, such as conformational changes of encapsulated molecules, have only begun to be investigated.<sup>37</sup> These investigations are needed, because conformational states of proteins determine their biological activity and chemical reactivity. Carbonic anhydrase is well suited for these studies in the glass because its unfolding in solution has been examined. Because gradual heating causes irreversible precipitation at 64 °C and higher temperatures,

this denaturation could not be monitored by spectroscopic methods; a more involved method had to be used.<sup>38</sup> Denaturation by guanidinium chloride (GdmCl) in solution, however, is a well-characterized, reversible process, conveniently followed by circular dichroism (CD) spectroscopy.<sup>30</sup>

The CD bands of bovine carbonic anhydrase II in the far-UV region are relatively weak, because  $\alpha$ -helical content is low. A minimum in ellipticity at 217 nm is diagnostic of the high content of antiparallel  $\beta$ -sheet. In the near-UV region, 240-320 nm, the spectrum is complex, with multiple Cotton effects. There are major bands at 245 and 270 nm and two minor ones above 280 nm. Because isozymes II of human and bovine carbonic anhydrases have very similar near-UV CD spectra, the same chain length, the same tryptophan residues (nos. 5 and 16 in one of the two clusters of aromatic residues, and nos. 97, 123, 192, 209, and 245 in the central  $\beta$ -sheet region), and many other similarities, reported properties of the mutants of the human enzyme are relevant to the bovine enzyme that we used.<sup>39</sup> All the tryptophan residues make positive contribution to the CD in the region 230-250 nm, but tyrosine residues make a minor negative contribution. Tryptophan residues nos. 5, 123, 209, and 245 contribute mainly to the band at 269 nm. Because the relatively many aromatic residues are distributed in various regions of the carbonic anhydrase molecule, its CD spectrum reflects the conformation of the whole protein, not only a part of it. (This advantage is absent in studies that use only one chromophore or fluorophore for monitoring of conformational changes). Our CD spectra of the enzyme in solution agree with those reported earlier.<sup>27</sup> As Figure 1 shows, encapsulation in silica causes only small changes in band intensities and shapes. Similar small changes were found upon encapsulation of

bacteriorhodopsin and zinc cytochrome *c* in silica glasses.<sup>14,40</sup> Studies of these two proteins showed that they are not significantly perturbed in the glass, and we conclude that neither is carbonic anhydrase. Both the backbone (far-UV) and the relevant side chains (near-UV) seem to retain upon encapsulation the general structure that they had in solution.

We monitored unfolding by measuring molar residue ellipticity,  $\theta$ , at 245 and 269 nm, wavelengths at which the spectral changes were largest. The corresponding plots obtained at these two wavelengths were always very similar because each reflected the changes in the tertiary structure of the whole enzyme molecule.

**Electrostatic Effect of the Silica Glass on Uptake of Ionic Species.** When a monolith of sol-gel silica is immersed in a solution, the solute will diffuse into the monolith. Even though the solute molecules may be much smaller than the pores in the glass, when an equilibrium is reached after long soaking concentrations of the solute inside the glass and in the surrounding solution may not be equal. This inequality will persist if the solute is an ionic species and the surface of the glass pores are charged. Since the isoelectric point of silica is 2.1, the pores of sol-gel glass are negatively charged at pH values 7.00 and 8.00, used in our experiments.<sup>41</sup> Research in this laboratory showed partial uptake of the solute when the charges of the solute and the glass are like and excessive uptake when the charges are opposite. These electrostatic effects can be abolished by raising ionic strength of the solution. In the presence of 0.600 M NaCl, at pH 7.00, concentrations of  $[\text{Fe}(\text{CN})_6]^{3-}$  ion and other ionic solutes “inside” the monolith and in the solution “outside” do become equal after sufficient time. We confirmed this result in experiments with  $[\text{Ru}(\text{NH}_3)_5\text{Cl}]\text{Cl}_2$ , a salt containing a colored complex cation. As Figure S2 in Supporting Information shows,

concentration of this doubly-charged cation inside and outside the silica monolith became equal in the buffer at pH 7.00 that was also 0.600 M in NaCl.

In studies of unfolding of encapsulated carbonic anhydrase with guanidinium chloride, concentration of the colorless  $\text{Gdm}^+$  cation in the glass could be known only if it were kept equal to that in the external solution. The 0.600 M NaCl, which proved sufficient even for the multiply-charged ions, was kept in all solutions. To permit correct comparisons of the unfolding process in the glass and in solution, 0.600 M NaCl was always used, although this salt was not necessary for precisely knowing the concentration of GdmCl in free solution.

**Unfolding of Carbonic Anhydrase in Solution.** A previous study<sup>38</sup> found that heating of the enzyme solution to 64 °C and higher temperatures causes precipitation that cannot be reversed by cooling. Denaturation had to be followed by monitoring of pH as a function of temperature.<sup>38</sup> The enzyme unfolds in the interval 55.0-70.0 °C; precipitation begins at 55.0 °C, and the precipitate remains up to 95.0 °C. The melting temperature  $T_m = 64.3$  °C.<sup>38</sup> As Figure S3 in the Supporting Information shows, our experiments confirm that onset of precipitation at 64 °C is accompanied by a large change of ellipticity and an increase in the spectral noise.

Unfolding by guanidinium chloride at room temperature proceeds via two intermediates. At the denaturant concentration of 3.83 M, bovine carbonic anhydrase II is completely unfolded.<sup>30</sup> Our results, shown in Figure 2A, confirm these results. We repeated the experiments with the enzyme in solution to allow comparisons with our original experiments with the enzyme in glass, to be described next.

**Unfolding of Carbonic Anhydrase in Silica Glass by Heating.** To determine the  $T_m$  value, CD measurements in Figure 3 were fitted to an approximate model containing two limiting states, folded and unfolded.<sup>42</sup> The result is independent of the wavelength, as it should be:  $54 \pm 3$  °C at 245 nm and  $49 \pm 3$  °C at 269 nm are practically the same temperature. We take an average value,  $T_m = 51 \pm 3$  °C. On a generally accepted assumption that the random-coil conformations obtained by chemical denaturation (Figure 2A) and by heating (Figure 3B) are indistinguishable, it turns out that the encapsulated enzyme becomes only 77 % unfolded. That the plot in Figure 3B levels off at  $f_u = 0.77$  is an indication that the encapsulated enzyme unfolds incompletely. Thermal unfolding of the enzyme causes precipitation in solution, as discussed above, but not in the silica glass. Both incomplete unfolding and lack of precipitation can be attributed to the influence of the silica matrix. The enzyme molecules are relatively constrained by this matrix, which restricts the mobility of the protein molecules that is required for complete unfolding. Because the enzyme molecules are isolated in separate “cages” in porous silica, they cannot aggregate together and precipitate. The relatively small slope (i.e., broad melting range) of the plots in Figure 3 may be an indication that the protein molecules exist in different microenvironments and have somewhat different stabilities toward unfolding.

As Figure 4 shows, the encapsulated enzyme at 74.0 °C shows an essentially featureless CD spectrum. Upon gradual cooling to 20.0 °C, the spectrum remains almost the same, except for the nonspecific change in the region 240-250 nm. Clearly, the unfolded protein does not refold upon cooling. This finding, again, indicates that the protein molecules are constricted by the surrounding silica matrix, which precludes the mobility required for

refolding. Previous studies of alkaline phosphatase, acid phosphatase, and flavoprotein oxidases showed these enzymes to be thermally more stable in silica glass than in solution. Although the  $T_m$  values for carbonic anhydrase in solution (64.3 °C) and in silica glass (51 ± 3 °C) were obtained by different methods, their comparison may be instructive. *This enzyme, unlike the aforementioned ones, seems to be somewhat destabilized toward unfolding by its encapsulation in silica.* Evidently, encapsulation in sol-gel glasses may differently affect stability of different proteins. More research is needed before generalizations can be made.

#### **Unfolding of Carbonic Anhydrase in Silica Glass by Guanidinium Chloride.**

Figure 2B shows, again, that the encapsulated enzyme is incompletely unfolded ( $f_u = 0.83$ ) at the denaturant concentrations higher than 3.71 M, at which the enzyme in solution was completely unfolded ( $f_u = 1.00$  in Figure 2A). We refrained from fitting the results in Figure 2B to some model because any fitting would require assumptions about the mechanism of unfolding. As Figure 5 shows, the CD spectrum retains some features even at the 3.71 M concentration of the denaturant. Although the spectral bands are very weak, their number and general shape clearly resemble those in Figure 1. Even in the presence of 4.35 M guanidinium chloride, the ellipticity does not reach the value characteristic of the unfolded conformation. The enzyme seems to retain some conformational features in the presence of the denaturant.

Thorough dialysis of the enzyme-doped monolith against buffer that was 0.600 M in NaCl removed the denaturant, but the near-UV CD spectrum of the encapsulated enzyme did not change, did not “recover” its intensity and features. Evidently, the enzyme cannot refold

inside the glass matrix. It remains almost completely unfolded in the absence of the denaturant.

#### **Effect of Encapsulation on Conformational Stability of Carbonic Anhydrase.**

Upon partial drying of the aged silica glass, the pores partially collapse, and the monolith shrinks. This collapse may affect the conformational stability, but we did not investigate this process. Very recent studies<sup>15,16</sup> showed that encapsulation in silica prolongs the lifetime of enzymes at higher temperatures. This important finding can be attributed to the enhanced thermodynamic stability of the enzymes, and our study may help explain this enhancement. Constrained in the silica matrix, protein molecules lack the mobility required for complete unfolding. Separated by this matrix, the molecules cannot aggregate and precipitate. Both of these effects may be considered stabilization with respect to the state of these proteins in solution. We note, however, that a simple property such as the melting point ( $T_m$ ) may not be a correct criterion of the protein “stability” because the concept of stability has multiple meanings, especially when applied to enzymes.

So far we discussed conformational stability, i.e., resistance of the protein to its unfolding by heating and by guanidinium ions. Next, we will discuss the enzymatic activity of carbonic anhydrase encapsulated in silica.

**Diffusion of Organic Compounds through Silica Glass.** Retardation by the glass matrix of movement of small molecules (such as acetone, acetonitrile, and chloroform) has been quantified by the so-called hindrance factors.<sup>35</sup> Because *p*-nitrophenyl acetate, the substrate for carbonic anhydrase (eq 3), is a larger molecule, it is expected to diffuse relatively slowly through silica. Partial hydrolysis of this ester would occur in this time and

complicate the study of its diffusion. Therefore we used *p*-nitroanisole,  $p\text{-CH}_3\text{O-C}_6\text{H}_4\text{-NO}_2$ , which resembles *p*-nitrophenyl acetate in size, composition, and shape but does not hydrolyze under the conditions of the diffusion experiments. Figure 6 shows that ca. 10 h are required for full penetration of this guest compound in the monolith, that is, for equalization of the guest concentrations inside the glass and in the external solution. The negative charge of the sol-gel glass at pH 8.00 does not affect the extent of uptake of this electroneutral guest molecule.

#### **Hydrolysis of *p*-Nitrophenyl Acetate by Encapsulated Carbonic Anhydrase.**

Biological function of carbonic anhydrase is to catalyze interconversion of  $\text{CO}_2$  and  $\text{HCO}_3^-$ , but this enzyme can also catalyze hydrolysis of esters.<sup>24,33</sup> The reaction in eq 3 in transparent monoliths of silica doped with the enzyme produced the yellow *p*-nitrophenoxide anion, and we followed its growing absorbance. Figure 7 shows that this yellow product of hydrolysis appears in minutes along the faces of the monolith and only after hours in its core. Evidently, the substrate is hydrolyzed as it diffuses into the monolith and first encounters the enzyme in the surface layers of silica. Agreement between the results in Figures 6 and 7 confirms that *p*-nitroanisole is a good mimic of *p*-nitrophenyl acetate so far as the diffusion rate is concerned.

**Michaelis-Menten Kinetics and Effect of Encapsulation on Activity of Carbonic Anhydrase.** Although our results do not show whether mass transfer of substrate and product of enzymatic catalysis determines the observed reaction rate, we assume that the latter is the case. Linearity of the plots in Figures 8 and 9 is evidence that the encapsulated enzyme obeys the Michaelis-Menten law of enzyme kinetics. Table 1 and Figure 10 show that specific



activity of the encapsulated enzyme is lowered to ca. 1 % of that of the dissolved enzyme and that it depends little on the extent of doping of silica by the enzyme. The small decrease in specific activity as the enzyme concentration in the monolith increases cannot be caused by partial loading, aggregation, or denaturation of the enzyme in glass. Evidence earlier in this article refutes all these three possibilities. If the decrease in activity is significant, it may be a consequence of a small decrease in accessibility of the enzyme to the substrate as the enzyme concentration increases. Similar, although somewhat larger, dependence of activity on concentration has been reported for encapsulated trypsin.<sup>17</sup> More such studies are needed, but these early results are promising. For use of sol-gel glasses in catalysts or biosensors, it is encouraging that activity seems to be only little affected by the extent of doping these glasses with enzymes.

Table 1 allows comparisons of encapsulated and dissolved carbonic anhydrase as a catalyst for the reaction in eq 3. The apparent Michaelis constant for the four different concentrations of the encapsulated enzyme  $K'_M = 16 \pm 8$  mM, is identical to the value  $K'_M = 14 \pm 3$  mM for the dissolved enzyme. Evidently, the affinity of the active site for the substrate is unaffected by encapsulation in silica. Indeed, CD spectra in Figure 1 show that the overall enzyme conformation is preserved in the silica matrix. This finding about  $K'_M$  value is interesting and possibly important, but its generality should be tested in studies of other enzymes.

The apparent turnover number,  $k'_{cat}$ , is diminished upon encapsulation. The average value for the four different concentrations of the encapsulated enzyme is  $4 \text{ min}^{-1}$ . Since the substrate does not penetrate the inner core of the monolith in the 10-min period over which

we studied the kinetics, the question arises as to what fraction of the encapsulated enzyme is responsible for catalysis. Unable to answer it accurately, we estimate on the basis of Figure 7 that only one-half of the total encapsulated enzyme actually catalyzes the observed reaction. Therefore a better estimate may be  $k'_{\text{cat}} = 8 \text{ min}^{-1}$ , although this very approximate value is ca. 2 % of the corresponding value for the dissolved enzyme, it is sufficiently high to justify further studies of enzyme activity in sol-gel glass.

### ***Conclusion***

There is keen interest in encapsulation of enzymes in glasses by the sol-gel method and in use of these doped glasses as catalysts, sensors, and composite biomaterials. For these applications to succeed, however, much has to be learned about the effects of the encapsulation on structure and activity of enzymes. We showed that some properties of the enzyme (overall conformation and  $K'_M$  value) are preserved, while others (propensity for unfolding and  $k'_{\text{cat}}$  value) are changed upon encapsulation. Slow diffusion of potential substrates and their interactions with the glass matrix, if not corrected by rising ionic strength, would limit application of doped monoliths. Spatial and steric constraints of the protein molecules by the glass matrix have important and unexpected consequences - the protein does not precipitate upon denaturation and cannot be either fully unfolded or refolded after it had been unfolded. These constraints should be understood in order to control protein-matrix interactions in ways that may allow selective adsorption, chemical sensing, and shape-selective catalysis.

**References**

- 1) Avnir, D.; Braun, S.; Lev, O.; Ottolenghi, M. *Chem. Mater.* **1994**, *6*, 1605-14.
- 2) Avnir, D. *Acc. Chem. Res.* **1995**, *28*, 328-34.
- 3) Rosenfeld, A.; Blum, J.; Avnir, D. *J. Catal.* **1996**, *164*, 363-368.
- 4) Wojcik, A. B.; Klein, L. C. *Appl. Organomet. Chem.* **1997**, *11*, 129-135.
- 5) Livage, J. *C. R. Acad. Sci., Ser. II: Mec., Phys., Chim., Astron.* **1996**, *322*, 417-27.
- 6) Dunn, B.; Zink, J. I. *Chem. Mater.* **1997**, *9*, 2280-2291.
- 7) Braun, S.; Rappoport, S.; Shtelzer, S.; Zusman, R.; Druckmann, S.; Avnir, D.; Ottolenghi, M. *Design and properties of enzymes immobilized in sol-gel glass matrices*; Kamely, D. C., Ananda M, Ed.; Kluwer, Boston, Mass, 1991, pp 205-18.
- 8) Reisfeld, R.; Joergensen, C. K. *Struct. Bonding (Berlin)* **1992**, *77*, 207-56.
- 9) Braun, S.; Shtelzer, S.; Rappoport, S.; Avnir, D.; Ottolenghi, M. *J. Non-Cryst. Solids* **1992**, *147-148*, 739-43.
- 10) Miller, J. M.; Dunn, B.; Valentine, J. S.; Zink, J. I. *J. Non-Cryst. Solids* **1996**, *202*, 279-289.
- 11) Zheng, L.; Reid, W. R.; Brennan, J. D. *Anal. Chem.* **1997**, *69*, 3940-3949.
- 12) Lan, E. H.; Dunn, B.; Valentine, J. S. V.; Zink, J. I. *J. Sol-Gel Sci. Technol.* **1996**, *7*, 109
- 13) Shen, C.; Kostić, N. M. *J. Electroanal. Chem.* **1997**, *438*, 61-65.
- 14) Shen, C.; Kostić, N. M. *J. Am. Chem. Soc.* **1997**, *119*, 1304-1312.
- 15) Chen, Q.; Kenausis, G. L.; Heller, A. *J. Am. Chem. Soc.* **1998**, *120*, 4582-4585.
- 16) Heller, J.; Heller, A. *J. Am. Chem. Soc.* **1998**, *120*, 4586-4590.

- 17) Shtelzer, S.; Rappoport, S.; Avnir, D.; Ottolenghi, M.; Braun, S. *Biotechnol. Appl. Biochem.* **1992**, *15*, 227-35.
- 18) Yamanaka, S. A.; Nishida, F.; Ellerby, L. M.; Nishida, C. R.; Dunn, B.; Valentine, J. S.; Zink, J. I. *Chem. Mater.* **1992**, *4*, 495-7.
- 19) Yamanaka, S. A.; Dunn, B.; Valentine, J. S.; Zink, J. I. *J. Am. Chem. Soc.* **1995**, *117*, 9095-6.
- 20) Braun, S.; Rappoport, S.; Zusman, R.; Avnir, D.; Ottolenghi, M. *Mater. Lett.* **1990**, *10*, 1-5.
- 21) Dosoretz, C.; Armon, R.; Starosvetzky, J.; Rothschild, N. *J. Sol-Gel Sci. Technol.* **1996**, *7*, 7-11.
- 22) Pocker, Y.; Meany, J. E. *Biochemistry* **1967**, *6*, 239-46.
- 23) Pocker, Y.; Storm, D. R. *Biochemistry* **1968**, *7*, 1202-14.
- 24) Anderson, J.; Byrne, T.; Woelfel, K. J.; Meany, J. E.; Spyridis, G. T.; Pocker, Y. *J. Chem. Educ.* **1994**, *71*, 715-18.
- 25) Thorslund, A.; Lindskog, S. *Eur. J. Biochem.* **1967**, *3*, 117-23.
- 26) Giletto, A.; Pace, C. N. *Protein stability*; Price, N. C., Ed.; Academic, San Diego, Calif, 1996, pp 233-239.
- 27) Wong, K.-P.; Tanford, C. *J. Biol. Chem.* **1973**, *248*, 8518-23.
- 28) Biltonen, R. L.; Lumry, R. *J. Amer. Chem. Soc.* **1969**, *91*, 4256-64.
- 29) Lee, J. C.; Timasheff, S. N. *J. Biol. Chem.* **1981**, *256*, 7193-201.
- 30) Uversky, V. N.; Ptitsyn, O. B. *J. Mol. Biol.* **1996**, *255*, 215-28.

- 31) Segel, I. H. *Enzyme Kinetics: Behavior and Analysis of Rapid Equilibrium and Steady-State Enzyme Systems*; Wiley-Interscience, New York, N. Y., 1975.
- 32) Wong, K.-P.; Hamlin, L. M. *Biochemistry* **1974**, *13*, 2678-83.
- 33) Christianson, D. W.; Fierke, C. A. *Acc. Chem. Res.* **1996**, *29*, 331-339.
- 34) Silverman, D. N.; Lindskog, S. *Acc. Chem. Res.* **1988**, *21*, 30-6.
- 35) Koone, N.; Shao, Y.; Zerda, T. W. *J. Phys. Chem.* **1995**, *99*, 16976-81.
- 36) Sieminska, L.; Zerda, T. W. *J. Phys. Chem.* **1996**, *100*, 4591-7.
- 37) Edmiston, P. L.; Wambolt, C. L.; Smith, M. K.; Saavedra, S. S. *J. Colloid Interface Sci.* **1994**, *163*, 395-406.
- 38) McCoy, L. F., Jr.; Wong, K.-P. *Biochemistry* **1981**, *20*, 3062-7.
- 39) Freskgaard, P.-O.; Maartensson, L.-G.; Jonasson, P.; Jonsson, B.-H.; Carlsson, U. *Biochemistry* **1994**, *33*, 14281-8.
- 40) Wu, S.; Ellerby, L. M.; Cohan, J. S.; Dunn, B.; El-Sayed, M. A.; Valentine, J. S.; Zink, J. I. *Chem. Mater.* **1993**, *5*, 115-20.
- 41) Yamanaka, S. A.; Nguyen, N. P.; Dunn, B.; Valentine, J. S.; Zink, J. I. *J. Sol-Gel Sci. Technol.* **1996**, *7*, 117-121.
- 42) Pace, C. N. *Methods Enzymol.* **1986**, *131*, 266-80.

**Table 1.** Michaelis-Menten parameters for hydrolysis of *p*-nitrophenyl acetate (eq 3) catalyzed by bovine carbonic anhydrase II in solution (the first row) and encapsulated in silica glass at four different concentrations (the next four rows). In all cases the solvent was a phosphate buffer at ionic strength of 10 mM and pH 8.00.

Enzyme conc. ( $\mu\text{M}$ )	$K'_M$ (mM)	$k'_{\text{cat}}$ ( $\text{min}^{-1}$ )	$k'_{\text{cat}} / K'_M$ ( $\text{M}^{-1} \text{min}^{-1}$ )	Spec. activity ( $\text{mg min}^{-1}$ $\text{mg enzyme}^{-1}$ )
3.3	$14 \pm 3$	388	27000	304
10	$22 \pm 15$	9	409	4.45
31	$10 \pm 3$	2	200	1.95
56	$9 \pm 4$	1	111	1.52
79	$22 \pm 14$	2	91	1.27

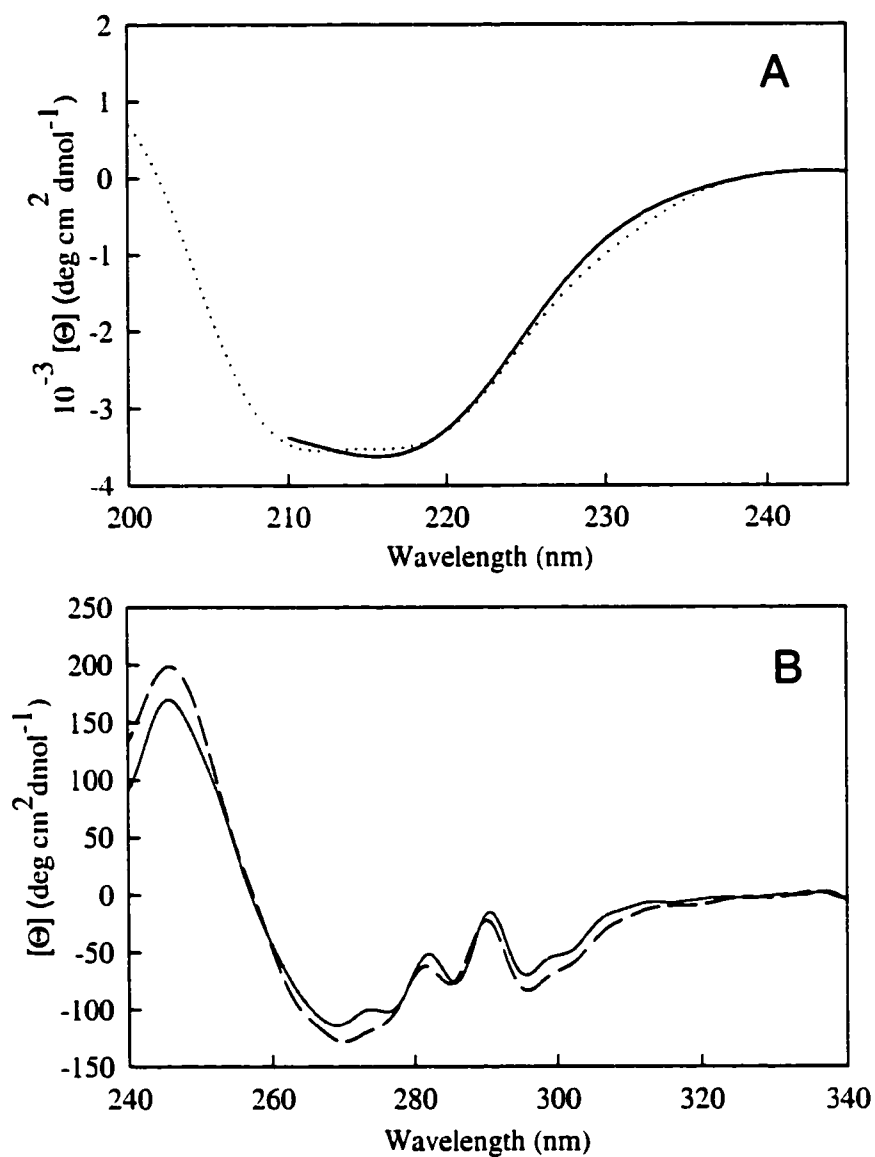


**Figure 1.** Far (A) and near-UV (B) CD spectra of bovine carbonic anhydrase II dissolved in a MOPS buffer having ionic strength 11.6 mM and pH 7.00 (dashed or dotted line) and encapsulated in silica glass (solid line). The protein concentrations and path length were 5  $\mu$ M and 1.0 mm (A) or 28  $\mu$ M and 8.00 mm (B). Molar ellipticity is normalized to the mean residue value.

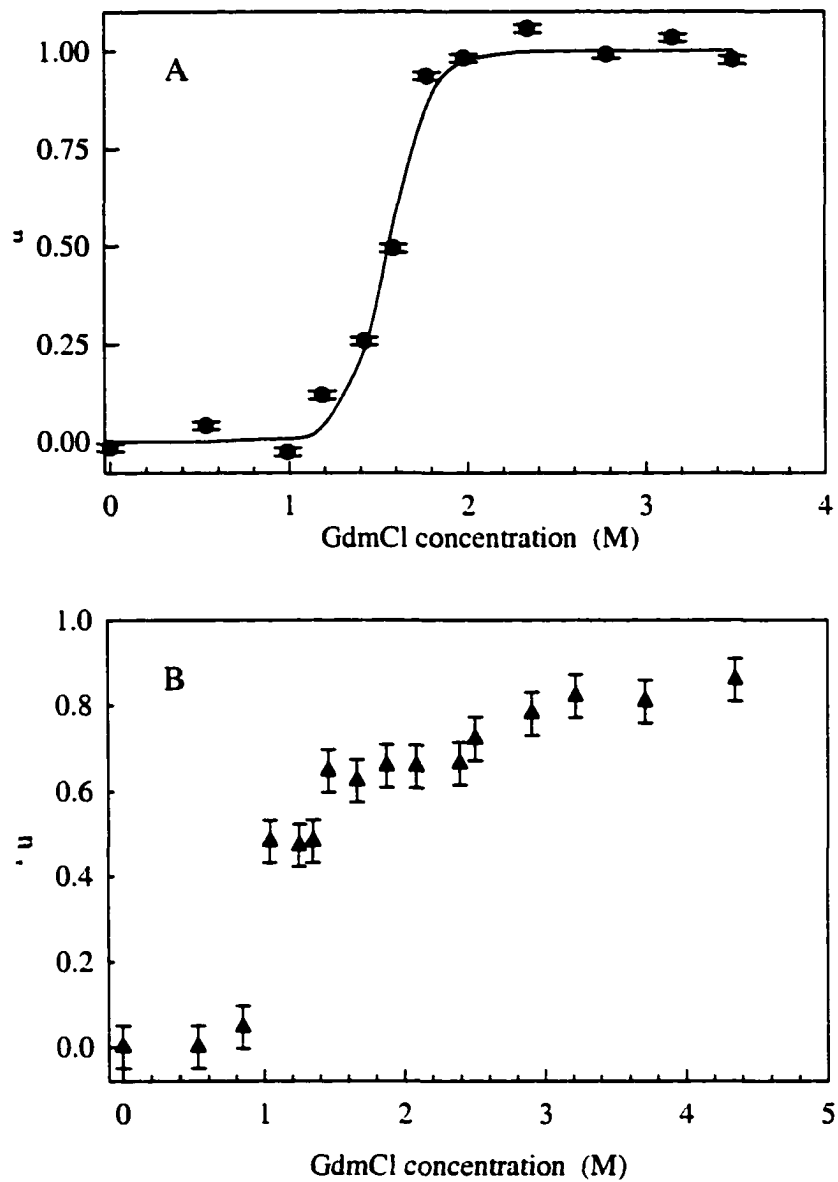


**Figure 2.** Unfolding by guanidinium chloride of bovine carbonic anhydrase II dissolved in a MOPS buffer having ionic strength 11.6 mM and pH 7.00 that was also 0.600 M in NaCl (A) and encapsulated in silica glass (B). The degree of unfolding,  $f_u$ , was calculated from the ellipticity at 269 nm. Each point was obtained with a different sample., but all the samples were prepared under the same conditions.



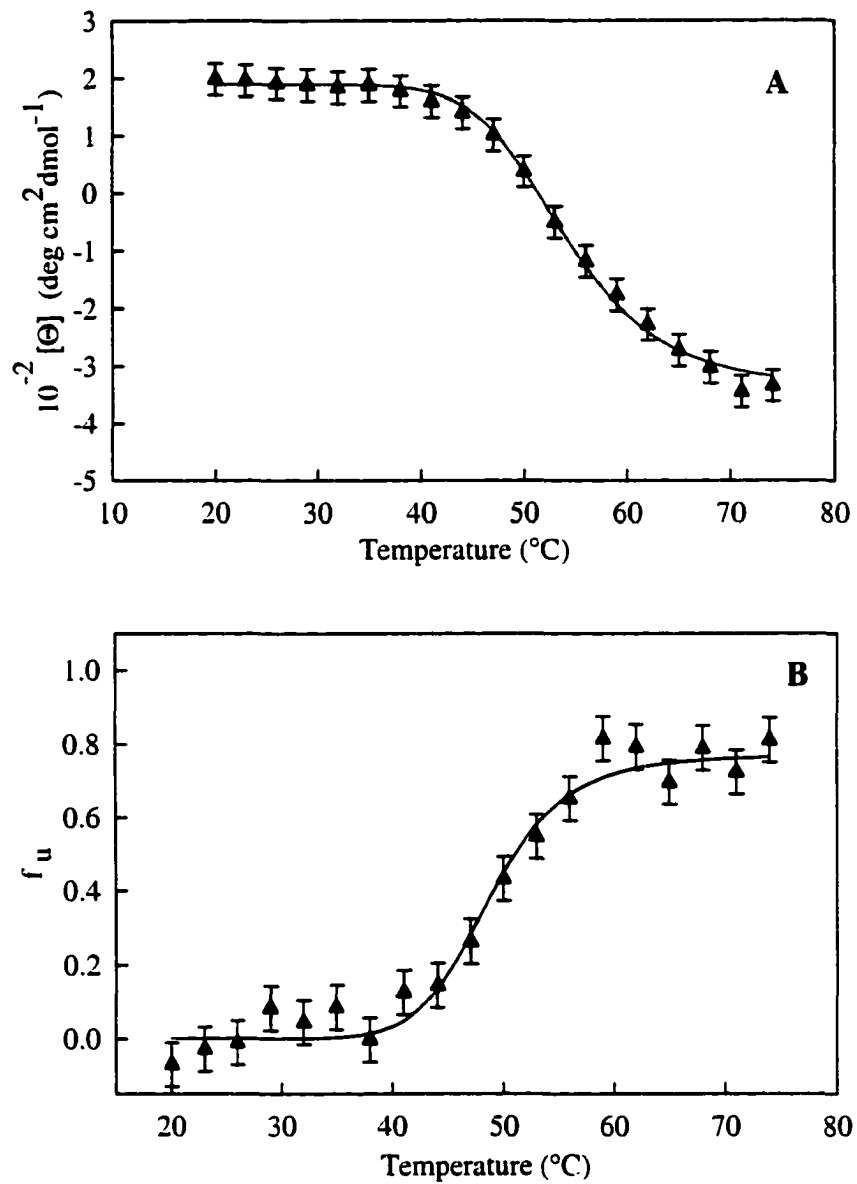


**Figure 3.** Unfolding by heating of bovine carbonic anhydrase II encapsulated in silica glass at the concentration of 28 mM, monitored at 245 nm (A), and 269 nm (B). Molar ellipticity was normalized to the mean residue value. The degree of unfolding,  $f_u$ , was calculated from the ellipticity at 269 nm.

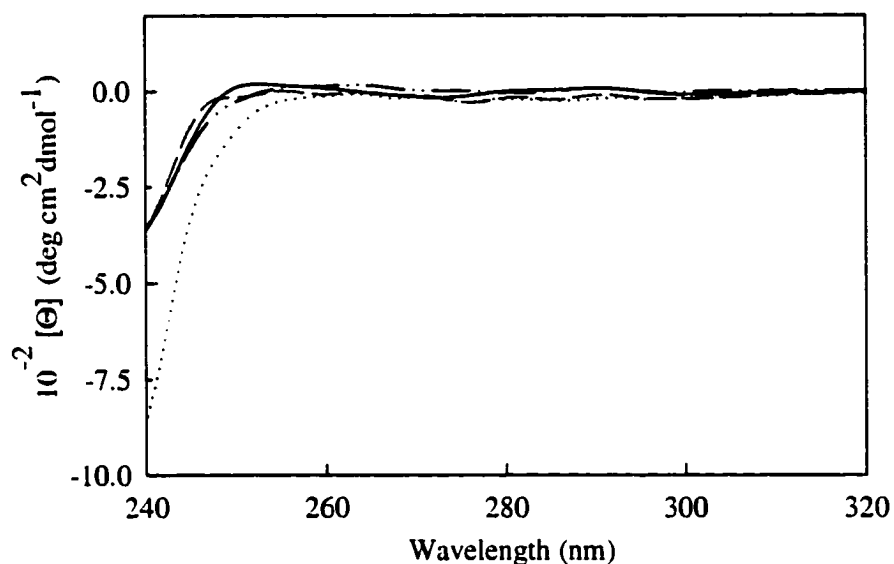


**Figure 4.** Near-UV CD spectra of BCA II encapsulated in silica glass at the concentration of 28  $\mu\text{M}$ . One sample, immersed in a MOPS buffer having ionic strength 11.6 mM and pH 7.0, was heated at the rate of 3.0  $^{\circ}\text{C}/\text{h}$  to 74.0  $^{\circ}\text{C}$  (dotted line) and then cooled at the same rate to 20  $^{\circ}\text{C}$  (dashed line). Another sample was infused with the MOPS buffer that was also 0.600 M in NaCl and 4.35 M in guanidinium chloride (solid line), and then guanidinium chloride was removed by dialysis against the aforementioned buffered NaCl solution (chain line), all at 20.0  $^{\circ}\text{C}$ .

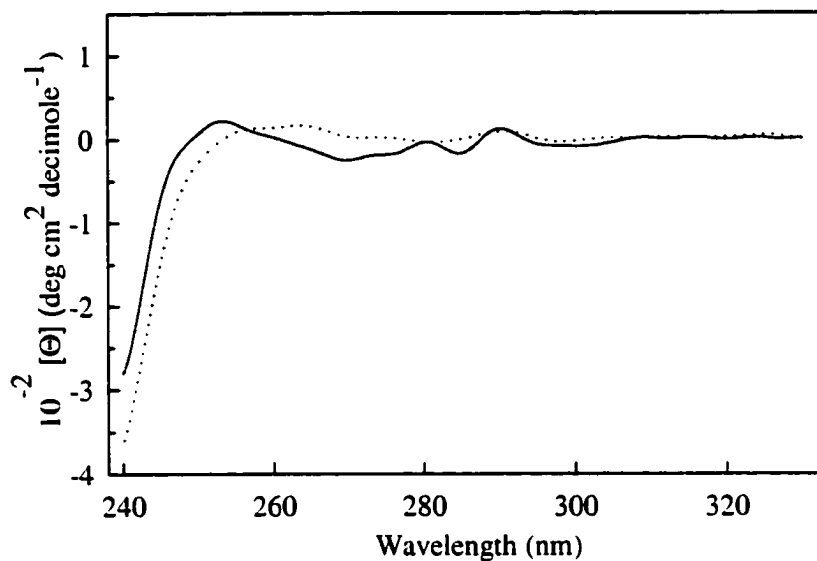


**Figure 5.** Near-UV circular dichroism spectra of bovine carbonic anhydrase II encapsulated in silica glass at the concentration 28  $\mu\text{M}$  (solid line) and dissolved at the concentration 26  $\mu\text{M}$  (dotted line) The glass monolith was immersed, and the enzyme was dissolved, in a MOPS buffer having ionic strength 11.6 mM and pH 7.00 that was 0.600 M in NaCl and that also contained guanidinium chloride, 3,710 M in the case of the encapsulated and 3.488 M in the case of the dissolved enzyme.

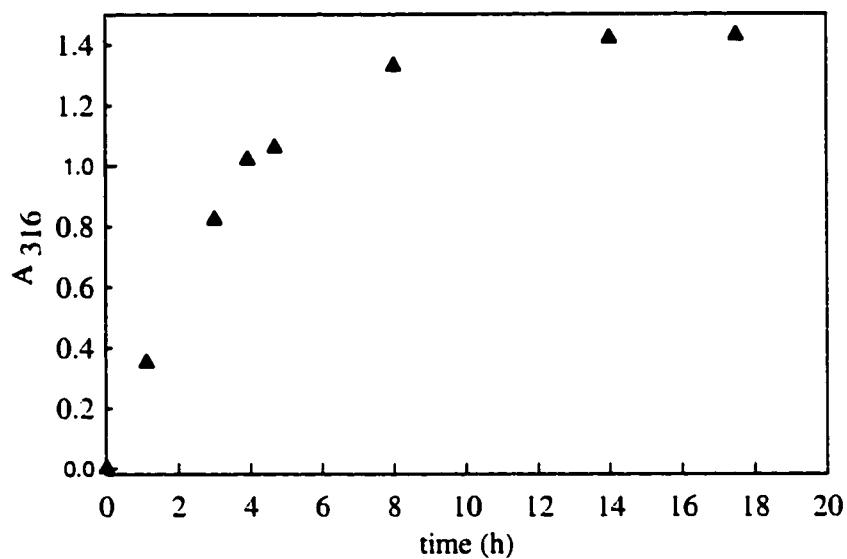


**Figure 6.** Absorbance at 316 nm of a silica monolith sized 8 x 8 x 27 mm immersed for various times in a 0.14 mM solution of p-nitroanisole in a 9:1 mixture by volume of a phosphate buffer having ionic strength 10 mM pH 8.00 and acetonitrile. As the guest enters the glass, absorbance of the glass increases.

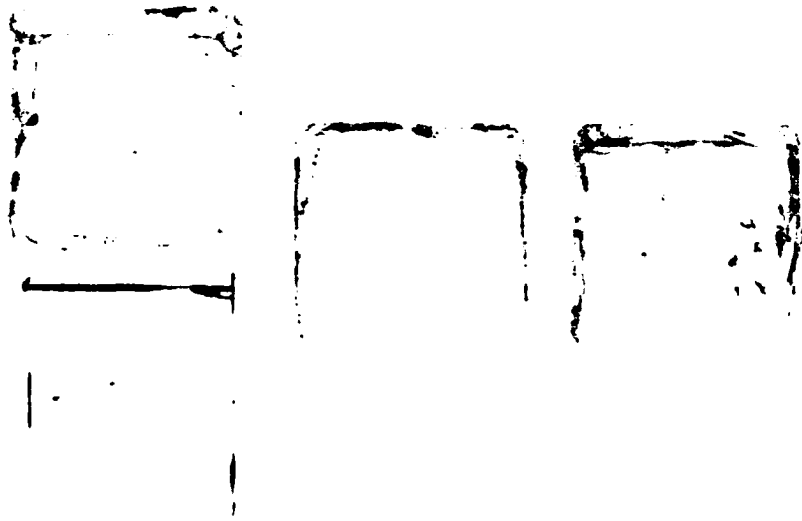


**Figure 7.** Cross sections of a silica monolith sized 8 x 8 x 27 mm that was doped with 28 mM bovine carbonic anhydrase II and immersed in 30 mL of a 1.00 mM solution of p-nitrophenyl acetate in a 9:1 mixture by volume of a phosphate buffer having ionic strength 10 mM pH 8.00 and acetonitrile. The encapsulated enzyme catalyzes hydrolysis of p-nitrophenyl acetate and formation of p-nitrophenoxide anion, which is yellow. The immersion times were (a) 0, (b) 10 min (c) 1.0 h, (d), 10 h. As the ester gradually penetrates the doped monolith, it encounters the enzyme and becomes hydrolyzed.

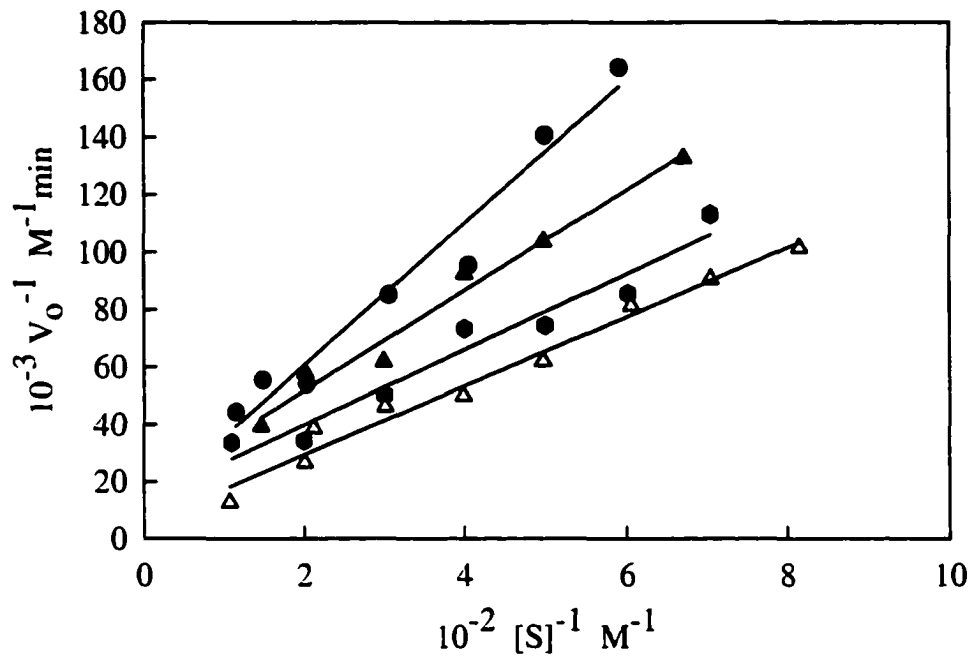


**Figure 8.** Lineweaver-Burk plots for hydrolysis at 25 °C of p-nitrophenyl acetate catalyzed by bovine carbonic anhydrase II in silica monoliths sized 8 x 8 x 27 mm. From the bottom to the top plot, concentrations of the enzyme in silica were 79, 56, 31, and 10  $\mu\text{M}$ . The ester was dissolved in a 9:1 mixture by volume of a phosphate buffer at ionic strength 10 mM and pH 8.00 and acetonitrile.

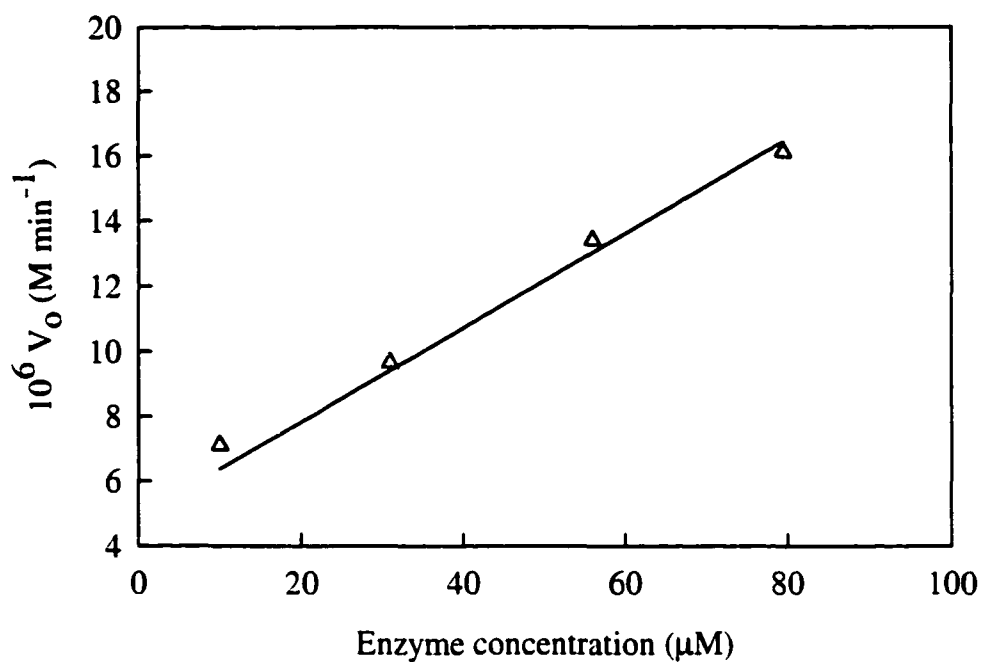


**Figure 9.** Initial rate at 25 °C for hydrolysis of p-nitrophenyl acetate catalyzed by bovine carbonic anhydrase II (eq.3) encapsulated at four concentrations in silica monoliths sized 8 x 8 x 27 mm. The monoliths were immersed in a 2.00 mM solution of a phosphate buffer having ionic strength 10 mM pH 8.00 and acetonitrile.

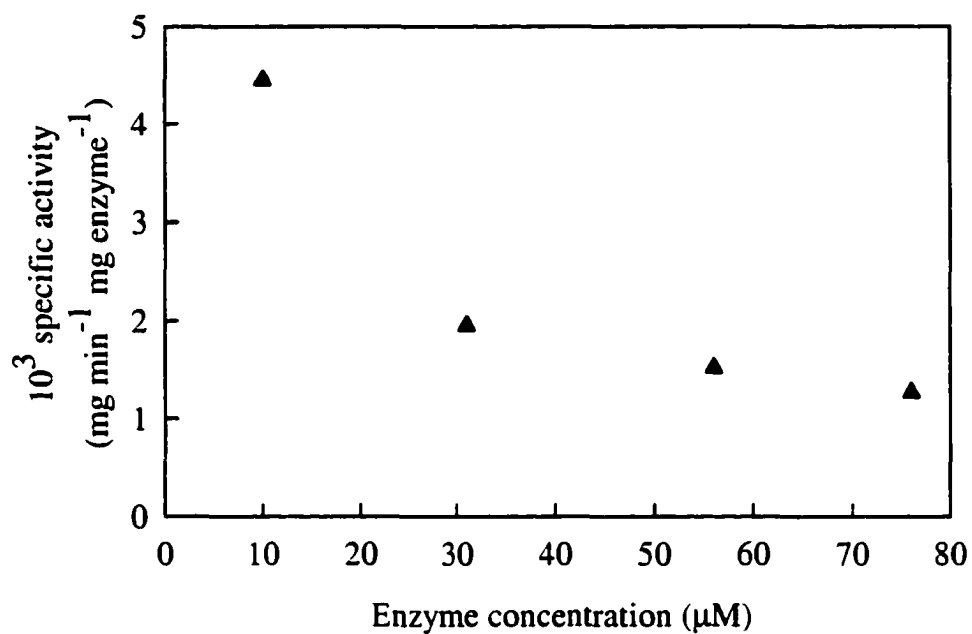


**Figure 10.** Specific activity at 25 °C of bovine carbonic anhydrase II encapsulated at four different concentrations in silica monolith sized 8 x 8 x 27 mm. The enzyme catalyzed hydrolysis (eq. 3) of p-nitrophenyl acetate dissolved in a 9:1 mixture by volume of a phosphate buffer at ionic strength 10 mM and pH 8.00 and acetonitrile.



**APPENDIX 1**

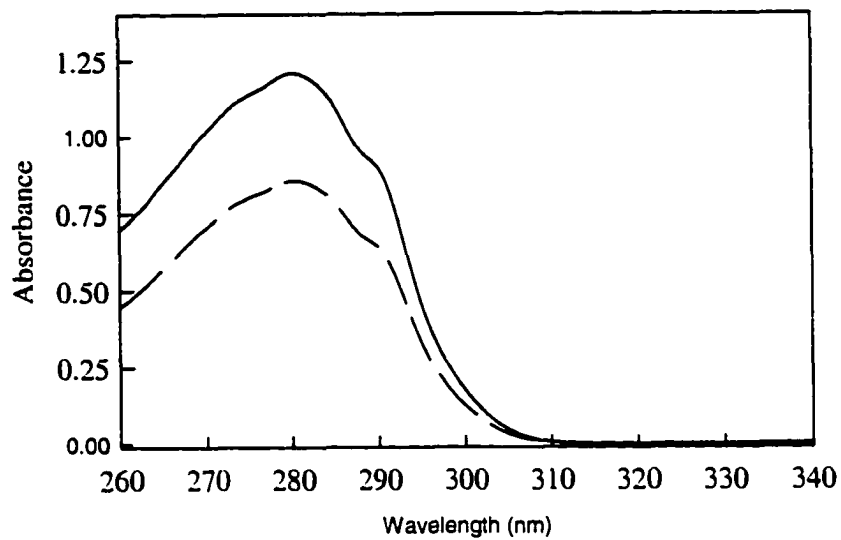


**Figure S1.** Absorption spectra of bovine carbonic anhydrase II. Dashed line: 19.4  $\mu\text{M}$  solution in a MOPS buffer having ionic strength 11.6 mM and pH 7.00. Solid line: silica monolith containing 27.8  $\mu\text{M}$  enzyme and immersed in the aforementioned buffer.

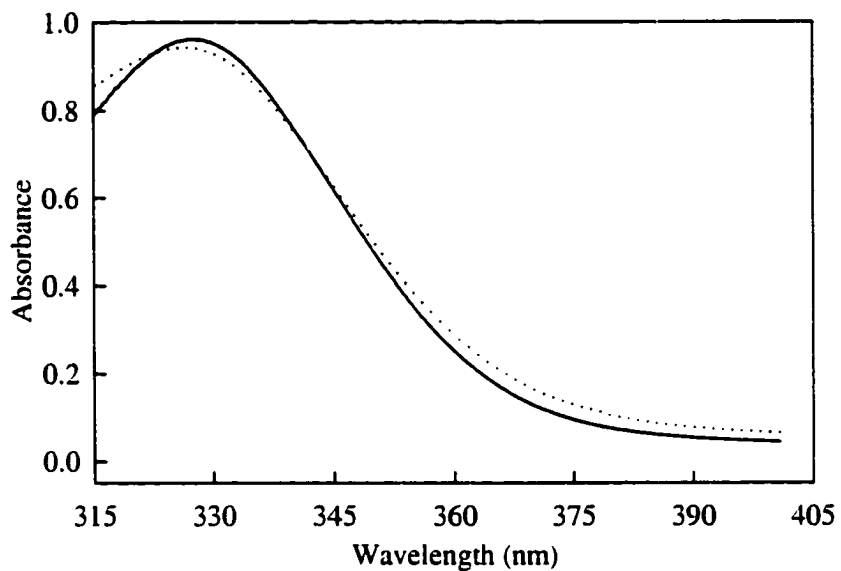


**Figure S2.** Absorption spectra of a silica monolith sized 8 x 8 x 27 mm immersed for 20 h in a  $5.20 \cdot 10^{-4}$  M solution of  $[\text{Ru}(\text{NH}_3)_5\text{Cl}]\text{Cl}_2$  in a MOPS buffer having ionic strength 11.6 mM and pH 7.00 that was 0.600 M in NaCl (solid line) and of that external solution itself (dashed line). The complex cation has the same concentration in the silica glass and in the external solution.

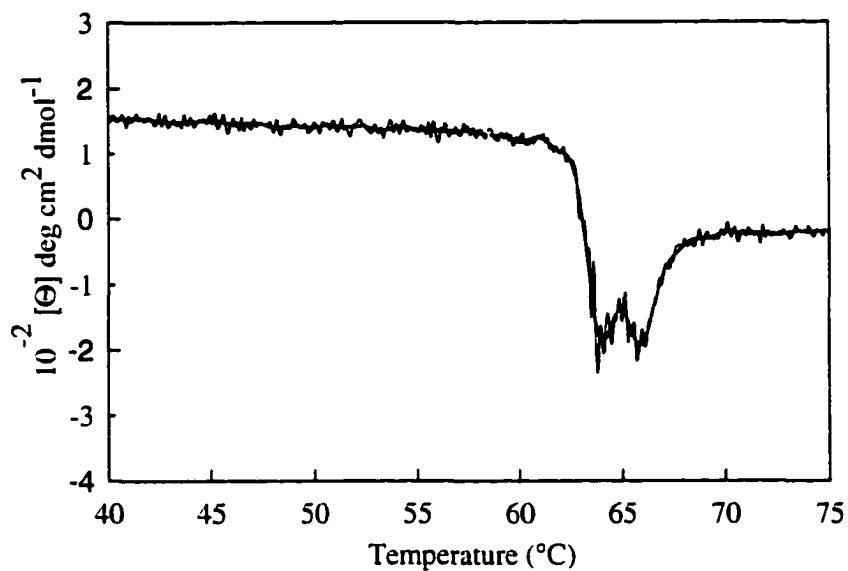


**Figure S3.** Molar ellipticity at 245 nm, normalized to the mean residue value, of a 0.764 mg/mL solution of bovine carbonic anhydrase II in a MOPS buffer having ionic strength 11.6 mM and pH 7.00. Irreversible precipitation occurs at 64 °C and higher temperatures.

**CHAPTER 3. BEHAVIOUR OF ORGANIC COMPOUNDS CONFINED  
IN MONOLITHS OF SOL-GEL SILICA GLASS. EFFECTS OF GUEST-  
HOST HYDROGEN BONDING ON UPTAKE, RELEASE, AND  
ISOMERIZATION OF THE GUEST COMPOUNDS**

A paper published in and reprinted from

*Journal of Materials Chemistry* **2001**, *11*, 408-418

Copyright 2001 The Royal Society of Chemistry

Jovica D. Badjić and Nenad M. Kostić

***Abstract***

Various proteins, catalysts, and other compounds can be encapsulated or diffused into porous sol-gel glasses, but little is known about their interactions with the glass matrix. We report unexpectedly large effects that hydrogen bonding between organic compounds and sol-gel silica has on equilibria and reactions involving these guest compounds. Silica monolith immersed in a solution absorbs the organic solute. Styrene, which is incapable of hydrogen bonding, becomes evenly distributed between external solution and the glass. Aniline and *N,N*-diethyl-*p*-anisidine, which are capable of hydrogen bonding, become extracted into the glass when the solvent (neat CCl<sub>4</sub>) does not interfere with their hydrogen bonding with silica. They become evenly distributed between the solution and the glass when a component of the solvent (DMF added to CCl<sub>4</sub>) or chemical modification

(trimethylsilylation) of the silica surface suppresses hydrogen bonding of these the guests with the surface. Ultraviolet spectra show that silica-guest interactions are present when the guest uptake is excessive and absent when this uptake is balanced. Ultraviolet spectra of aniline show that the hydrogen atoms are donated by silica to the guest. Not only the extent, but also the rate, of uptake is enhanced when the guest makes hydrogen bonds to the silica matrix; suppression of these bonds lowers the uptake rate. Silica monolith extracts *trans*-3,3'-diacetyl azobenzene from a CCl<sub>4</sub> solution 1250-fold. Upon addition of DMF, hydrogen bonds are broken, and the monolith completely releases the solute into the external solution. Five derivatives of azobenzene (3,3'-dimethyl-, 3-acetyl-, 3,3'-diacetyl-, 3,5-diacetyl-, and 3,3',5,5'-tetraacetyl azobenzene), which differ in the propensity for accepting hydrogen atoms from the silica matrix, served as photochromic probes and showed the effect of hydrogen bonding on reactivity. Both the photoinduced (*trans*-to-*cis*) and the subsequent thermal (*cis*-to-*trans*) isomerizations of the five derivatives obey the first-order law in glass as well as in free solution. When the solvent (neat CCl<sub>4</sub>) allows hydrogen bonding, the proportion of the isomers in the photostationary state differs between the glass and solution, and the rate constant for the thermal reaction is two to four times (in different derivatives) smaller in the glass than in solution. Evidently, hydrogen bonding retards the rearrangement of the probe molecules in the silica matrix. When hydrogen bonding is abolished (by addition of DMF to CCl<sub>4</sub>), the compositions of the photostationary state in the glass and in solution become equal, and so do the rate constants. Effects of hydrogen bonding on enzymes encapsulated in sol-gel glass and on the distribution of analytes between the glass monolith

and the sample solution should be taken into consideration when designing accurate biosensors.

### ***Introduction***

Controlled hydrolysis of alkoxides and polymerization of the resulting oxyacids, the sol-gel method, is useful in several branches of chemistry and engineering. Moderate processing conditions enable encapsulation of various organic, inorganic, and biological molecules in glasses having adjustable properties.<sup>1-8</sup> The method is used for the fabrication of sensors, catalyst supports, coatings, special polymers, and other new materials.<sup>9-19</sup>

The guest compounds can be added at the onset of the polymerization and encapsulated in the glass, or they can be diffused into the porous solid after it had solidified. In either case interactions at the molecular level between glass matrix and guest molecules, which govern mobility and chemical reactivity of those guests, are poorly understood. To examine these interactions, we determine affinity of sol-gel silica glass toward various organic compounds as guests, and we study dynamical properties of some of these guests inside the matrix. Research of this kind has begun recently.<sup>20-24</sup>

Work in our laboratory has shown that small molecules may behave quite differently in free solution and in the same solvent but confined in the pores of a hydrogel.<sup>25-27</sup> Soaking of silica glass in electrolyte solutions, no matter how prolonged, may not ensure equal partitioning of a certain ions between the glass and the solution. At a pH value at which the pore walls are negatively charged, anions, such as  $[\text{Fe}(\text{CN})_6]^{3-}$ , are only partially taken up, whereas cations, such as  $[\text{Ru}(\text{NH}_3)_6]^{3+}$ , are excessively taken up by the glass from the

surrounding solution. In either case, internal and external concentrations of the ion remain unequal after the equilibrium is reached. If the electrostatic interactions are left unchecked, the unequal distribution of an ionic analyte would invalidate a biosensor.

Hydrogen bonding is subtler and more specific than electrostatic interactions.<sup>28,29</sup> Evidence for the existence of this bonding in sol-gel silica glass has been reported.<sup>21,30-33</sup> However, to our knowledge, there is no published evidence for the effects of hydrogen bonding on equilibria and reactions involving the guest compounds within sol-gel silica.

Because hydrogen bonds are relatively strong and directional, they may greatly affect physical and chemical processes in doped glasses. Not much is known about these important interactions, which are likely to affect properties and performance of biosensors, immobilized catalysts, and various composite materials prepared by the sol-gel method. These phenomena deserve thorough investigation, and this study is a piece of it. We detected hydrogen bonding, found examples of its enormous effect on uptake of guests by silica, learned how to enhance and abolish this bonding, and showed that it can affect mobility of guest molecules and rate of their reaction. By studying hydrogen bonding and its influence on thermodynamic and kinetic properties of absorbed and encapsulated molecules in sol-gel silica monoliths, one can learn to control chemical processes inside the matrix and to prepare silica glasses with specific and desired properties.

### ***Experimental Procedures***

**Instrumentation.** Proton and <sup>13</sup>C NMR spectra were recorded with a Varian 400 MHz instrument; infrared spectra, with a Bio Rad FTS-7 instrument; UV absorption spectra,



with a Perkin-Elmer Lambda 18 spectrophotometer whose cuvette holder was connected to the thermostated circulator bath Model 9500 from Fisher Scientific Co. Photochemical reactions were done with a Rayonet 100 reactor, which has six fluorescent tubes designated 3500 Å.

**Chemicals.** Distilled water was further demineralized to a resistivity greater than 17 MΩ cm. Tetramethyl orthosilicate and acetonitrile were purchased from Fisher Chemical Co; aniline, styrene, thionyl chloride, *p*-anisic acid, nitrosobenzene, 3-amino-acetophenon, hexamethyldisilazane (HMDSZ), carbon tetrachloride, benzene, and anhydrous *N,N*-dimethylformamide (DMF), from Aldrich Chemical Co; and 3,3'-dimethyl azobenzene, from Trade TCI Mark.

**Hazards.** Tetramethyl orthosilicate, benzene and CCl<sub>4</sub> are highly toxic; the last two chemicals may cause cancer. Protective gloves and effective fume hood must be used in experiments with these compounds.

**Preparation of Silica Monoliths.** The silica sol was prepared by a standard procedure.<sup>34</sup> A mixture of 15.76 g of tetramethyl orthosilicate, 3.38 g of water, and 0.30 g of 0.040 M HCl was kept in an ice-cooled ultrasonic bath for 30 min. Upon addition of 36.26 mL of a 10 mM sodium phosphate buffer having pH 7.00, gelation began. The sol was quickly poured into polystyrene cuvettes sized 10 x 10 x 40 mm, and left at 4 °C. During the aging for 14 days, the samples were kept soaked and were washed with water twice a day. The aged samples were exposed to air, still at 4 °C, for another 14 days of partial drying and shrinking. The resulting transparent monoliths, prisms sized 8 x 8 x 27 mm, were soaked in acetonitrile and stored at 4° C for further use. All monoliths used in this study had this size.

Defective or nonstandard monoliths were rejected, for the sake of reproducibility and accuracy of the experiments.

**Dehydration of Silica Monoliths.** Two silica monoliths sized 8 x 8 x 27 mm were soaked in 300 mL of stirred acetonitrile in a capped 500-mL Erlenmeyer flask. The solvent was replaced with fresh 300-mL portions twice, after 2 h and again after 21 h. This last soaking lasted for an additional 24 h. The monoliths were then soaked in 150 mL of stirred  $\text{CCl}_4$  in a capped 250-mL Erlenmeyer flask. The solvent was replaced with a fresh 150-mL portion after 24 h, and the soaking continued for an additional 24 h. In some experiments, the second solvent was a 9 : 1 v/v mixture of  $\text{CCl}_4$  and DMF. The Erlenmeyer flasks were always capped, to protect the dry solvents from the moisture in the air. Dehydrated silica monoliths were stored for further experiments in a fresh portion of the same solvent in which they had been soaked last – pure  $\text{CCl}_4$  or a 9 : 1 v/v mixture of  $\text{CCl}_4$  and DMF.

**Trimethylsilylation of Silica Monoliths.** A silica monolith sized 8 x 8 x 27 mm was exhaustively soaked, with stirring, in a succession of relatively large volumes of many solvents and solutions. These liquids, the volume of their portions, the time of the soaking in each fresh portion, the number of fresh portions, and the function of each liquid were as follows: Acetonitrile, 350 mL, 24 h, one, for rinsing; a mixture of 90 mL acetonitrile and 10 mL acetyl chloride, 2 h, one, for removal of water; acetonitrile, 400 mL, 12 h, six, for removal of acetyl chloride and reaction products; a mixture of 90 mL acetonitrile and 10 mL hexamethyldisilazane (HMDSZ) under the nitrogen atmosphere, 24 h, five, for trimethylsilylation;  $^{35}\text{S}$  acetonitrile, 400 mL, four, for removal of HMDSZ and reaction products; and finally  $\text{CCl}_4$ , 150 mL, 24 h, two, for removal of previous solvents. Upon first

contact with HMDSZ the transparent monolith turned cloudy white, but it became transparent again later. This procedure was repeated with several monoliths. The silylated monoliths were stored in  $\text{CCl}_4$  for further experiments.

**Infrared Spectra of Dehydrated and Silylated Silica Glass.** Silica monoliths of both kinds were ground in a mortar, the powder was dried in a vacuum desiccator for 1 h, and the spectroscopic sample was placed between NaCl plates.

**Pretreatment of Silica Monoliths with Acid and Base.** Two silica monoliths sized 8 x 8 x 27 mm were soaked in 200 mL of a 0.10 M HCl solution, and the other two were soaked in 200 mL of a  $3.2 \cdot 10^{-4}$  M NaOH solution, all in capped 500-mL Erlenmeyer flasks, with stirring overnight. All four monoliths were then dehydrated by the procedure described above.

**General Procedure for Uptake Experiments.** Stock solutions of guest compounds in  $\text{CCl}_4$  were 2.05 mM in styrene, 0.48 mM in aniline, and 0.43 mM in *N,N*-diethyl-*p*-anisamide, so that their absorbances are measured accurately. Dehydrated silica monoliths sized 8 x 8 x 27 mm were the hosts. Each monolith was soaked in 50.0 mL of a stock solution in a capped vial. The monolith stood upright, with one of its 8 x 8 mm sides resting on the flat bottom of the vial and the other five sides exposed to the solution. From time to time the monolith without the surrounding solution would be transferred to the 10-mm quartz cuvette kept in the sample holder of the spectrophotometer. An identical but undoped silica monolith made in the same batch as the doped monolith would be put in another 10-mm quartz cuvette, kept in the reference holder. Both monoliths were held in the same place and the same position in all experiments, so that their absorbances could be accurately compared.

The UV spectra would be scanned at the rate of 120 nm/min, and the doped monolith would be returned to the solution of the guest compound (the dopant) and soaked further. The UV measurements were more frequent early in the experiment, while the uptake was relatively fast, and less frequent later, when the uptake slowed down. At the end of the uptake experiment, the UV spectrum of the soaking solution partially depleted of the guest compound was compared with the UV spectrum of the stock solution of this guest. The width ( $w$ , in mm) of the soaked monolith was measured with the caliper, and the absorbance of this monolith multiplied by  $10/w$ , so that it can be compared with the absorbance of the stock solution.

**Uptake and Release of *trans*-3,3'-Diacetyl azobenzene.** This compound was chosen for determination of the maximum uptake of a guest compound by the sol-gel silica glass. A dehydrated monolith sized 8 x 8 x 27 mm was soaked in 200 mL of a stirred  $9.30 \cdot 10^{-4}$  M solution of the title compound in  $\text{CCl}_4$ . The capped Erlenmeyer flask was wrapped in aluminum foil, to prevent photoisomerization of the *trans* isomer. Decrease of its concentration in the external solution was monitored occasionally by UV spectroscopy. Aliquots of ca. 0.30 mL of the external solution were diluted by ca. 2.5 mL of  $\text{CCl}_4$ , to lower their absorbance below 1.0; both the aliquot and the solvent were weighed with an analytical balance, so that the accurate dilution factor be known. Then the UV spectrum was recorded, and from it the concentration of the title compound in the external solution was determined. Slight decreases in the volume of the soaking solution after each successive removal of aliquots were taken into account in the successive determinations of its concentration. When this concentration almost ceased decreasing with time, the uptake experiment was ended.

The release of the title compound by the monolith was triggered by adding 20.0 mL of DMF to the external solution. Increase in the concentration of the title compound in the external solution was followed by UV spectroscopy, as described above. When this concentration nearly reached the initial value of  $9.30 \cdot 10^{-4}$  M, the experiment was ended.

**Calculation of the Volume Required for Trans-to-Cis Isomerization.** We accepted a published mechanism for isomerization of azobenzene.<sup>36-39</sup> Conformation of the trans isomer was optimized with the program Hyperchem 4.5. All five stages of the isomerization were examined separately for each azobenzene derivative.<sup>40</sup> The structures at each of the five stages were superimposed and treated as one structure, the van der Waals volume of which was then calculated by the program GRASP 1.2. This volume can accommodate the entire isomerization process of the given derivative. This procedure was repeated for each of the five derivatives of azobenzene.

**Determination of Absorptivities of Azobenzene Derivatives.** The following procedure was used for the trans isomers of all five azobenzene derivatives. A sample of ca. 17 mg, weighed to 0.01 mg, was dissolved in  $500.0 \pm 0.2$  mL  $\text{CCl}_4$ , in a volumetric flask. The UV spectrum of this solution allowed direct calculation of absorptivities of the trans isomer at various wavelengths.

Absorptivities of the cis isomer were determined indirectly. A sample of ca. 1.0 mg of the trans isomer was dissolved in 10.0 mL of a 95 : 5 v/v mixture of  $\text{CCl}_4$  and  $\text{CDCl}_3$ , in a volumetric flask. The UV spectrum was recorded, and the solution was irradiated (by the procedure to be described next) until its UV spectrum ceased to change, i.e., until the photostationary state (designated pss) for the isomerization was reached. The relative

concentrations of the trans and cis isomers were determined from the intensities of the  $^1\text{H}$  NMR resonances for the acetyl groups in these isomers. Although thermal isomerization is very slow and the composition of the pss is practically constant over a relatively short time (see below), for the sake of accuracy the NMR spectrum was taken promptly. From the known initial concentration and absorptivity of the trans isomer, the UV spectrum of the mixture of isomers, and the composition of this mixture, the absorptivity of the cis isomer was determined. The results are given in Table S1 in the Supporting Information.

**Trans-to-Cis Photoisomerization of Azobenzene.** To a quartz cuvette sized 10 x 10 x 40 mm and having all walls transparent (so-called fluorescence cuvette) was fused a ground-glass joint. The joint could be closed, to prevent evaporation of the solvent held (together with the doped monolith) in the cuvette. The following procedure was used for all five derivatives of azobenzene. A dehydrated silica monolith sized 8 x 8 x 27 mm was soaked in 50.0 mL of a solution of the trans isomer in a 9 : 1 v/v mixture of  $\text{CCl}_4$  and DMF; DMF ensured that the guest compound uniformly penetrates into silica (see the general description of uptake experiments). The uptake was followed by UV spectrophotometry. When the absorbance of the trans isomer in silica reached that in the external solution, the monolith and 1.50 mL of the soaking solution were transferred to the special cuvette and always kept in the same position inside it. The capped cuvette was irradiated, always in the same position with respect to the lamps. The walls transmitted UV light from all sides. Ultraviolet spectrum of the monolith was taken occasionally. When it ceased changing, photostationary state (pss) was reached. Absorbances were converted to concentrations according to eqs 1 and 2, in which  $A$  is absorbance,  $\epsilon$  is absorptivity, subscript o denotes

initial state, and lack of a subscript denotes the time of measurement.<sup>41</sup> The experimental results were fitted to by the linear least-square method eq 3, in which  $t$  is time and  $k_1$  is the apparent first-order rate constant for the intramolecular photoisomerization.<sup>41</sup>

$$[\text{cis}] = \frac{1 - \frac{A}{A_0}}{1 - \frac{\epsilon_{\text{cis}}}{\epsilon_{\text{trans}}}} [\text{trans}]_0 \quad (1)$$

$$[\text{trans}] = [\text{trans}]_0 - [\text{cis}] \quad (2)$$

$$\ln \frac{[\text{trans}]_0 - [\text{trans}]_{\text{pss}}}{[\text{trans}] - [\text{trans}]_{\text{pss}}} = \frac{[\text{trans}]_0}{[\text{trans}]_0 - [\text{trans}]_{\text{pss}}} k_1 \cdot t \quad (3)$$

**Cis-to-Trans Thermal Isomerization of Azobenzene.** The following procedure was used for all five derivatives of azobenzene. A dehydrated silica monolith sized 8 x 8 x 27 mm was soaked in 50.0 mL of a  $5 \cdot 10^{-5}$  M solution of the pure trans isomer. The solvents were two. In one series of experiments it was neat  $\text{CCl}_4$ . In the other series, it was a 9 : 1 v/v mixture of  $\text{CCl}_4$  and DMF. As before, when absorbance of the monolith reached that of the surrounding solution, the monolith was transferred to the special cuvette for UV irradiation. This time, the photoisomerization was just a method for preparing the cis isomer, whose thermal isomerization was the reaction of interest. When the solvent was neat  $\text{CCl}_4$ , the monolith was transferred without the external solution, to avoid continued uptake of azobenzene during irradiation. When the solvent was the mixture, the monolith was transferred with 1.50 mL of the soaking solution, because in this case there was no danger of continued uptake.

The capped cuvette was irradiated in the photochemical reactor (as described above) until the UV spectrum ceased changing, a sign that the photostationary state was reached. To the monolith free of the solvent was then added 1.5 mL of neat CCl<sub>4</sub>, and the monolith that had been immersed in the mixture of CCl<sub>4</sub> and DMF was left so. The liquid around the monolith is needed to conduct the heat to the monolith. In either case, the sealed cuvette was immersed above the level of the monolith and the surrounding liquid in the water bath at 50.0 ± 0.5 °C; thermal isomerization at a lower temperature would be impractically slow. The cuvette would occasionally be transferred to the spectrophotometer, and thermal isomerization would be followed by recording UV spectra. When the isomerization was completed, in experiments employing neat CCl<sub>4</sub> its spectrum was also taken, as a precaution against leakage of the azobenzene from the monolith.

Ultraviolet bands of the five azobenzene derivatives reach their maxima at different wavelengths. The maximum absorbance was converted to the concentration of the trans isomer according to eqs 1 and 2. The change of concentration in time was fitted by the linear least-squares method to eq 4, in which  $k_2$  is the first-order rate constant for thermal isomerization. Other quantities were defined in connection with eq 3.<sup>41</sup>

$$\ln \frac{[\text{trans}]_0 - [\text{trans}]_{\text{pss}}}{[\text{trans}]_0 - [\text{trans}]} = k_2 \cdot t \quad (4)$$

**Preparation of *N,N*-Diethyl-*p*-anisamide.** To a solution of 17.4 g (0.11 mol) of *p*-anisic acid in 50.0 mL of benzene was added 17.6 mL of thionyl chloride. The mixture was refluxed in a strong fume hood until gas evolution ceased, for ca. 2 hours. Benzene was



cautiously evaporated under reduced pressure, and *p*-anisoyl chloride was obtained in almost theoretical yield. It was used without further purification.

A solution 21.8 g of *p*-anisoyl chloride (0.13 mol) of in 50.0 mL of diethyl ether was added slowly in a dropping funnel to a solution of 40 mL of diethyl amine (0.39 mol) in 150 mL of diethyl ether, kept at 0 °C. Upon complete addition of *p*-anisoyl chloride, the reaction mixture was stirred for 2 h at room temperature and extracted with 200 mL of diethyl ether. The organic layer was washed with three 150-mL portions of water and one portion of brine and dried with magnesium sulfate. The organic solvent was evaporated, and crude title compound was recrystallized from methanol. The yield was 18.9 g or 70 %; mp 42-43 °C, as reported;<sup>42</sup> <sup>1</sup>H NMR in CDCl<sub>3</sub>: δ 1.17 (br, 6 H), δ 3.40 (br, 4 H), δ 3.82 (s, 3 H), δ 6.89 (m, 2H), and δ 7.34 (m, 2H).

**Preparation of Azobenzenes.** See Scheme 1.<sup>43,44</sup> All derivatives of nitrosobenzene were synthesized by oxidation of the corresponding derivatives of aniline with Caro's acid.<sup>45</sup> A solution containing 3.0 mmol of nitrosobenzene or its derivative and 3.0 mmol of a derivative of aniline in 15 mL of glacial acetic acid was heated at 60 °C for 12 h, poured to ice-cold, saturated aqueous solution of NaHCO<sub>3</sub>, and extracted with benzene. Evaporation of benzene gave a crude solid. Its purification on a silica-gel column yielded a pure azobenzene derivative. Chromatographic conditions are given below.

*3-Acetyl azobenzene.* Eluent was a 9 : 1 v/v mixture of benzene and ethyl acetate. Orange needles had mp 88-89 °C (cf 88-90 °C);<sup>43</sup> <sup>1</sup>H NMR in CDCl<sub>3</sub>: δ 2.68 (s, 3 H), δ 7.51 (m, 3 H), δ 7.61 (t, 1 H), δ 7.93 (m, 2 H), δ 8.08 (m, 2 H), and δ 8.46 (s, 1 H);<sup>13</sup>C NMR in

$\text{CDCl}_3$ :  $\delta$  26.9,  $\delta$  122.9,  $\delta$  123.1,  $\delta$  127.0,  $\delta$  129.2,  $\delta$  129.5,  $\delta$  130.3,  $\delta$  131.5,  $\delta$  138.1,  $\delta$  152.5,  $\delta$  152.7, and  $\delta$  197.6.

*3,5-Diacetyl azobenzene*. Eluent was a 6 : 4 v/v mixture of benzene and ethyl acetate. Orange needles had mp 87-89 °C.  $^1\text{H}$  NMR in  $\text{CDCl}_3$ :  $\delta$  2.72 (s, 6 H),  $\delta$  7.54 (m, 3 H),  $\delta$  7.96 (m, 2 H),  $\delta$  8.62 (t, 1 H), and  $\delta$  8.64 (d, 2 H);  $^{13}\text{C}$  NMR in  $\text{CDCl}_3$ :  $\delta$  27.0,  $\delta$  123.3,  $\delta$  126.5,  $\delta$  129.3,  $\delta$  129.5,  $\delta$  132.0,  $\delta$  138.5,  $\delta$  152.3,  $\delta$  153.0, and  $\delta$  196.9; LRMS-CI: calcd for  $\text{M}^+$  of  $\text{C}_{16}\text{H}_{14}\text{N}_2\text{O}_2$  266, found 266.

*3,3',5,5'-Diacetyl azobenzene*. Eluent was a 8 : 2 v/v mixture of benzene and ethyl acetate; mp 133-134°C (cf 131-134 °C);<sup>46</sup>  $^1\text{H}$  NMR in  $\text{CDCl}_3$ :  $\delta$  2.67 (s, 6 H),  $\delta$  7.61 (m, 2 H),  $\delta$  8.07 (m, 4 H), and  $\delta$  8.46 (s, 2 H).  $^{13}\text{C}$  NMR in  $\text{CDCl}_3$ :  $\delta$  26.9,  $\delta$  123.1,  $\delta$  127.2,  $\delta$  129.6,  $\delta$  130.8,  $\delta$  138.2,  $\delta$  152.5, and  $\delta$  197.5.

*3,3',5,5'-Tetraacetyl azobenzene*. Eluent was a 5 : 2 : 3 v/v/v mixture of benzene, ethyl acetate, and chloroform; mp 221-224 °C;  $^1\text{H}$  NMR in  $\text{CDCl}_3$ :  $\delta$  2.75 (s, 12 H),  $\delta$  8.67 (t, 2 H), and  $\delta$  8.70 (d, 4 H);  $^{13}\text{C}$  NMR in  $\text{CDCl}_3$ :  $\delta$  27.0,  $\delta$  126.7,  $\delta$  130.3,  $\delta$  138.6,  $\delta$  152.5, and  $\delta$  196.7; LRMS-CI: calcd for  $\text{M}^+$  of  $\text{C}_{20}\text{H}_{18}\text{N}_2\text{O}_4$  350, found 350.

## **Results and Discussion**

**Hydrogen Bonding between Silica Glass and Guest Compounds.** Hydrogen bonds between sol-gel silica and guest compounds embedded in it (during formation of the glass) or absorbed in it (by diffusion into the preformed glass) are widely assumed to exist, but direct detection of these bonds was reported recently.<sup>21,30-33</sup> Not much is known about these important interactions, which are likely to affect properties and performance of biosensors,

immobilized catalysts, and various composite materials prepared by the sol-gel method. Beyond detecting hydrogen bonding, we wish to understand their effect on equilibria and reactions of guest compounds within sol-gel silica monolith.

**Treatment of the Silica Monolith.** After aging and partial drying, the pores in the silica monoliths contain water that must be removed lest it interfere with hydrogen bonds under study. We extracted water with a succession of solvents chosen so that each dilutes and removes the previous one. These exhaustive procedures took considerable time. The dehydration procedure achieved the overall dilution factor of ca.  $10^{11}$ . The trimethylsilylation procedure was applied to the dehydrated glass and included chemical as well as extractive dehydration. The additional dilution factor in the trimethylsilylation procedure reached ca.  $10^4$ . Much smaller factors probably would have been sufficient, but we strove for very accurate experiments.

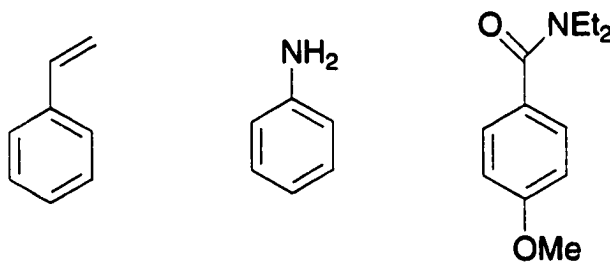
Trimethylsilylated silica does not show any bands in the  $1650 - 1790 \text{ cm}^{-1}$  region in the infrared spectrum (Figure 5). The absence of carbonyl groups proves that acetyl chloride does not react with silanol hydroxyl groups during the dehydration preceding treatment with hexamethyldisilazane.

#### **Balanced and Excessive Uptake of the Guest Compounds by Silica Glass.**

Because sol-gel silica is porous, it is widely assumed that molecules smaller than the pores can diffuse in and out of the matrix and that their concentrations in the matrix and in the surrounding solution will become equal, i.e., that the uptake will be balanced. Research in this laboratory has already refuted this assumption in cases when both the silica matrix and the guest are charged.<sup>25-27</sup> If these charges are like, the host matrix partially rejects the

guest; if the charges are opposite, the matrix takes the guest up excessively. We term this phenomenon *imbalanced uptake*.

Electrostatic interactions, which we studied before, are strong and isotropic. In this study we examine the consequences of subtler interactions. Hydrogen bonding is relatively strong but also anisotropic and selective. These characteristics make hydrogen bonding extremely important for equilibria and chemical reactivity.<sup>28,47-49</sup> The three compounds serving as guests are shown below. Styrene is incapable of hydrogen



bonding; aniline can both accept and donate hydrogen atoms; and *N,N*-diethyl-*p*-anisamide can only accept them. These three compounds as probes allowed us to examine the capacity of sol-gel silica monolith as both acceptor and donor of hydrogen. We also managed to enhance and abolish hydrogen bonding simply by adjusting the solvent properties, as will be explained below.

Figure 1 shows that when the solvent was neat  $\text{CCl}_4$ , uptake of styrene was balanced, whereas the uptake of the other two guests was excessive. Figure 2 shows that when  $\text{CCl}_4$  contained 10 % by volume of DMF, the uptake of these two guests became balanced as well.

Excessive uptake of relatively nonpolar organic molecules into the highly polar matrix such as silica is unexpected on the basis of the well-known principles of extraction and partition chromatography. When excessive uptake occurs, there must exist special

attractive interactions between the host and the guest. Interaction of  $\text{CCl}_4$  with silica have just been reported.<sup>50</sup> These interactions are to be expected because chlorine atoms in organic molecules are known to form weak hydrogen bonds.<sup>51</sup> Styrene, which lacks heteroatoms and is incapable of hydrogen bonding, lacks special attraction to silica surface and cannot displace  $\text{CCl}_4$  from the silica surface. Consequently, its uptake by silica monolith is balanced. The other two guests have nitrogen and oxygen atoms, which can form relatively strong hydrogen bonds to silica, and therefore displace  $\text{CCl}_4$  from silica surface. Consequently, their uptake by silica is excessive. When the hydrogen-bonding solvent DMF is present in large excess, it abolishes excessive uptake of these two guests.

**Ultraviolet-Spectroscopic Evidence for Hydrogen Bonding.** Figure S1 in the Supporting Information shows that absorption spectrum of styrene does not change when this compound enters the silica matrix. The absence of interaction with the matrix is consistent with the balanced uptake observed for styrene. Figure S2 in the Supporting Information shows that the spectrum of *N,N*-diethyl-*p*-anisamide does change when its uptake is excessive (from neat  $\text{CCl}_4$ ), but does not change when its uptake is balanced (in the presence of DMF). Perturbation of the chromophore is diagnostic of its interaction with silica. That perturbation and excessive uptake occur together probably is more than coincidence; it likely is a casual relation.

Because UV spectrum of aniline is well understood, this compound is used as a reliable probe for hydrogen bonding. Blue shift signifies hydrogen acceptance; red shift, hydrogen donation.<sup>52-55</sup> Figure 3 shows a large blue shift when aniline is taken up from the solution in neat  $\text{CCl}_4$  and no spectral change when aniline is taken up from the solution

containing also DMF. Evidently, aniline accepts hydrogen from the silica matrix when the silanol groups on its surfaces are available. When, however, silanol groups are saturated with DMF, a good acceptor, hydrogen bonding between silica and aniline is abolished.

**Immense Uptake and Complete Release of *trans*-3,3'-Diacetyl azobenzene by Silica Glass.** As Figure 1 shows, concentration of hydrogen-bonding guests becomes approximately three times greater in the glass than in the external solution after approximately three hours of soaking, when these experiments were ended. To find out the maximum capacity of silica for a guest, we chose the title compound, which contains two hydrogen-accepting acetyl groups, because we had a good supply of it. The experiment lasted for 11 days, until the uptake practically ceased. The results are shown in Figure 4. We define the uptake coefficient as the ratio of the guest concentrations in the glass and in the solution surrounding the glass. Concentration of the guest in 200 mL of solution decreased from  $9.3 \cdot 10^{-4}$  M to  $1.2 \cdot 10^{-4}$  M in a sealed container. The “departed” quantity of it must have accumulated in the silica monolith, whose overall volume is 1.7 mL. Because only ca. 65 % of this volume is pores<sup>25</sup> and therefore accessible to the guest, the aforementioned ratio of concentration “inside” and “outside” is  $1.5 \cdot 10^{-1}$  M to  $1.2 \cdot 10^{-4}$  M, or 1250. We did not thoroughly study the other derivatives of azobenzene, but they too are likely to show greatly excessive uptake.

This surprisingly large number shows how important hydrogen bonding between silica matrix and guests compounds can be. Clearly, this bonding must be taken into consideration in studies of diffusion and partition of solutes between sol-gel materials and

surrounding media and in careful studies of equilibria and rates of reactions inside sol-gel materials.

Upon addition of DMF to the depleted external solution, the absorbed guest was fully released by the silica monolith in ca. 75 h, much faster than it had been taken up. Clearly, hydrogen bonds between silica and the guest can be broken by a competing hydrogen-acceptor.

Our finding holds promise for practical applications of sol-gel silica. This material can efficiently extract from solution a solute with complementary hydrogen-bonding ability and then release this solute upon addition of a small amount of a suitable solvent. This cycle is reminiscent of molecular sieves, analytical and preparative separations, and controlled delivery of drugs.

**Nearly-Balanced Uptake of the Guest Compounds by Chemically-Modified Silica Glass.** Upon exhaustive treatment of silica monolith with hexamethyldisilazane, hydroxyl groups on the surfaces were “capped” with the  $\text{Si}(\text{CH}_3)_3$  groups. As Figure 5 shows, these organic groups are evident by the infrared bands at ca.  $3000$  and  $1260\text{ cm}^{-1}$ , corresponding to C-H and Si-C vibrations, respectively.

Both compounds that show excessive uptake by pristine silica (Figures 1b and 1c) show nearly-balanced uptake by the modified silica (Figures 6a and 6b) even though the solvent,  $\text{CCl}_4$ , allows hydrogen bonding. We attribute the absence of this bonding to trimethylsilylation. Hydroxylic hydrogen atoms to be donated to the guests are absent, and the oxygen atoms that might accept hydrogen atoms from aniline are protected by the bulky  $\text{Si}(\text{CH}_3)_3$  groups. Figure 6 shows that concentration of each guest in the silica host levels off

slightly below the concentration in the external solution. If real, this small “underachievement” may be the result of the steric bulk of the capping groups.

The chromophores that were markedly perturbed by the pristine silica (Figure 3) are only slightly affected by the modified silica (Figure S3 in the Supporting information). Because hydrogen bonding is suppressed, the slight change presumably is a result of a nonspecific effect of the altered medium. Again, excessive uptake coincides with marked spectral change, whereas nearly or completely balanced uptake coincides with little or no spectral change.

Evidently, excessive uptake of hydrogen-bonding guests can be abolished not only by adding a competing solvent but also by modifying the silica surface. This finding corroborates our view, stated above, that the competing solvent DMF lines the surfaces of porous silica and prevents the guest molecules from forming hydrogen bonds with these surfaces.

**Rate of Uptake of the Guest Compounds by Silica Monoliths.** The time in which the concentration of the guest compound inside the silica monolith becomes equal to the concentration in the external solution may be taken as an approximate measure of the rate of uptake if, as in our experiments, the external concentrations are similar in all experiments. In the case of balanced uptake, internal concentration levels off with time. In the case of excessive uptake, internal concentration continues to increase.

As Figure 2 shows, the equalization time was ca. 400 min for both guests that are capable of hydrogen bonding. When this bonding was suppressed, they were taken up at the



same rate. As Figures 1b and 1c show, the two rates became greater and quite different when hydrogen bonding was allowed; then the equalization times were 75 and 35 min.

In attempts to alter the uptake rates, we treated silica monolith with acid or with base before dehydration. Figure S4 in the Supporting Information shows, however, that the differently-treated monoliths resembled each other and untreated monoliths in the rates of uptake of the same hydrogen-bonding guest in  $\text{CCl}_4$ , the solvent that allows this bonding.

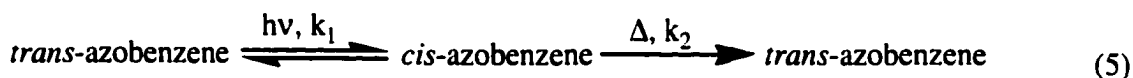
When silica surface was modified with the bulky  $\text{Si}(\text{CH}_3)_3$  groups, the uptake slowed down; the equalization time for both guest compounds exceeded 1000 min. Again, suppression of hydrogen bonding seems to lower the rate of uptake.

Clearly, rate of uptake varies greatly when hydrogen bonding is allowed or abolished and when the silica surface is chemically modified. Even before quantitative studies of the rate are done, our semiquantitative finding should be taken into account in studies of equilibria and chemical reactions involving sol-gel glasses doped with enzymes and other chemicals.

**Kinetics of Azobenzene Isomerization.** Isomerization of azobenzene has been used to explore microstructure and rigidity of solid polymers.<sup>56-58</sup> In principle, this process can be used in optical storage systems, nanodevices, and molecular switches. Other researchers have applied this elegant method to assess the steric constraint of sol-gel glass on molecules contained in it.<sup>41,59,60</sup> Function of this glass in various applications depends on the mobility and chemical reactivity of the dopant.<sup>23</sup> Because hydrogen bonding greatly affects the extent and the rate of uptake and release of guest compounds by the host glass, we study quantitatively the influence of hydrogen bonding on a reaction of a series of guest molecules

absorbed in the host matrix. Interconversion of geometric (cis and trans) isomers of azobenzene is shown in eq 5. It is a simple reaction, amounting to motion of molecular parts.

We chose it because its kinetics is well known.<sup>61-63</sup>

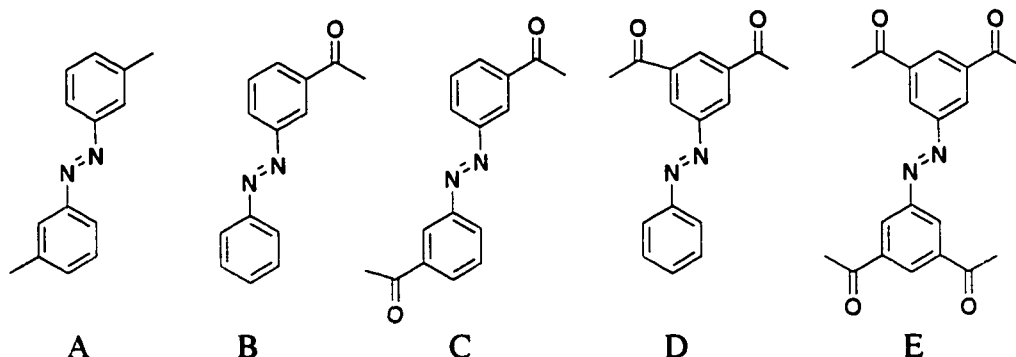


The so-called forward reaction is effected by UV light, and it is relatively fast. The so-called back reaction is spontaneous at room temperature but slow. We studied it at 50.0 °C, in the dark.

Study of the forward reaction presents pitfalls. The first-order rate constant for photoisomerization changes when the amount of light absorbed by the irradiated sample changes. The absorbed amount, in turn, depends on concentration of the sample and on the irradiation wavelength. To avoid errors in kinetic analysis, we determine the order of the reactions of the various azobenzene derivatives, but do not calculate or compare the rate constants  $k_1$ . Fortunately, study of the back reaction is straightforward. This was shown with various photochromic molecules, which proved useful for exploration of polymers.<sup>40,41,56,59,60,64-69</sup> Above the glass-transition temperature the back reaction inside the polymer is monophasic, as in solution. Below this temperature, however, the reaction inside the polymer is biphasic or multiphasic. This change in kinetics has been attributed to heterogeneity of the matrix and variability of the free volume felt by the photochromic molecules.

**The Azobenzene Derivatives.** We purchased the compound designated A and synthesized and purified those designated B to E. Their propensity for accepting hydrogen

atoms increases with the number of acetyl substituents. We studied the effect of these substituents, and therefore of hydrogen bonds, on the thermal isomerization shown in eq 5.



**Uptake and Isomerization of Azobenzene in Silica Glass when Hydrogen Bonds are Absent.** In these experiments the solvent was a 9 : 1 v/v mixture of  $\text{CCl}_4$  and DMF. The latter component, a hydrogen acceptor, binds to silica and forestalls its hydrogen bonding to azobenzene derivative. All five guests showed balanced uptake into the silica monoliths. Both photoinduced and thermal reactions in eq 5 for all five compounds absorbed in silica were monophasic, as linear plots in Figures 7 and 8 show. Table 1 shows that the rate constants  $k_2$  for thermal isomerization (the second reaction in eq 5) are virtually the same in solution and in the glass. Table 2 shows that the photoisomerization (the first reaction in eq 5) occurs to the same extent in solution and in the glass. Evidently, in the absence of hydrogen bonding these two media are equal as environments for the isomerization. When azobenzene cannot make hydrogen bonds to the matrix, this photoprobe does not differentiate between bulk solvent and solvent confined in the glass pores. Similar conclusion was reached in a study of isomerization in which hydrogen bonding was not possible because the protic solvent was present.<sup>41,59,60</sup> Clearly, the glass matrix itself does not restrict the motion required for the isomerization.

The largest photoprobe, the one designated E, requires the volume of ca.  $505 \text{ \AA}^3$  for isomerization. A sphere of this volume has a diameter of ca.  $30 \text{ \AA}$ . Evidently, the pores in sol-gel silica are larger than this size.

**Uptake and Isomerization of Azobenzene in Silica Glass when Hydrogen Bonds are Present.** In these experiments the solvent was neat  $\text{CCl}_4$ . All five azobenzene derivatives showed excessive uptake by silica monoliths because of hydrogen bonding to silica. In the case of the compound C, which we studied in detail (see above), this excess is 1250-fold.

Thermal back reaction (the second step in eq 5) of all five photoprobes was studied separately in solution and inside silica. Because these probes are different compounds, which differ in the substituents and in electron delocalization, “vertical” comparisons in Table 3 are unwarranted.<sup>62,70-73</sup> We make only “horizontal” comparisons, those of the same compound in two environments. As Figure 7 shows, isomerization of all five photoprobes in solution, and of all except B in silica, were monophasic. The reaction of the compound B in silica appeared biphasic.

At the end of the long kinetic experiments, the neat  $\text{CCl}_4$  surrounding the monoliths was checked by UV spectrophotometry. The compounds A and B leaked from the silica, and the compounds C, D, and E did not. The biphasic reaction of B probably is caused by the simultaneous isomerization, at different rates, of this compound in silica and in the surrounding solution. The reaction of A may appear monophasic if the rates in silica and in solution are comparable. For the sake of accuracy, we omitted compounds A and B from Table 3.

Kinetic results for the compounds C, D, and E are not complicated by leakage. They are given in Table 3. Thermal isomerization is slower in silica than in solution. Mobility of azobenzene within silica seems to be hindered by hydrogen bonding to the pore surfaces. Both photoprobes having two acetyl groups (C and D) show similar rate of isomerization and the same degree of hindrance, 3.5-fold. The photoprobe having four acetyl groups (E) shows a lesser hindrance, but this fact may be an indirect, not a direct consequence of hydrogen bonding. The more extensive bonding of E with silica hindered already the photoinduced reaction, the trans-to-cis isomerization, so that only ca. one-half of the trans isomer initially present in silica was converted to the cis isomer. Only that half of the total compound E within the glass underwent the thermal conversion back to the trans configuration.

### ***Conclusion***

Specific interaction between the host matrix and the guest molecules may restrict or broaden the applicability of doped sol-gel glasses in chemistry, biochemistry, and materials science. Hydrogen bonding is an important interaction, whose implications are partially explored.

This study shows that sol-gel silica can donate hydrogen atoms to acceptor molecules present in the silica monolith. Hydrogen bonding can cause enormous excess in uptake of hydrogen-bonding solutes from solution and can modulate reactivity of the compounds trapped in glass monoliths. When hydrogen bonding is suppressed, the uptake becomes balanced, and the reactivity becomes normal. These results should caution those who design biosensors and other devices that depend on uptake and other equilibria involving sol-gel

glasses. The same results, however, encourage those who seek new applications of sol-gel glasses as molecular sieves and means for gradual or controlled delivery of substances such as drugs.

**Acknowledgment.** This work was supported by the U.S. National Science Foundation.

### **References**

- (1) Livage, J. *Bull. Mater. Sci.* **1999**, *22*, 201-5.
- (2) Schmid, L.; Rohr, M.; Baiker, A. *Chem. Commun. (Cambridge)* **1999**, 2303-4.
- (3) Gill, I.; Ballesteros, A. *J. Am. Chem. Soc.* **1998**, *120*, 8587-98.
- (4) Wojcik, A. B.; Klein, L. C. *Appl. Organomet. Chem.* **1997**, *11*, 129-35.
- (5) Livage, J. *C. R. Acad. Sci., Ser. II: Mec., Phys., Chim., Astron.* **1996**, *322*, 417-27.
- (6) Avnir, D. *Acc. Chem. Res.* **1995**, *28*, 328-34.
- (7) Reetz, M.; Zonta, A.; Simpelkamp, J. *Angew. Chem., Int. Ed. Engl.* **1995**, *34*, 301-3.
- (8) Avnir, D.; Braun, S.; Lev, O.; Ottolenghi, M. *Chem. Mater.* **1994**, *6*, 1605-14.
- (9) Sanchez, C.; Ribot, F.; Lebeau, B. *J. Mater. Chem.* **1999**, *9*, 35-44.
- (10) Lan, E. H.; Dave, B. C.; Fukuto, J. M.; Dunn, B.; Zink, J. I.; Valentine, J. S. *J. Mater. Chem.* **1999**, *9*, 45-53.
- (11) Gelman, F.; Avnir, D.; Schumann, H.; Blum, J. *J. Mol. Catal. A: Chem.* **1999**, *146*, 123-8.
- (12) Blum, J.; Rosenfeld, A.; Gelman, F.; Schumann, H.; Avnir, D. *J. Mol. Catal. A: Chem.* **1999**, *146*, 117-22.
- (13) Obert, R.; Dave, B. C. *J. Am. Chem. Soc.* **1999**, *121*, 12192-3.

- (14) Husing, N.; Schubert, U. *Angew. Chem., Int. Ed.* **1998**, *37*, 22-45.
- (15) Levy, D.; Del Monte, F.; Oton, J. M.; Fiksdan, G.; Matias, I.; Datta, P.; Lopez-Amo, M. *J. Sol-Gel Sci. Technol.* **1997**, *8*, 931-5.
- (16) Levy, D. *Chem. Mater.* **1997**, *9*, 2666-70.
- (17) Loy, D. A.; Shea, K. J. *Chem. Rev.* **1995**, *95*, 1431-42.
- (18) Reisfeld, R.; Joergensen, C. K. *Struct. Bonding (Berlin)* **1992**, *77*, 207-56.
- (19) Hench, L. L.; West, J. K. *Chem. Rev.* **1990**, *90*, 33-72.
- (20) Rottman, C.; Grader, G.; Hazan, Y. D.; Melchior, S.; Avnir, D. *J. Am. Chem. Soc.* **1999**, *121*, 8533-43.
- (21) Spange, S.; Zimmermann, Y.; Graeser, A. *Chem. Mater.* **1999**, *11*, 3245-51.
- (22) Rao, M. S.; Dave, B. C. *J. Am. Chem. Soc.* **1998**, *120*, 13270-1.
- (23) Dunn, B.; Zink, J. I. *Chem. Mater.* **1997**, *9*, 2280-91.
- (24) Ueda, M.; Kim, H.-B.; Ikeda, T.; Ichimura, K. *J. Mater. Chem.* **1995**, *5*, 889-94.
- (25) Shen, C.; Kostić, N. M. *J. Electroanal. Chem.* **1997**, *438*, 61-5.
- (26) Shen, C.; Kostić, N. M. *J. Am. Chem. Soc.* **1997**, *119*, 1304-12.
- (27) Badjić, J. D.; Kostić, N. M. *Chem. Mater.* **1999**, *11*, 3671-9.
- (28) Joesten, M. D.; Schaad, L. J. *Hydrogen Bonding*; New York : M. Dekker: New York, 1974.
- (29) Etter, M. C. *Acc. Chem. Res.* **1990**, *23*, 120-6.
- (30) Matsui, K.; Nozawa, K.; Yoshida, T. *Bull. Chem. Soc. Jpn.* **1999**, *72*, 591-6.
- (31) Sieminska, L.; Zerda, T. W. *J. Phys. Chem.* **1996**, *100*, 4591-7.
- (32) Nikiel, L.; Zerda, T. W. *J. Phys. Chem.* **1991**, *95*, 4063-9.

- (33) Matsui, K.; Matsuzuka, T.; Fujita, H. *J. Phys. Chem.* **1989**, *93*, 4991-4.
- (34) Yamanaka, S. A.; Nishida, F.; Ellerby, L. M.; Nishida, C. R.; Dunn, B.; Valentine, J. S.; Zink, J. I. *Chem. Mater.* **1992**, *4*, 495-7.
- (35) Cossy, J.; Pale, P. *Tetrahedron Lett.* **1987**, *28*, 6039-40.
- (36) Cimiraglia, R.; Asano, T.; Hofmann, H.-J. *Gazz. Chim. Ital.* **1996**, *126*, 679-84.
- (37) Cimiraglia, R.; Hofmann, H.-J. *Chem. Phys. Lett.* **1994**, *217*, 430-5.
- (38) Kobayashi, S.; Yokoyama, H.; Kamei, H. *Chem. Phys. Lett.* **1987**, *138*, 333-8.
- (39) Nishimura, N.; Tanaka, T.; Sueishi, Y. *J. Chem. Soc., Chem. Commun.* **1985**, 903-4.
- (40) Victor, J. G.; Torkelson, J. M. *Macromolecules* **1987**, *20*, 2241-50.
- (41) Ueda, M.; Kim, H.-B.; Ichimura, K. *Chem. Mater.* **1994**, *6*, 1771-5.
- (42) McCabe, E. T.; Barthel, W. T.; Gertler, S. I.; Hall, S. I. *J. Org. Chem.* **1954**, *19*, 493-8.
- (43) Badger, G. M.; Joshua, C. P.; Lewis, G. E. *Aust. J. Chem.* **1965**, *18*, 1639-44.
- (44) Ulrich, P.; Cerami, A. *J. Med. Chem.* **1984**, *27*, 35-40.
- (45) Gowenlock, B. G.; Pfab, J.; Young, V. M. *J. Chem. Soc., Perkin Trans. 2* **1997**, 1793-8.
- (46) Rosengaus, J.; Willner, I. *J. Chem. Soc., Chem. Commun.* **1993**, 1044-5.
- (47) Wijnen, J. W.; Engberts, J. B. F. N. *J. Org. Chem.* **1997**, *62*, 2039-44.
- (48) Kropp, P. J.; Breton, G. W.; Craig, S. L.; Crawford, S. D.; Durland, W. F., Jr.; Jones, J. E., III; Raleigh, J. S. *J. Org. Chem.* **1995**, *60*, 4146-52.
- (49) Lewis, F. D.; Stern, C. L.; Yoon, B. A. *J. Am. Chem. Soc.* **1992**, *114*, 3131-3.
- (50) Ruetten, S. A. *J. Phys. Chem. B* **1999**, *103*, 9285-94.
- (51) Patai, S.; Editor *The Chemistry of the Carbon-Halogen Bond, Pts. 1 and 2*, 1973, pp 1215 pp.



- (52) Nakagaki, R.; Aoyama, I.; Shimizu, K.; Akagi, M. *J. Phys. Org. Chem.* **1993**, *6*, 261-72.
- (53) Pal, T. K.; Mallik, G. K.; Laha, S.; Chatterjee, K.; Ganguly, T.; Banerjee, S. B. *Spectrochim. Acta, Part A* **1987**, *43A*, 853-9.
- (54) Suppan, P. *J. Photochem. Photobiol., A* **1990**, *50*, 293-330.
- (55) Cumper, C. W. N.; Singleton, A. *J. Chem. Soc., B* **1968**, 649-51.
- (56) Grebenkin, S. Y.; Bol'shakov, B. V. *J. Photochem. Photobiol., A* **1999**, *122*, 205-9.
- (57) Mita, I.; Horie, K.; Hirao, K. *Macromolecules* **1989**, *22*, 558-63.
- (58) Paik, C. S.; Morawetz, H. *Macromolecules* **1972**, *5*, 171-7.
- (59) Ueda, M.; Kim, H. B.; Ikeda, T.; Ichimura, K. *Chem. Mater.* **1992**, *4*, 1229-33.
- (60) Ueda, M.; Kim, H.-B.; Ikeda, T.; Ichimura, K. *J. Non-Cryst. Solids* **1993**, *163*, 125-32.
- (61) Bunce, N. J.; Ferguson, G.; Forber, C. L.; Stachnyk, G. J. *J. Org. Chem.* **1987**, *52*, 394-8.
- (62) Asano, T.; Okada, T. *J. Org. Chem.* **1984**, *49*, 4387-91.
- (63) Nishimura, N.; Kosako, S.; Sueishi, Y. *Bull. Chem. Soc. Jpn.* **1984**, *57*, 1617-25.
- (64) Grebenkin, S. Y.; Bol'shakov, B. V. *Chem. Phys.* **1998**, *234*, 239-48.
- (65) Gardlund, Z. G. *J. Polym. Sci., Polym. Lett. Ed.* **1968**, *6*, 57-61.
- (66) Sung, C. S. P.; Lamarre, L.; Chung, K. H. *Macromolecules* **1981**, *14*, 1839-41.
- (67) Lamarre, L.; Sung, C. S. P. *Macromolecules* **1983**, *16*, 1729-36.
- (68) Kryszewski, M.; Nadolski, B.; North, A. M.; Pethrick, R. A. *J. Chem. Soc., Faraday Trans. 2* **1980**, *76*, 351-68.
- (69) Priest, W. J.; Sifain, M. M. *J. Polym. Sci., Part A-1* **1971**, *9*, 3161-8.

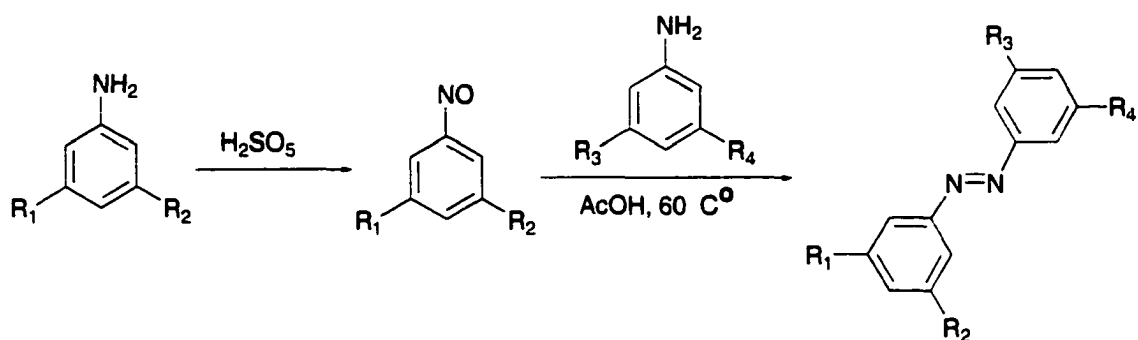
(70) King, N. R.; Whale, E. A.; Davis, F. J.; Gilbert, A.; Mitchell, G. R. *J. Mater. Chem.* **1997**, *7*, 625-30.

(71) Siampiringue, N.; Guyot, G.; Monti, S.; Bortolus, P. *J. Photochem.* **1987**, *37*, 185-8.

(72) Nishimura, N.; Sueyoshi, T.; Yamanaka, H.; Imai, E.; Yamamoto, S.; Hasegawa, S. *Bull. Chem. Soc. Jpn.* **1976**, *49*, 1381-7.

(73) Whitten, D. G.; Wildes, P. D.; Pacifici, J. G.; Irick, G., Jr. *J. Amer. Chem. Soc.* **1971**, *93*, 2004-8.

Scheme 1



symbol	R <sub>1</sub>	R <sub>2</sub>	R <sub>3</sub>	R <sub>4</sub>
B	H	H	CH <sub>3</sub> CO	H
C	CH <sub>3</sub> CO	H	CH <sub>3</sub> CO	H
D <sup>44</sup>	H	H	CH <sub>3</sub> CO	CH <sub>3</sub> CO
E	CH <sub>3</sub> CO	CH <sub>3</sub> CO	CH <sub>3</sub> CO	CH <sub>3</sub> CO

**Table 1.** Estimated volume needed for thermal (cis-to-trans) isomerization of five azobenzene derivatives and first-order rate constants  $k_2$  in the absence of hydrogen bonding in solution and inside sol-gel silica glass. the solvent in both cases is a 9 : 1 v/v mixture of  $\text{CCl}_4$  and DMF.

compound	symbol	volume, $\text{\AA}^3$	$10^3 k_2, \text{min}^{-1}$	
			in solution	in silica
3,3'-dimethyl azobenzene	A	334	$3.02 \pm 0.02$	$2.73 \pm 0.02$
3-acetyl azobenzene	B	392	$1.72 \pm 0.02$	$1.56 \pm 0.01$
3,3'-diacetyl azobenzene	C	425	$1.21 \pm 0.01$	$1.29 \pm 0.01$
3,5-diacetyl azobenzene	D	462	$2.10 \pm 0.08$	$1.80 \pm 0.03$
3,3',5,5'-tetraacetyl azobenzene	E	505	$0.78 \pm 0.02$	$0.78 \pm 0.02$

**Table 2.** Percentage of the cis isomer in the photostationary state reached in trans-to-cis isomerization of five azobenzene derivatives in solution and inside sol-gel silica glass when hydrogen bonding between these derivatives and silica is absent and present.

compound	symbol	in solution <sup>a</sup>	in silica	
			without H-bonding <sup>b</sup>	with H-bonding <sup>c</sup>
3,3'-dimethyl azobenzene	A	92 ± 4	92 ± 4	80 ± 4
3-acetyl azobenzene	B	89 ± 4	89 ± 4	82 ± 4
3,3'-diacetyl azobenzene	C	78 ± 4	82 ± 4	75 ± 4
3,5-diacetyl azobenzene	D	70 ± 4	70 ± 4	68 ± 4
3,3',5,5'-tetraacetyl azobenzene	E	49 ± 3	48 ± 3	19 ± 2

<sup>a</sup> Solvent is CCl<sub>4</sub>

<sup>b</sup> Solvent is a 9 : 1 v/v mixture of CCl<sub>4</sub> and DMF

<sup>c</sup> Solvent is CCl<sub>4</sub>

**Table 3.** First-order rate constants  $k_2$  and their ratio for thermal (cis-to-trans) isomerization of four azobenzene derivatives in solution and inside sol-gel silica glass when hydrogen bonding between azobenzene and silica is present. The solvent in both cases is  $\text{CCl}_4$ .

compound	symbol	$10^3 k_2, \text{min}^{-1}$		$k_2^{\text{solution}}/k_2^{\text{silica}}$
		in solution	in silica	
3,3'-diacetyl azobenzene	C	$1.63 \pm 0.02$	$0.46 \pm 0.02$	3.5
3,5-diacetyl azobenzene	D	$2.09 \pm 0.08$	$0.60 \pm 0.02$	3.5
3,3',5,5'- tetraacetyl azobenzene	E	$0.83 \pm 0.02$	$0.41 \pm 0.02$	2.0

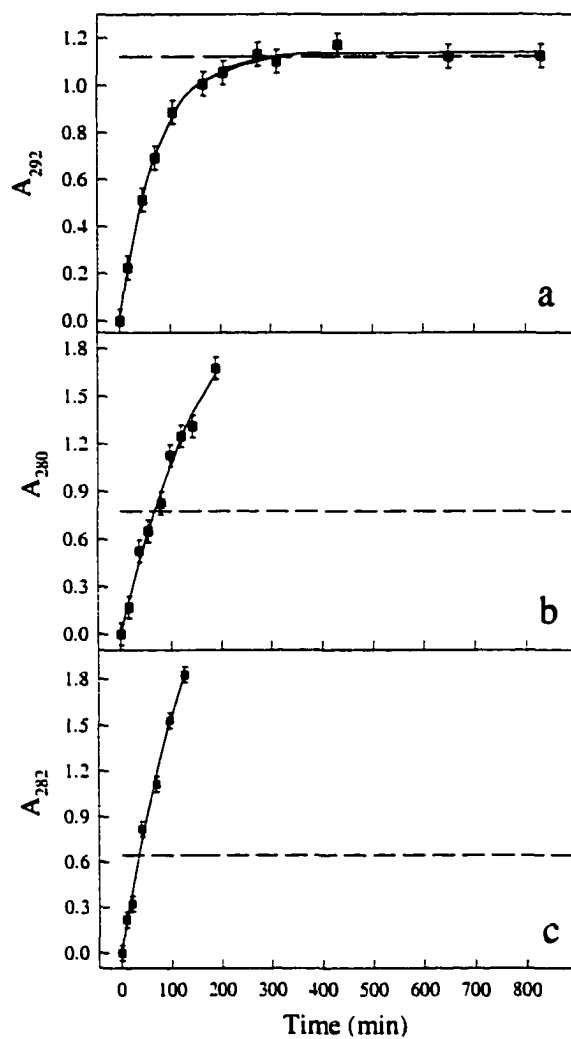


**Figure 1.** Uptake of (a) styrene, (b) aniline, and (c)  $N,N$ -diethyl- $p$ -anisidine by sol-gel silica glass when it is capable of hydrogen bonding to the guest compounds. Glass monolith sized 8 x 8 x 27 mm is soaked in 50.0 mL solution of each solute in  $\text{CCl}_4$ . As the guest enters, its absorbance in the glass increases. The dashed line marks the absorbance of the external solution. Uptake is balanced in (a) and excessive in (b) and (c).

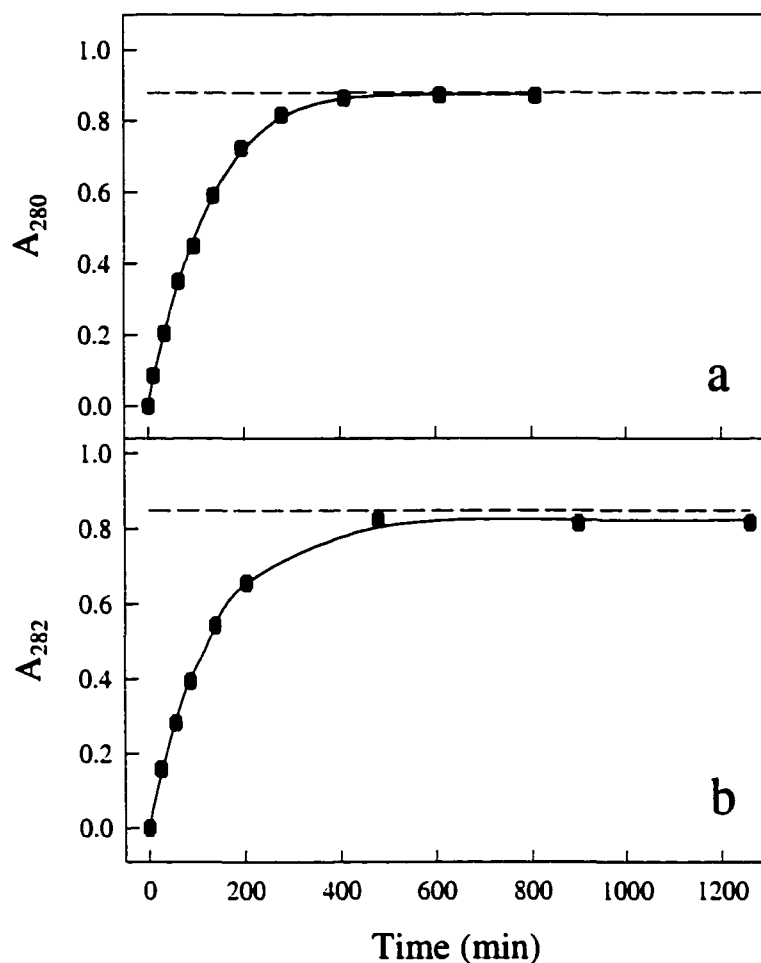


**Figure 2.** Uptake of (a) aniline, and (b) *N,N*-diethyl-*p*-anisidine by sol-gel silica glass when it is incapable of hydrogen bonding to the guest compounds. Glass monolith sized 8 x 8 x 27 mm is soaked in 50.0 mL of a 9 : 1 v/v mixture of CCl<sub>4</sub> and DMF; the latter solvents prevents hydrogen bonding between silica and the guest. As the guest enters, its absorbance in the glass increases. The dashed line marks the absorbance of the external solution. Uptake is balanced in both cases.



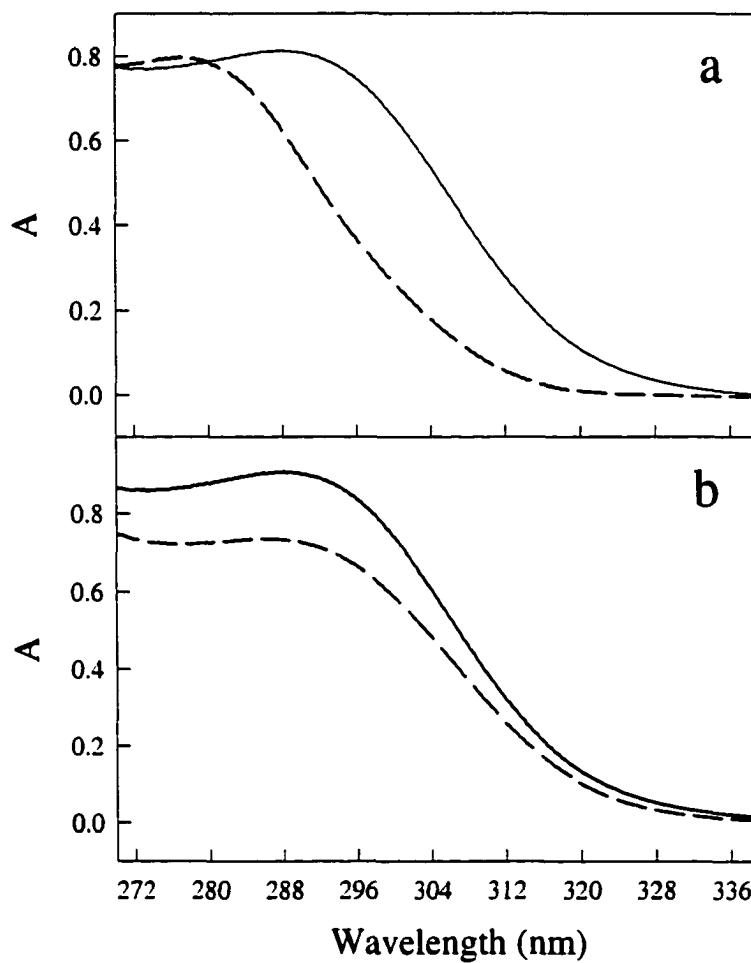


**Figure 3.** Absorption spectra of aniline in solution (solid line) and inside sol-gel silica glass (dashed line). The solvent is (a)  $\text{CCl}_4$  and (b) a 9 : 1 v/v mixture of  $\text{CCl}_4$  and DMF. Note the large blue shift in (a) as aniline enters the glass from the solution. Hydrogen bonding between aniline and silica is present in (a) and absent in (b).

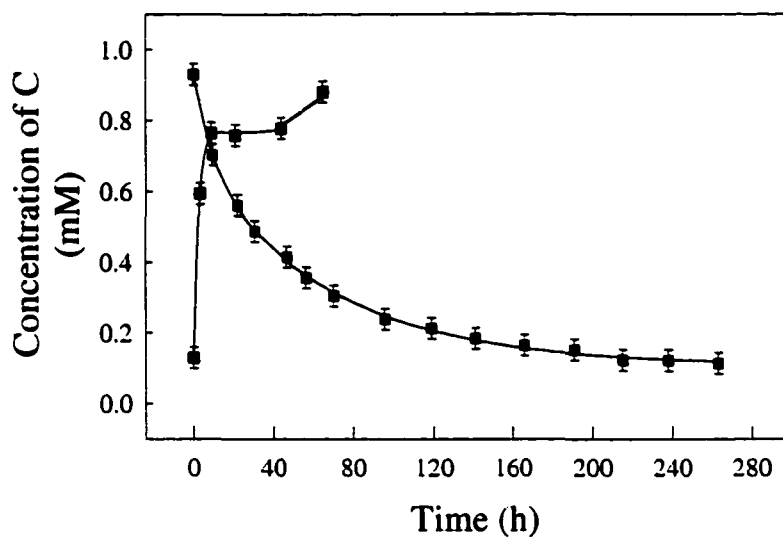


**Figure 4.** Uptake (the downward plot) and release (the upward plot) of *trans*-3,3'-diacetyl azobenzene (designated C) by sol-gel silica glass, followed by the UV spectrophotometry of C in the external solution. The glass monolith sized 8 x 8 x 27 mm was soaked in 200.0 mL of a stirred  $9.30 \cdot 10^{-4}$  M solution of C in  $\text{CCl}_4$ . For release, 20 mL of DMF was added to the external solution.

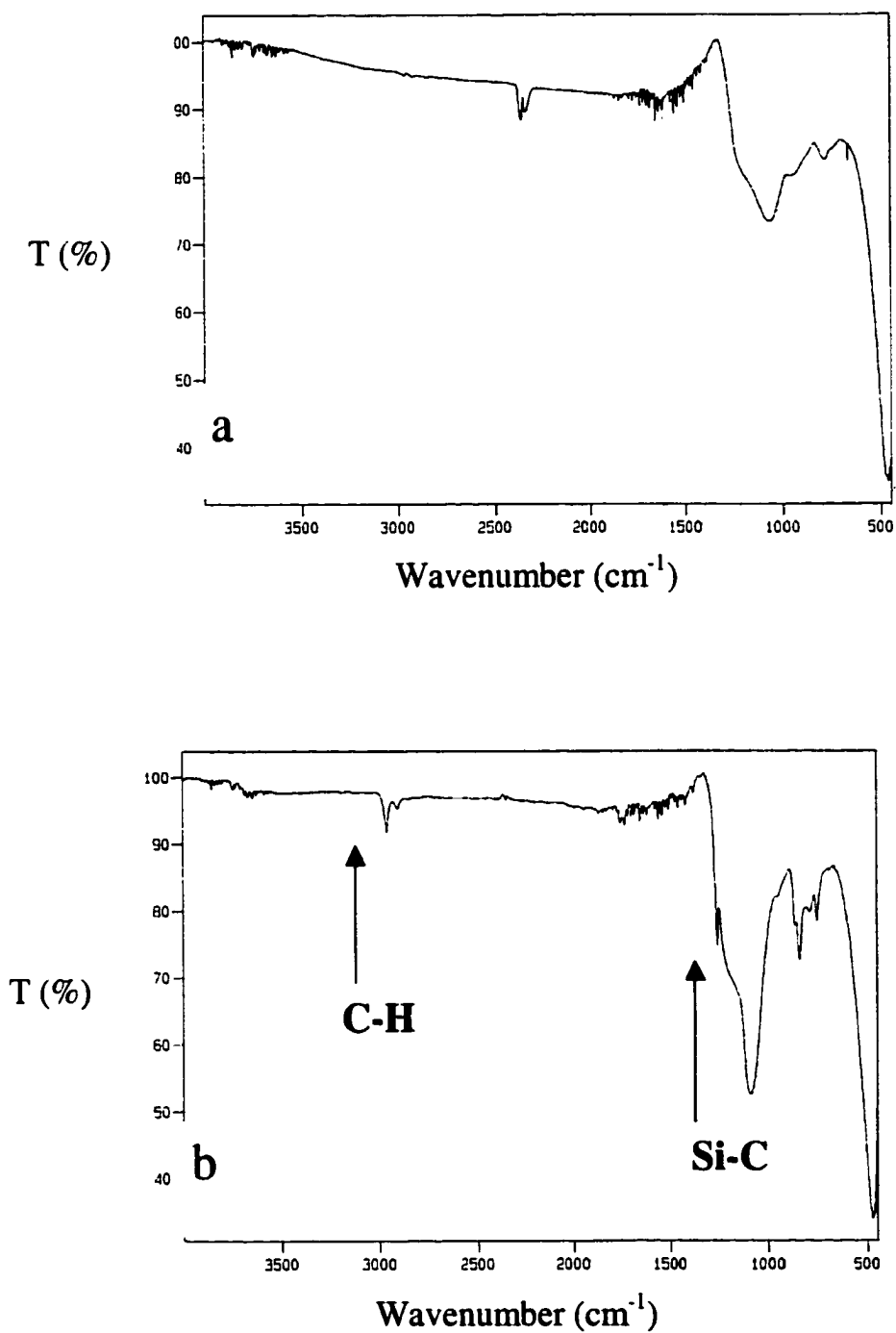


**Figure 5.** Infrared spectra of pulverized sol-gel silica monoliths (a) before and (b) after treatment with hexamethyldisilazane. The highlighted bands in (b) are characteristic of the Si(CH<sub>3</sub>)<sub>3</sub> groups.

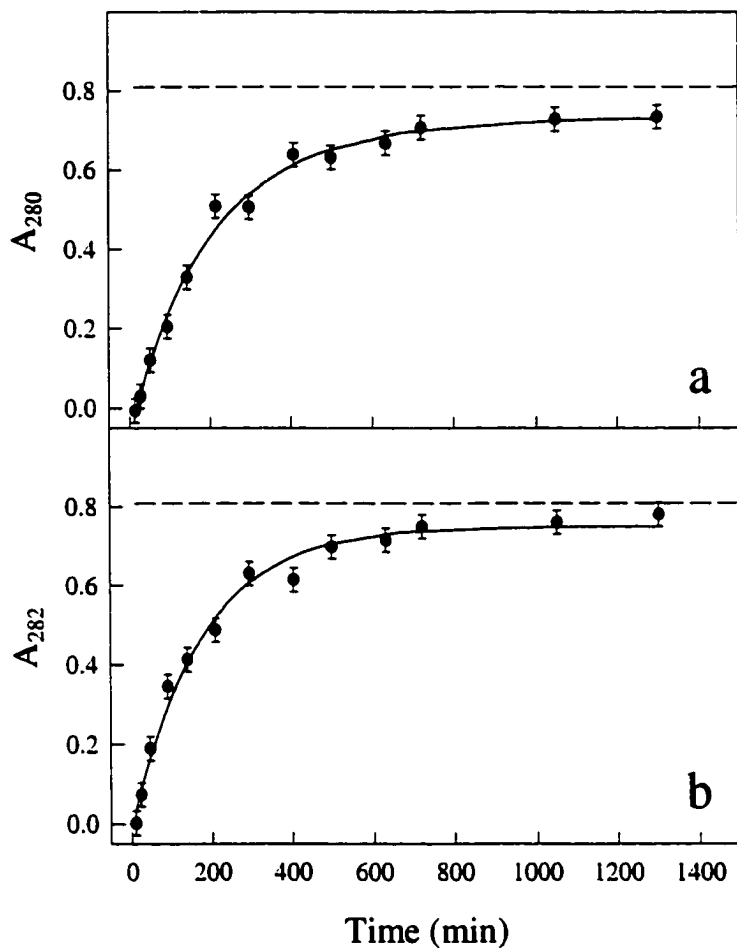


**Figure 6.** Uptake of (a) aniline and (b)  $N,N$ -diethyl- $p$ -anisidine by sol-gel silica glass chemically modified with  $\text{Si}(\text{CH}_3)_3$  groups, which preclude hydrogen bonding between the guest compounds and silica. For conditions, see caption to Figure 1.

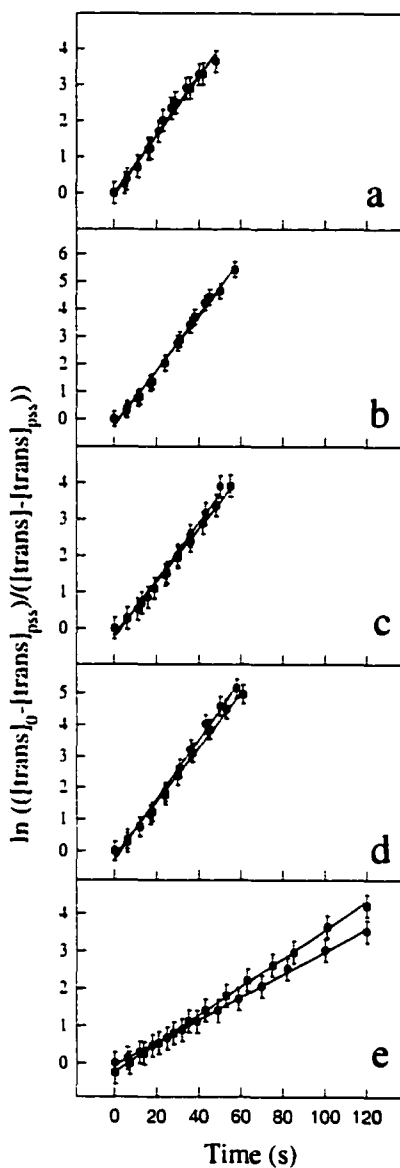


**Figure 7.** Kinetics of photoinduced (trans-to-cis) isomerization of (a) 3,3'-dimethyl azobenzene, designated A, (b) 3-acetyl azobenzene, designated B, (c) 3,3'-diacetyl azobenzene, designated C, (d) 3,5-diacetyl azobenzene, designated D, and (e) 3,3',5,5'-tetraacetyl azobenzene, designated E, in solution (■) and inside sol-gel silica glass (●) when hydrogen bonding between the azobenzene derivatives and silica is suppressed. The solvent in all experiments was a 9 : 1 v/v mixture of  $\text{CCl}_4$  and DMF; the latter component makes hydrogen bonds to silica. Solid lines are fittings to first-order rate law.

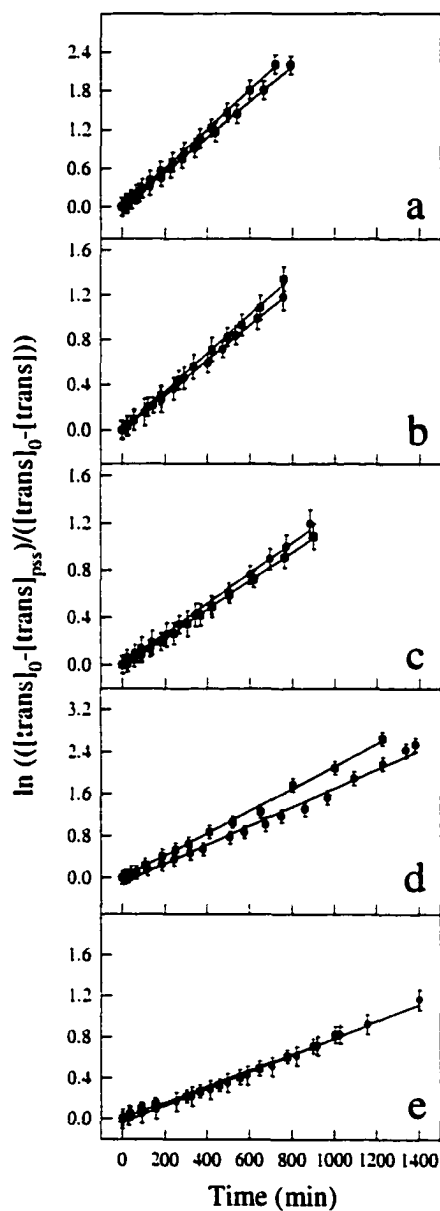


**Figure 8.** Thermal (cis-to-trans) isomerization of (a) 3,3'-dimethyl azobenzene, designated A, (b) 3-acetyl azobenzene, designated B, (c) 3,3'-diacetyl azobenzene, designated C, (d) 3,5-diacetyl azobenzene, designated D, and (e) 3,3',5,5'-tetracetyl azobenzene, designated E, in solution (■) and inside sol-gel silica glass (●) when hydrogen bonding between the azobenzene derivatives and silica is suppressed. The solvent in all experiments was a 9 : 1 v/v mixture of CCl<sub>4</sub> and DMF; the latter component makes hydrogen bonds to silica. Solid lines are fittings to first-order rate law.

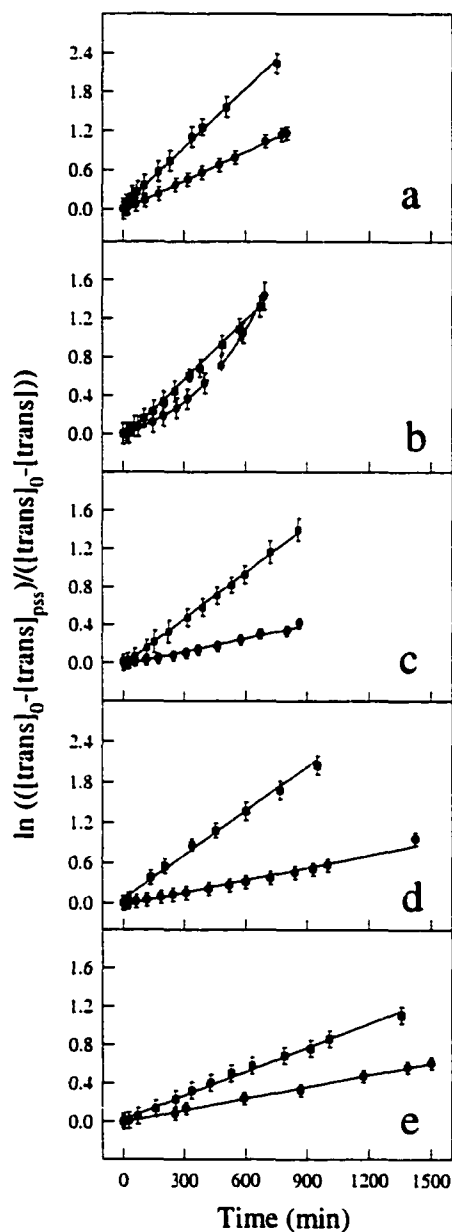


**Figure 9.** Thermal (cis-to-trans) isomerization of (a) 3,3'-dimethyl azobenzene, designated A, (b) 3-acetyl azobenzene, designated B, (c) 3,3'-diacetyl azobenzene, designated C, (d) 3,5-diacetyl azobenzene, designated D, and (e) 3,3',5,5'-tetracetyl azobenzene, designated E, in solution (■) and inside sol-gel silica glass (●) when hydrogen bonding between the azobenzene derivatives and silica is present. The solvent in all experiments was  $\text{CCl}_4$ . Solid lines are fittings to first-order rate law.

**APPENDIX 2**



**Table S1.** Ultraviolet absorptivities of trans and cis isomers of azobenzene derivatives.

compound	symbol	wavelength (nm)	$\epsilon$ trans ( $M^{-1}cm^{-1}$ )	
			trans	cis
3,3'-dimethyl azobenzene	A	324.6	21474	1317
3-acetyl azobenzene	B	320.0	19516	1931
3,3'-diacetyl azobenzene	C	320.0	19354	2012
3,5-diacetyl azobenzene	D	319.0	20243	1006
3,3',5,5'-tetraacetyl azobenzene	E	314.0	16896	2623

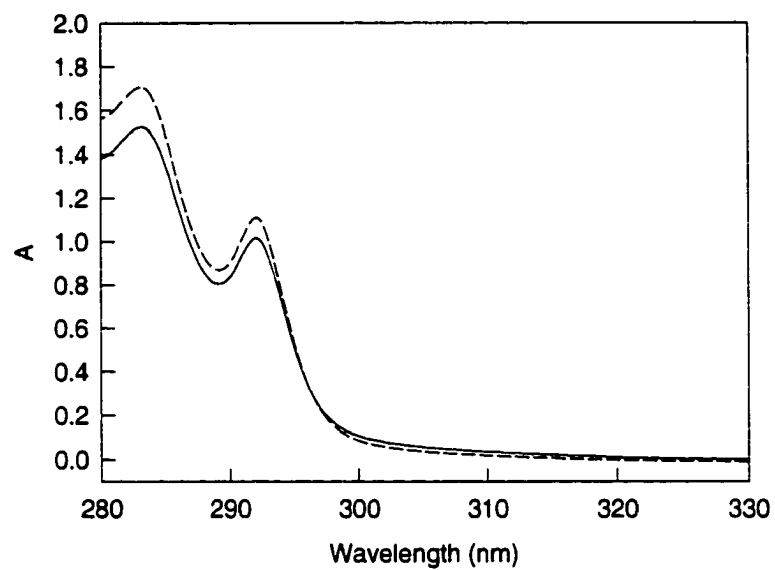


**Figure S1.** Absorption spectrum of styrene in solution (solid line) and inside sol-gel silica glass (dashed line). In both cases solvent was in  $\text{CCl}_4$ . Lack of perturbation of the spectrum is evidence against hydrogen bonding between styrene and silica.

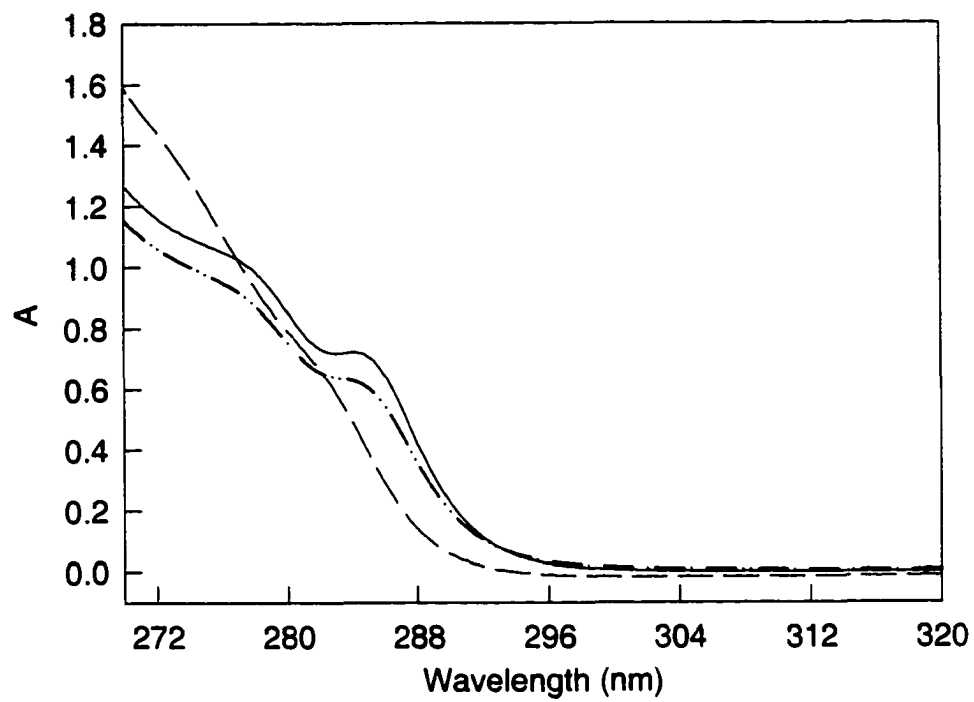


**Figure S2.** Absorption spectra of *N,N*-diethyl-*p*-anisidine in solution (dash-dotted line) and inside sol-gel silica glass (solid line), in both cases in a 9 : 1 v/v mixture of CCl<sub>4</sub> and DMF, and inside sol-gel silica glass in CCl<sub>4</sub> (dashed line).

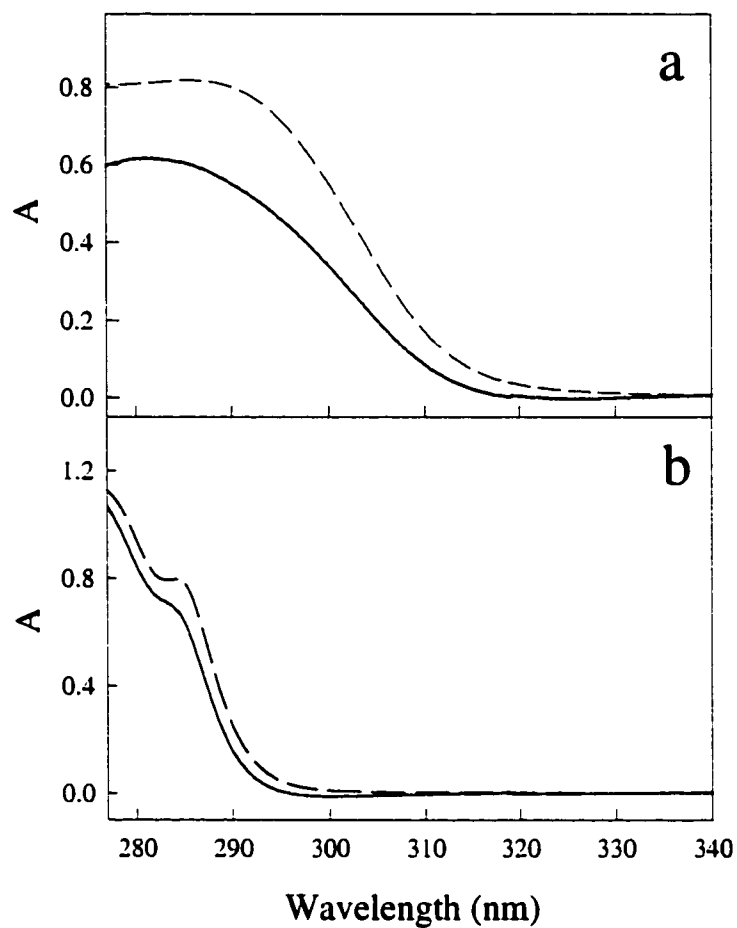


**Figure S3.** Absorption spectra a compound in solution (dashed line) and inside trimethylsilylated sol-gel silica glass (solid line); in both cases the solvent is  $\text{CCl}_4$ . The compound is (a) aniline and (b) *N,N*-diethyl-*p*-anisidine.

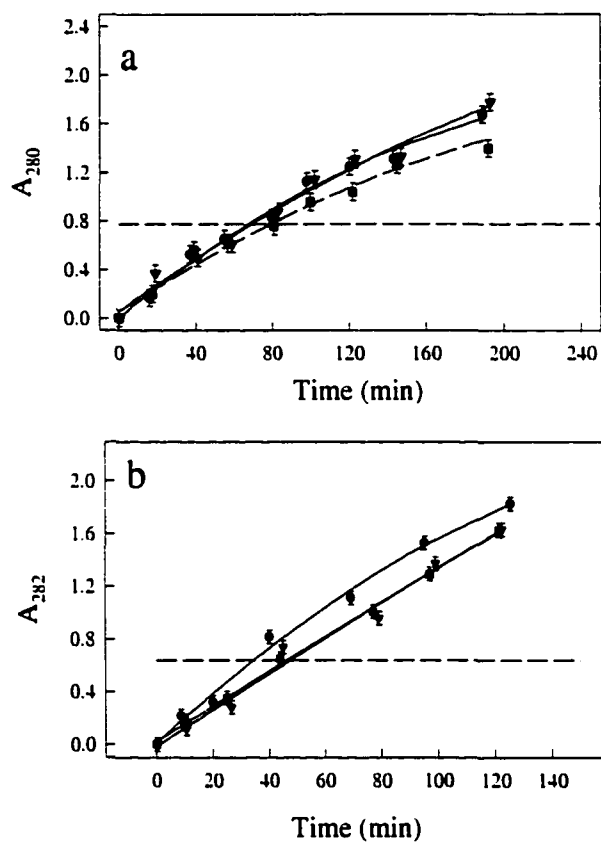


**Figure S4.** Uptake of (a) aniline and (b)  $N,N$ -diethyl- $p$ -anisidine by sol-gel silica glass when it is capable of hydrogen bonding to the guest compounds. The silica glass before the uptake experiments was treated with HCl ( $\blacktriangledown$ ), NaOH ( $\blacksquare$ ), or neither compound ( $\bullet$ ). Glass monolith sized 8 x 8 x 27 mm is soaked in 50.0 mL solution of each solute in  $\text{CCl}_4$ . The dashed line marks the absorbance of the external solution.

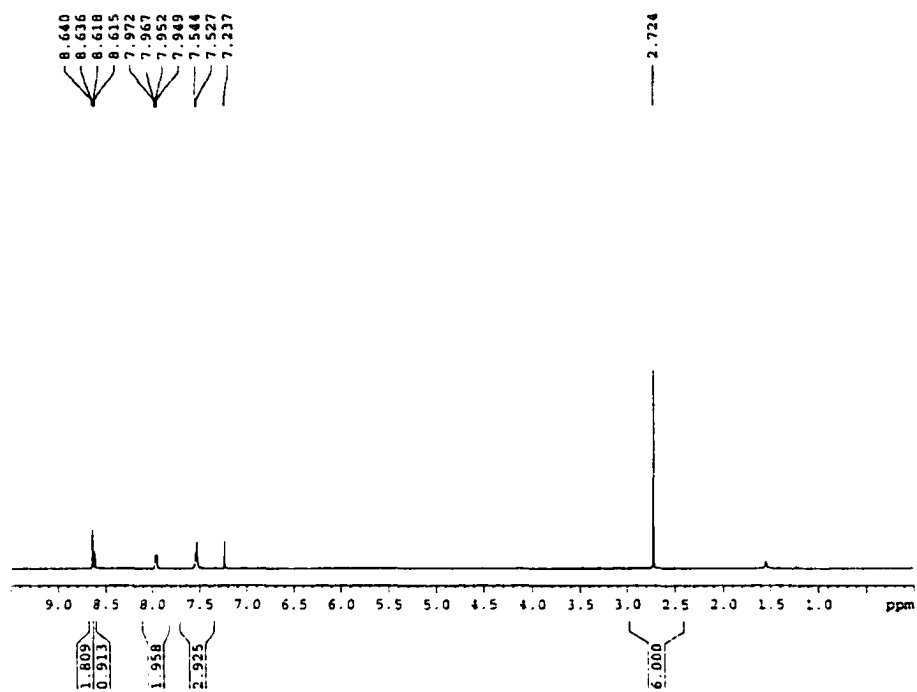


**Figure S5.**  $^1\text{H}$  NMR spectrum of 3,5-diacetyl azobenzene in  $\text{CDCl}_3$ .

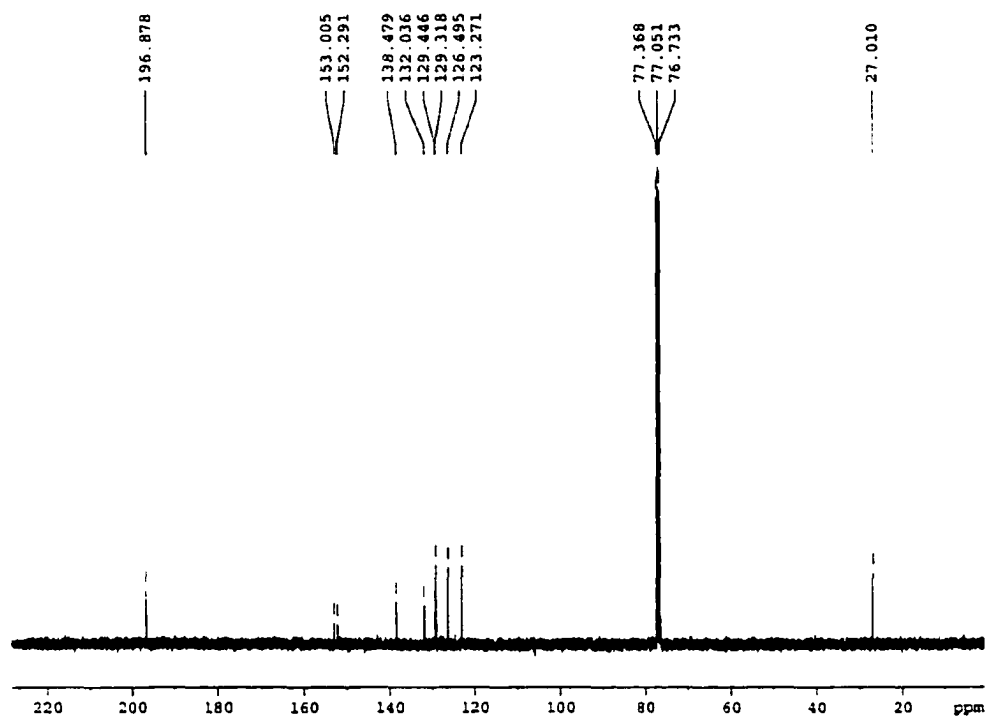


**Figure S6.**  $^{13}\text{C}$  NMR spectrum of 3,5-diacetyl azobenzene in  $\text{CDCl}_3$ .

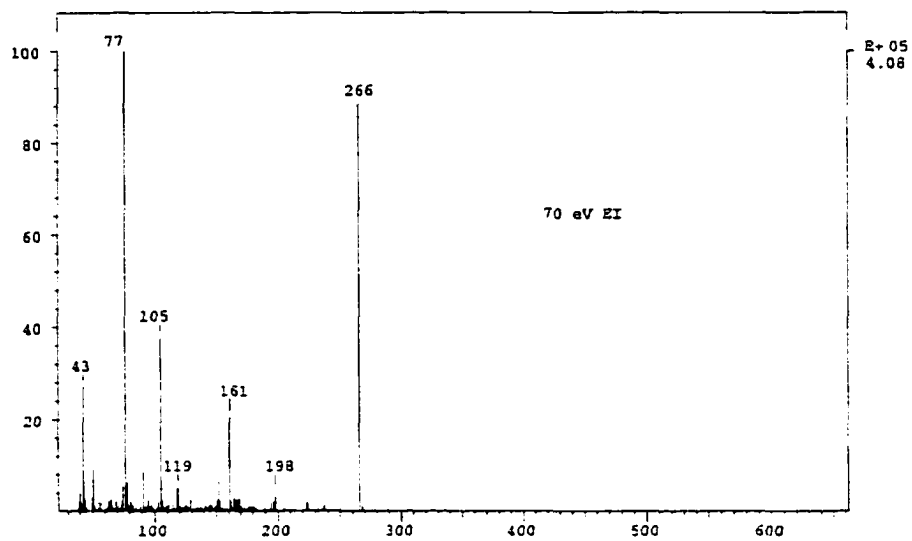


**Figure S7.** Low-resolution mass spectrum (CI) of 3,5-diacetyl azobenzene.



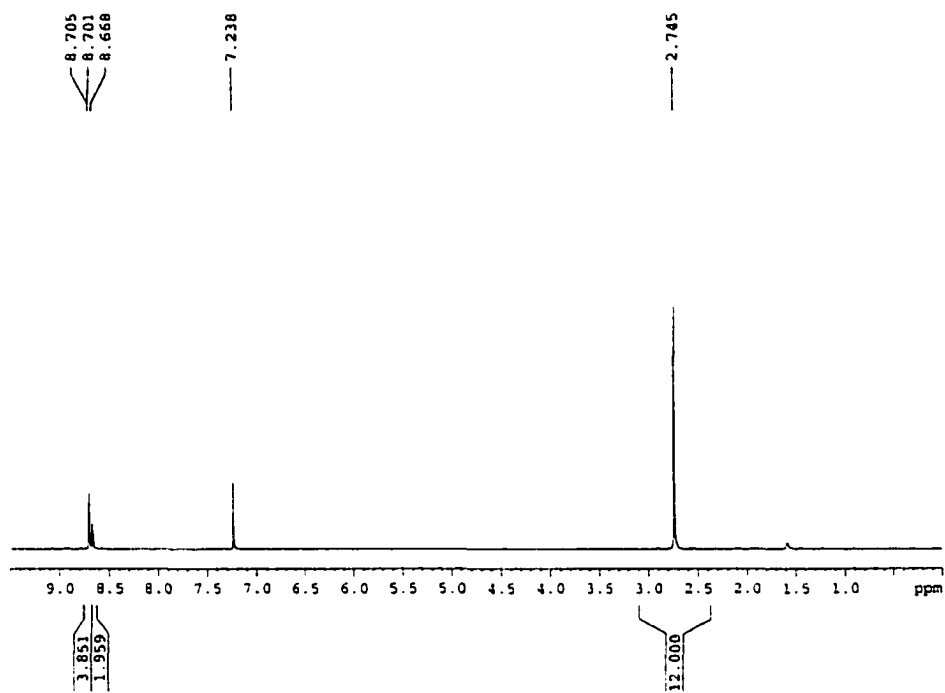


**Figure S8.**  $^1\text{H}$  NMR of 3,3',5,5'-tetraacetyl azobenzene spectrum in  $\text{CDCl}_3$ .

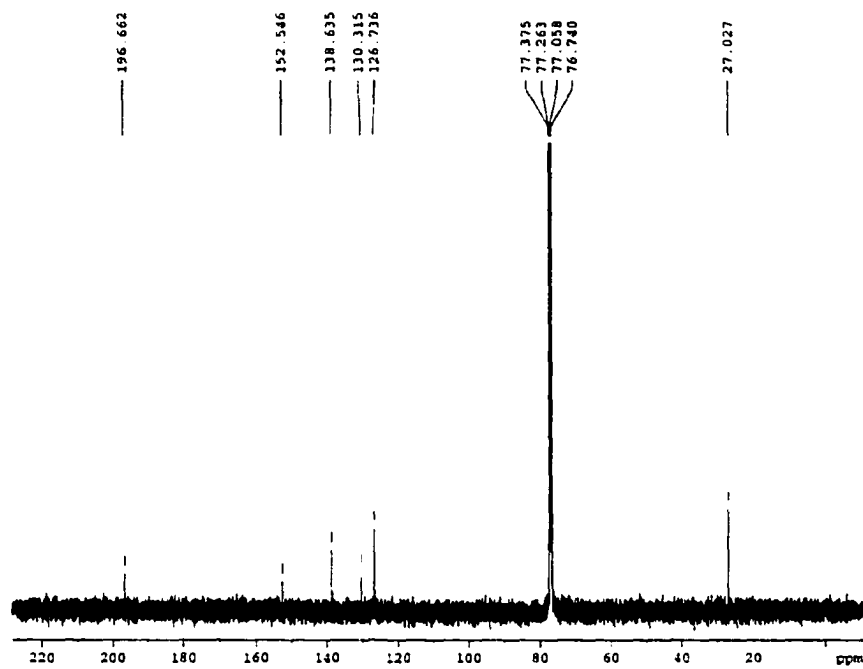


**Figure S9.** <sup>13</sup>C NMR of 3,3',5,5'-tetraacetyl azobenzene in CDCl<sub>3</sub>.

**CHAPTER 4. UNEXPECTED INTERACTIONS BETWEEN SOL-GEL SILICA GLASS AND GUEST MOLECULES. EXTRACTION OF AROMATIC HYDROCARBONS INTO POLAR SILICA FROM HYDROPHOBIC SOLVENTS**

A paper published in and reprinted from

*Journal of Physical Chemistry B* **2000**, *104*, 11081-11087

Copyright 2000 American Chemical Society

Jovica D. Badjić and Nenad M. Kostić

***Abstract***

Properties of a solute may differ greatly between a free solution and that solution confined in pores of a sol-gel glass. We studied the entry of various aromatic organic compounds from solution into the monolith of sol-gel silica immersed in this solution. Partitioning of the solute is quantified by the uptake coefficient, the ratio of its concentrations in the glass and in the surrounding solution at equilibrium. The dependence of this coefficient on the solvent gives insight into possible interactions between the solute and the silica matrix. We report the uptake of 31 compounds altogether: 18 halogen derivatives of benzene; 5 condensed (fused) aromatics; and stilbene and three substituted derivatives of it, each in both *cis* and *trans* configurations. When the solvent is hexane, the uptake coefficients are as follows: 1.0 – 1.9 for the halobenzenes; 3.0 – 4.6 for the hydrocarbons; and 3.3 – 4.9 for the

stilbenes. When the solvent is carbon tetrachloride or dichloromethane, the uptake coefficient become 0.82 – 1.39 for the hydrocarbons and 0.90 – 1.25 for the stilbenes. The excessive uptake of organic compounds from hexane is unexpected for it amounts to extraction of nonpolar or slightly polar solutes from a nonpolar solvent to a polar interior of silica glass. The solute-silica interactions responsible for this extraction are not of van der Waals type. Our findings are consistent with hydrogen bonding between the aromatic  $\pi$  system in the solutes and the hydroxyl groups on the silica surface. Hexane cannot interact with this surface but dichloromethane and carbon tetrachloride can, shielding the hydroxyl groups from the organic solvents and thus suppressing the hydrogen bonding. This explanation is supported by the emission spectra of the aromatic compound pyrene when it is dissolved in acetonitrile, dichloromethane, cyclohexyl chloride, and hexane and when it is taken up by monoliths of sol-gel silica from these four solutions. The relative intensities of the emission bands designated III and I change greatly when pyrene is taken up from hexane but remain unchanged when it is taken up from the other three solvents. Evidently, hexane does not, whereas the other three solvents do, line the silica surface and shield it from approach by pyrene molecules. Even though solute molecules are much smaller than the pores in the sol-gel glass, diffusion of these molecules into the monolith may result in an uneven partitioning at equilibrium. This fact must be taken into consideration in the design of biosensors, immobilized catalysts, and other composite materials because their function depends on entry of analytes, substrates, and other chemicals into the glass matrix.

## ***Introduction***

The preparation of glasses by the sol-gel method is very useful in many branches of chemistry and materials science. Mild reaction conditions allow encapsulation of various organic, inorganic, and biological compounds into porous and transparent matrices.<sup>1-6</sup> Because physical and chemical properties of the doped glasses can be altered by varying the experimental conditions during the preparation process, this method can be used for the fabrication of sensors, catalyst supports, coatings, special polymers, and other new materials.<sup>7-14</sup>

The guest compounds can be encapsulated in silica as this matrix is being formed, or they can be diffused into the preformed glass from solution. The interactions at the molecular level between the glass matrix and the guest molecules may change the physical and chemical properties of the confined molecules. Understanding and control of these interactions is essential for purposeful design of doped sol-gel materials having desired properties.<sup>15-19</sup>

Work in our laboratory has shown that interactions between the silica matrix on the one side and proteins, metal complexes, and organic compounds on the other can change mobility and chemical reactivity of these guests.<sup>20-23</sup> After studies of electrostatic interactions and of classical hydrogen bonding involving heteroatoms,<sup>20</sup> we turn our attention to even subtler and weaker forces, such as van der Waals interactions and non-classical hydrogen bonding. These interactions of the guests with the sol-gel host surface may change the reaction rate inside the porous host, availability of the immobilized molecules to the guests, and chemical equilibria inside the silica matrix. The interactions are

important because they may affect properties and performance of biosensors, immobilized catalysts, and other composite materials.

### ***Experimental Procedures***

**Instrumentation.** Proton,  $^{19}\text{F}$ , and  $^{13}\text{C}$  NMR spectra were recorded with a Varian 400 MHz instrument; UV absorption spectra, with a Perkin-Elmer Lambda 18 spectrophotometer; and emission spectra, with a Jobin Yvon Fluoromax-2 fluorimeter.

**Chemicals.** Tetramethyl orthosilicate, acetonitrile, dichloromethane, and hexane were purchased from Fisher Chemical Co.; carbon tetrachloride, naphthalene, cyclohexyl chloride, 2,7-di-*tert*-butylnaphthalene, 4-methylbenzyl bromide, 2',4',6'-trimethylacetophenone, triphenylphosphine, carbon tetrabromide, 18-crown-6, and anthracene, from Aldrich Chemical Co.; pyrene, azulene, *trans*- and *cis*-stilbene, from Fluka Chemical Co.; and 3,4,5-trifluorobenzaldehyde, from Oakwood Products Inc. Distilled water was further demineralized to a resistivity greater than 17 M $\Omega$  cm.

**Hazards.** Aromatic compounds used in our study are either toxic or carcinogenic. Protective gloves and effective fume hood must be used in experiments with these compounds!

**Preparation of Silica Monoliths.** The silica sol was prepared by a standard procedure.<sup>24</sup> A mixture of 15.76 g of tetramethyl orthosilicate, 3.38 g of water, and 0.30 g of 0.040 M HCl was kept in an ice-cooled ultrasonic bath for 30 min. Upon addition of 36.3 mL of a 10 mM sodium phosphate buffer having pH 7.00, gelation began. The sol was quickly poured into polystyrene cuvettes sized 10 x 10 x 40 mm and left at 4 °C. During the aging for

14 days, the monoliths were kept soaked and were washed with water twice a day. The aged monoliths were exposed to air, still at 4 °C, for another 14 days of partial drying and shrinking. The resulting transparent monoliths, prisms sized 8 x 8 x 27 mm, were soaked in acetonitrile and stored at 4 °C for further use. Defective monoliths and those deviating from the standard dimensions were rejected, for the sake of reproducibility and accuracy of the experiments.

**Dehydration of Silica Monoliths.** Two silica monoliths sized 8 x 8 x 27 mm were soaked together in a series of stirred solvents, in a capped Erlenmeyer flask. The first soaking was in 300 mL of acetonitrile, which was changed three times, after 2, 24, and 48 h; the last soaking lasted for an additional 24 h. Second, in 150 mL of carbon tetrachloride, which was changed after 24 h, and the soaking continued for an additional 24 h. Third, in 300 mL of hexane, which was changed three times, after 2, 24, and 48; the last soaking lasted for an additional 24 h. In one series of experiments, the third step (instead of hexane) was 150 mL of cyclohexyl chloride, which was changed after 24 h. and the soaking continued for an additional 24 h. In another series of experiments, two monoliths were similarly soaked first in 300 mL of acetonitrile, as above, and then in 300 mL of dichloromethane, which was replaced three times, after 2, 24, and 48 h. In all experiments the Erlenmeyer flasks were chosen according to the solvent volume and were capped, to protect the dry solvents from the moist air. Dehydrated silica monoliths were stored for further experiments in a fresh portion of the solvent in which they had been soaked last.

**General Procedure for Uptake Experiments.** The concentration of each guest compound in stock solution was  $1.8 \cdot 10^{-5}$  M. The dehydrated silica monoliths sized 8 x 8 x

27 mm were the hosts. Each monolith was soaked in 50.0 mL of a stock solution in a capped vial. The monolith stood upright, with one of its small sides resting on the flat bottom of the vial and with the other five sides exposed to the solution. From time to time the monolith (without the surrounding solution) would be transferred to quartz cuvette sized 10 x 10 x 40 mm, kept in the sample holder of the spectrophotometer. An identical but undoped silica monolith made in the same batch as the doped monolith would be placed in another quartz cuvette, kept in the reference holder. Each monolith would be held in the same place and in the same position in all experiments, so that their absorbances could be accurately compared. The UV spectra would be scanned at the rate of 120 nm/min, and the doped monolith would be returned to the solution of the guest compound (the dopant) and soaked further.

Ultraviolet-visible spectra of different undoped monoliths prepared in the same batch were identical. Moreover, UV-vis spectra of doped monoliths did not change when different undoped monoliths from the same batch were kept in the reference beam of the spectrophotometer. The UV measurements were more frequent early in the experiment, while the uptake was relatively fast, and less frequent later, when the uptake slowed down. The uptake was considered finished when the absorbance of the guest in the silica monolith ceased to change in time.

**Uptake Coefficients.** We define the uptake coefficient as the ratio at equilibrium of the guest concentrations in the glass (internal) and the surrounding solution (external) at the end of the uptake process. The external concentration was kept nearly constant during the uptake. To correct the absorbance for the path length, the raw ratio is divided by the width of the monolith, determined with the caliper. This final number is the uptake coefficient that we



report. The standard deviation of all the absorbance ratios between the internal and external guests population taken at every 0.2 nm over the UV-vis spectral range examined constitutes the error margins in tables of uptake coefficients. Since these coefficients may depend on the external concentration of the guest, we kept that constant, at  $1.8 \cdot 10^{-5}$  M. This concentration gave absorbances in the range of the greatest photometric accuracy. We avoided low or high absorbances because of the inherent accuracy in their recording. With stilbene as the guest, we varied the concentration while keeping the stilbene absorbance in the accurate range and found only small variations (less than 20 %) in the uptake coefficients.

**General Procedure for Fluorescence Experiments.** Steady-state fluorescence spectra of pyrene were recorded both in solution and in the sol-gel silica monolith. The excitation was at 330 nm, and each spectrum was an average of three scans. The ratio of emission intensities at 383.2 nm (band III) and 371.8 nm (band I) is the III/I quotient.

A  $1.0 \cdot 10^{-5}$  M aqueous stock solution of pyrene in a 100-mL volumetric flask was purged with nitrogen for 10 minutes, and a 2.5-mL aliquot was transferred to a 10-mm fluorescence cuvette, which was capped and put in the fluorimeter.

The silica monolith sized 8 x 8 x 27 mm was immersed upright in 50 mL of the pyrene stock solution held in a vial, as in the uptake experiments. From time to time the vial would be opened, and the solution purged with nitrogen for 5 min. First the monolith, and then 1.0 mL of the surrounding solution, were transferred to a cuvette, which was then capped, and the fluorescence spectrum was recorded. During the acquisition, the monolith adhered to those two walls of the cuvette that faced the source and the detector. In this way, the excitation beam avoided the surrounding solution, the emission from pyrene in the glass

was maximized, and the emission from pyrene in the surrounding solution was minimized. This external solution was necessary, to avoid cracking of the glass monolith during the acquisition of the spectrum.

**Synthesis of the Substituted Benzyl Alcohol, (1).** *3,4,5-Trifluorobenzyl alcohol (1c)*. Sodium tetrahydroborate (0.23 g, 6.3 mmol) was added over 5 min to a stirred solution of 3,4,5-trifluorobenzaldehyde (2.0 g, 12.5 mmol) in 15 mL of ethanol. Stirring was continued for 30 min at room temperature. Volume was reduced in vacuo to ca. 2 mL, and 50 mL of water was added. The mixture was extracted with diethyl ether (3 x 50 mL). The combined organic phases were washed with saturated NaCl solution (2 x 50 mL) and dried over MgSO<sub>4</sub>. The evaporation of the organic phase yielded the crude alcohol, which was purified by flash chromatography on silica (hexane : acetone, 9 : 1). <sup>1</sup>H NMR in CDCl<sub>3</sub>, δ: 2.51 (br, 1 H), 4.61 (s, 2H), and 6.96 (m, 2H); <sup>13</sup>C NMR in CDCl<sub>3</sub>, δ: 63.6 (s), 110.3 (m), 137.1 (m), 138.9 (m), and 151.2 (m).

*3,4,5-Trimethylbenzyl alcohol (1b)*. The synthesis followed a published procedure.<sup>25,26</sup> Baddeley rearrangement of 2',4',6'-trimethylacetophenone in the presence of AlCl<sub>3</sub> yielded 3',4',5'-trimethylacetophenone. Oxidation of this compound by NaOCl to 3,4,5-trimethylbenzoic acid, followed by reduction with LiAlH<sub>4</sub>, afforded the desired alcohol. <sup>1</sup>H NMR in CDCl<sub>3</sub> δ: 2.17 (s, 3 H), 2.29 (s, 6H), 4.59 (s, 2H), and 7.01 (s, 2H); <sup>13</sup>C NMR in CDCl<sub>3</sub>, δ: 15.2, 20.6, 65.4, 126.5, 134.6, 136.8, and 137.7.

**Synthesis of the Substituted Benzyl Bromide, (2).** A solution of the derivatized benzyl alcohol **1b** or **1c** (10.5 mmol) in 25 mL of diethyl ether containing triphenylphosphine (2.75 g, 10.5 mmol) and carbon tetrabromide (3.48 g, 10.5 mmol) was stirred at 25° C for 40

minutes, filtered, and concentrated in vacuo. The residue was subjected to flash chromatography on silica with hexane as an eluent, to yield the pure bromide derivative **2b** or **2c**.

*3,4,5-Trimethylbenzyl bromide (2b)*.  $^1\text{H}$  NMR in  $\text{CDCl}_3$ ,  $\delta$ : 2.14 (s, 3 H), 2.25 (s, 6H), 4.41 (s, 2H), and 7.02 (s, 2H);  $^{13}\text{C}$  NMR in  $\text{CDCl}_3$ ,  $\delta$ : 15.4, 20.6, 34.2, 128.3, 134.6, 135.8, and 137.1.

*3,4,5-Trifluorobenzyl bromide (2c)*.  $^1\text{H}$  NMR in  $\text{CDCl}_3$ ,  $\delta$ : 4.37 (s, 2 H), and 7.03 (m, 2H);  $^{13}\text{C}$  NMR in  $\text{CDCl}_3$ ,  $\delta$ : 31.0 (s), 113.3 (m), 133.9 (m), 139.6 (m), and 151.1 (m).

**Synthesis of Alkylphosphonium Salts, (3).**<sup>27</sup> A solution of the derivatized benzyl bromide **1a**, **1b**, or **1c** (1.1 mmol) and triphenylphosphine (0.29 g, 1.1 mmol) in benzene (10 mL) was stirred under reflux for 12 h. The initially-clear solution rapidly become cloudy, and the phosphonium salt precipitated as a colorless solid. The solution was cooled in ice, filtered, and washed with 100 mL of cold benzene (carcinogen!). The benzene was evaporated in a rotary evaporator, and the phosphonium salt was recrystallized from benzene; both procedures were done inside an effective fume hood.

**Synthesis of Stilbene, (5).**<sup>28</sup> To the alkylphosphonium salt **3** (0.9 mmol) and potassium *tert*-butoxide (0.10 g, 0.9 mmol) in dichloromethane (10 mL) was added 3,4,5-trifluorobenzaldehyde **4** (0.13 g, 0.8 mmol) and 18-crown-6 (15 mg). The mixture was stirred overnight at room temperature, and then the solvent was evaporated. The residue was washed three times with 50 mL of hexane, and the washings were filtered through silica gel. Evaporation of the solvent yielded crude mixture of the trans and cis isomers **5**, which were then separated and purified by column chromatography on silica with hexane as an eluent.

*trans-3,4,5-Trifluoro-4'-methyl stilbene.*  $^1\text{H}$  NMR in  $\text{CDCl}_3$ ,  $\delta$ : 2.36 (s, 3H), 6.86 (d, 1 H,  $J = 16.4$  Hz), 6.97 (d, 1H,  $J = 16.4$  Hz), 7.06 (m, 2H); 7.17 (d, 2H), and 7.37 (d, 2H);  $^{13}\text{C}$  NMR in  $\text{CDCl}_3$ ,  $\delta$ : 21.3 (s), 110.0 (m), 124.7 (m), 126.7 (s), 129.6 (s), 131.0 (m), 133.5 (s), 133.9 (m), 137.0 (s), 139.0 (m), 151.4 (m);  $^{19}\text{F}$  NMR in  $\text{CDCl}_3$ ,  $\delta$ : -133.1 (m), and -160.2 (m); LRMS-Cl: calcd for  $\text{M}^+$  of  $\text{C}_{15}\text{H}_{11}\text{F}_3$  248, found 248.

*cis-3,4,5-Trifluoro-4'-methyl stilbene.*  $^1\text{H}$  NMR in  $\text{CDCl}_3$ ,  $\delta$ : 2.33 (s, 3H), 6.35 (d, 1 H,  $J = 12.0$  Hz), 6.63 (d, 1H,  $J = 12.0$  Hz), 6.83 (m, 2H); and 7.08 (m, 4H);  $^{13}\text{C}$  NMR in  $\text{CDCl}_3$ ,  $\delta$ : 21.3 (s), 112.8 (m), 126.5 (m), 128.7 (s), 129.3 (s), 132.5 (s), 133.0 (s), 133.5 (m), 137.8 (s), 138.9 (m), and 151.0 (m);  $^{19}\text{F}$  NMR in  $\text{CDCl}_3$ ,  $\delta$ : -133.4 (m), and -160.5 (m); LRMS-Cl: calcd for  $\text{M}^+$  of  $\text{C}_{15}\text{H}_{11}\text{F}_3$  248, found 248.

*trans-3,4,5-Trifluoro-3',4',5'-trimethyl stilbene.*  $^1\text{H}$  NMR in  $\text{CDCl}_3$ ,  $\delta$ : 2.18 (s, 3H), 2.30 (s, 6H), 6.84 (d, 1H,  $J = 16.4$  Hz), 6.91 (d, 1H,  $J = 16.4$  Hz), 7.05 (m, 2 H), and 7.13 (s, 2H);  $^{13}\text{C}$  NMR in  $\text{CDCl}_3$ ,  $\delta$ : 15.5 (s), 20.7 (s), 109.9 (m), 124.3 (m), 126.0 (s), 131.2 (m), 133.1 (s), 134.1 (m), 135.9 (s), 136.9 (s), 139.0 (m), and 151.6 (m);  $^{19}\text{F}$  NMR in  $\text{CDCl}_3$ ,  $\delta$ : -133.1 (m), and -160.7 (m); LRMS-Cl: calcd for  $\text{M}^+$  of  $\text{C}_{17}\text{H}_{15}\text{F}_3$  276, found 276.

*cis-3,4,5-Trifluoro-3',4',5'-trimethyl stilbene.*  $^1\text{H}$  NMR in  $\text{CDCl}_3$ ,  $\delta$ : 2.15 (s, 3H), 2.20 (s, 6H), 6.30 (d, 1H,  $J = 12.0$  Hz), 6.58 (d, 1H,  $J = 12.0$  Hz), and 6.87 (m, 4 H);  $^{13}\text{C}$  NMR in  $\text{CDCl}_3$ ,  $\delta$ : 15.3 (s), 20.5 (s), 112.8 (m), 126.1 (m), 128.4 (m), 132.7 (br), 132.8 (s), 133.6 (m), 135.0 (s), 136.6 (s), 138.9 (m), and 150.9 (m);  $^{19}\text{F}$  NMR in  $\text{CDCl}_3$ ,  $\delta$ : -133.4 (m), and -160.5 (m); LRMS-Cl: calcd for  $\text{M}^+$  of  $\text{C}_{17}\text{H}_{15}\text{F}_3$  276, found 276.

*trans-3,3',4,4',5,5'-Hexafluoro stilbene.*  $^1\text{H}$  NMR in  $\text{CDCl}_3$ ,  $\delta$ : 6.84 (s, 2H), and 7.09 (m, 4H);  $^{13}\text{C}$  NMR in  $\text{CDCl}_3$ ,  $\delta$ : 110.5 (m), 128.0 (s), 132.5 (m), 139.6 (m), and 151.6

(m);  $^{19}\text{F}$  NMR in  $\text{CDCl}_3$ ,  $\delta$ : -132.2 (m), and -158.2 (m); LRMS-Cl: calcd for  $\text{M}^+$  of  $\text{C}_{14}\text{H}_6\text{F}_6$  288, found 288.

*cis-3,3',4,4',5,5'-Hexafluoro stilbene*.  $^1\text{H}$  NMR in  $\text{CDCl}_3$ ,  $\delta$ : 6.52 (s, 2H), and 6.80 (m, 4H);  $^{13}\text{C}$  NMR in  $\text{CDCl}_3$ ,  $\delta$ : 112.8 (m), 129.4 (s), 131.9 (m), 139.2 (m), and 151.3 (m);  $^{19}\text{F}$  NMR in  $\text{CDCl}_3$ ,  $\delta$ : -132.1 (m), and -158.8 (m); LRMS-Cl: calcd for  $\text{M}^+$  of  $\text{C}_{14}\text{H}_6\text{F}_6$  288, found 288.

### ***Results and Discussion***

**Interactions between Silica Glass and Guest Compounds.** It is widely assumed that molecules (including ions) smaller than the pores in the sol-gel glass can freely diffuse in and out of this glass when it is immersed in the solution of these molecules. This assumption underlies the design of various biosensors, which can function only if the guest concentrations in the matrix and in the surrounding solution are equalized relatively quickly. We refer to this equalization or near equalization, regardless of the time required for its attainment, as balanced uptake. Research in our laboratory<sup>20-23</sup> has shown that, when repulsive or attractive interactions exist between the glass and the guests, the sol-gel silica matrix takes up the guest partially or excessively. We call this uptake imbalanced. Electrostatic interactions and conventional hydrogen bonds between sol-gel silica and guests with guests have been documented.<sup>15,20,22,23</sup> Now we search for even subtler and weaker interactions. Study of adsorption of aromatic compounds on silica has begun, but little is known about this phenomenon.<sup>29-33</sup> Our goal is not to analyze these weak interactions as such, but to examine their unexpected consequences for the doping of sol-gel glasses with

chemicals and for the function of these doped glasses. This study deals less with spectroscopy and more with materials science.

**Dehydration of Silica Monolith.** After aging and partial drying, the pores in the sol-gel silica monoliths contain water that must be removed lest it affect, or altogether prevent, the interaction with the guests. We extracted water with a succession of solvents chosen so that each dilutes and removes the previous one. Over time, this exhaustive procedure achieved the overall dilution factor of ca.  $10^{16}$ . Smaller factors probably would have sufficed, but we strove for accurate experiments.

The averaged pore size of silica xerogel prepared by the sol-gel method, and completely dried at high temperature, is ca.  $20 \text{ \AA}$ .<sup>34</sup> The average pore size of our silica glass, which is only partially dried at  $4^\circ \text{ C}$ , is greater than ca.  $30 \text{ \AA}$ <sup>20</sup> but smaller than ca.  $100 \text{ \AA}$ . Indeed our slabs do not scatter visible light.<sup>23</sup> The experimental methods for determination of surface area (BET) and pore size distribution (BJH) are inapplicable to our partially-dried silica monoliths because they shrink, and therefore change their physical properties, during their preparation for the experiment. Infrared spectrum of a pulverized silica monolith used in the uptake experiments does not show residual water or carbon-containing compounds.<sup>20</sup>

**Nearly Balanced Uptake of Aromatic Halides by Silica Glass.** Monosubstituted, 1,2- and 1,4-disubstituted, and 1,2,3- and 1,3,5-trisubstituted halo derivatives of benzene differ in dipole moment and polarizability (Table 1).<sup>35</sup> We tested whether these compounds form van der Waals interactions with the sol-gel silica glass. The experiments were done in hexane since this solvent is nonpolar and has very low polarizability and therefore is not expected to compete with the guest molecules for the host sites on silica. (This assumption

was vindicated in experiments with pyrene emission, to be discussed later.) The results of uptake exemplified by Figure 1 are shown in Table 1. The uptake coefficients for all the aromatic halides examined fall between 1.0 and 1.9. The 1,2,3-trisubstituted derivatives, which have the greatest dipole moments, showed the highest values. The 1,3,5-trisubstituted and 1,4-disubstituted chloro and bromo derivatives, which have no dipole moments, showed low values. Iodo derivatives, especially 1,4-diiodo benzene, and some other compounds in Table 1, however, refute the correlation between the dipole moment of the guest and the extent of its uptake by the silica matrix. Likewise, there is no correlation between polarizability of compounds and their uptake coefficients. We conclude that dipolar and van der Waals interactions are not responsible for the uptake of aromatic halides with the coefficients exceeding 1.0.

**Uptake of Polycyclic Aromatic Hydrocarbons and Control of It.** We chose six aromatic hydrocarbons that differ in polarizability, size, and structure. Their uptake by sol-gel silica from the solutions in hexane, dichloromethane, and carbon tetrachloride is quantified in Table 2. The uptake coefficients in the range 3.0 to 4.6 show that all the six compounds are excessively taken up from hexane into the silica matrix. On the contrary, the coefficients in the range 0.82 to 1.39 show balanced or nearly balance uptake from carbon tetrachloride and dichloromethane. The excessive uptake from hexane by sol-gel glass amounts to extraction of nonpolar hydrocarbons from a nonpolar hydrocarbon solvent into the polar environment characteristic of porous silica. This finding intrigued us, for it violates the well-known principles of extraction and partition chromatography. 36-38

Propensity of aromatic compounds to act as hydrogen-bond acceptors is well documented,<sup>39-46</sup> but there is no scale quantifying this propensity. We assume that it generally increases as the size (and also polarizability) of the molecule increases. Silanol groups in the sol-gel silica are hydrogen-bond donors. As Table 2 shows, the uptake coefficients generally increase downward, as the guest molecules become larger. This finding is consistent with hydrogen bonding involving the aromatic system as the cause of the unexpected extraction. All the solvents used in uptake experiments have near-zero  $\alpha$  and  $\beta$  Kamlet-Taft parameters, which reflect, hydrogen-bonding acceptor and donor abilities, respectively.<sup>47,48</sup> Therefore these solvents do not make hydrogen bonds with guest molecules. The  $\pi^*$  parameter, which reflects dipolarity/polarizability, is  $-0.081$ ,  $0.82$ , and  $0.28$  for hexane, dichloromethane, and carbon tetrachloride, respectively.<sup>49,50</sup> Therefore, these solvents may differ in their van der Waals interactions with the guest molecules and the silica matrix. Dichloromethane and carbon tetrachloride are known to adsorb on silica.<sup>30,51,52</sup> This silica-solvent interaction would suppress the silica-guest interaction; the solvent molecules, present in great excess, would displace the aromatic molecules from the pore surfaces in sol-gel glass. The result is balanced or nearly balanced uptake of the aromatics.

**Silica-Solvent Interactions Probed with Pyrene.** We tested the hypothesis that some solvents do, while others do not, adsorb on the sol-gel silica glass under the conditions of our experiments. Emission spectrum of pyrene consists of five bands, designated I through V. The ratio of the intensities of the third and the first band, the III/I quotient, is widely used as a measure of the polarity of the medium surrounding the fluorophore.<sup>53-57</sup>



Figure 2 a, b, and c and the first three rows in Table 3 show that the  $\text{III/I}$  quotient remains unchanged as the fluorophore moves from the polar or chlorine-containing solvent to the glass interior. Evidently, pyrene “feels” the same environment in these solvents and inside the porous sol-gel silica monolith immersed in the solutions containing polar or chlorine-containing solvents. Figure 2 d and last row in Table 3, however, show that the  $\text{III/I}$  quotient changes greatly as the fluorophore moves from hexane to the glass. Evidently, pyrene “feels” greatly different environments when dissolved in hexane and inside the sol-gel glass impregnated by this solution. The  $\text{III/I}$  quotient of  $0.75 \pm 0.04$  in our study is similar to the values of 0.65-0.75, reported for pyrene inside silica and modified silica.<sup>57-62</sup>

Uptake of pyrene into silica from the first three solvents is nearly balanced – the coefficients are equal (within the margins of error) and near unity. But uptake from hexane is excessive. Even when pyrene was maximally extracted into silica from hexane, at the end of the uptake experiments, there was no sign of the excimer formation in the emission spectrum (Figure 3), which is diagnostic of pyrene aggregation.<sup>63-64</sup> Evidently, pyrene accumulates in the porous glass because it interacts with silica, not with itself.

These experiments confirm our conclusion in the preceding subsection. Polar or chlorine-containing solvents line the pore surfaces in the glass, so that the pyrene “feels” this solvent inside the glass as well as in the solution. Hexane, however, does not adsorb on the glass surfaces and does not shield pyrene from the silica matrix. Consequently, pyrene “feels” a great difference between the glass interior and the hexane solution. Pyrene, like the guest compounds in Table 2, accepts hydrogen bonds from silica and thus becomes extracted into the glass matrix from the hexane solution.

**Uptake of Stilbene and Its Derivatives.** Because stilbene showed the highest affinity for sol-gel silica, we examined its uptake in some detail. Besides the parent compound, we synthesized three of its derivatives, according to Scheme 1. Compounds **1a**, **1b**, **2a**, **3a**, and **4** are known. Compounds **1c**, **2b**, **2c**, **3b**, and **3c**, which are intermediates in the syntheses, have not been reported before. Most important, all six compounds designated **5** (three substituted derivatives of stilbene, two geometrical isomers of each) are new.

There are altogether eight guest compounds, which differ in configuration and aromatic electron density. A trans isomer is more nearly planar than its cis isomer. Hexafluoro stilbene is poorer in electrons than the other derivatives. As Table 4 shows, all the eight compounds are extracted by porous sol-gel silica from the hexane solution. The molecular configuration (cis and trans) has a small effect on the uptake coefficient, possibly because the pore surfaces are irregular. Because hydroxyl groups on these surfaces are capable of hydrogen bonding in various directions, the precise orientation of the aromatic rings is not critical for adsorption. The substituents do not seem to affect adsorption in a discernable way. Dichloromethane as a solvent suppresses adsorption of stilbene and brings about the balanced uptake of all eight guest compounds.

### ***Conclusion***

Extraction of aromatics into porous sol-gel silica from hexane, but not from solvents capable of hydrogen bonding, seems to be a general property of aromatic compounds. We document it with many halo derivatives of benzene and also with polynuclear and conjugated aromatic compounds. This unexpected behavior is consistent with hydrogen bonding

between the aromatic guests and silanol groups on the surfaces of the glass pores. These interactions have recently been recognized.<sup>29</sup> Nothing was known before this study about these interactions in sol-gel materials. The goal of this research was not to continue the study of hydrogen bonding itself, but to examine its consequences for the adsorption of aromatics on sol-gel silica and the unexpected extraction of organic compounds into an inorganic matrix from organic solvents. This phenomenon should be taken into consideration in the design and use of various composite materials containing sol-gel silica, such as enzymes in biosensors and in immobilized catalysts. If balanced uptake is required for the function of sensors and other molecular devices, the unwanted extraction can be suppressed by the use of hydrogen-bonding solvents, which reliably prevent the adsorption and cause the aromatic guests to be evenly distributed between the glass matrix and the surrounding solution.

**Acknowledgment.** We thank Professor Victor Shang-Yi Lin of this department for permission to use the fluorimeter. This work was supported by the U.S. National Science Foundation.

### **References**

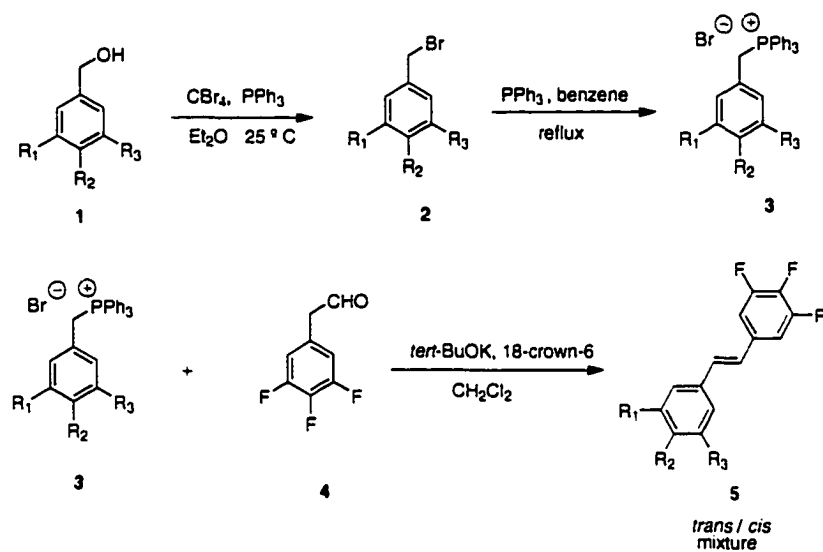
- (1) Livage, J. *Bull. Mater. Sci.* **1999**, 22, 201-5.
- (2) Schmid, L.; Rohr, M.; Baiker, A. *Chem. Commun. (Cambridge)* **1999**, 2303-4.
- (3) Gill, I.; Ballesteros, A. *J. Am. Chem. Soc.* **1998**, 120, 8587-98.
- (4) Livage, J. *C. R. Acad. Sci., Ser. II: Mec., Phys., Chim., Astron.* **1996**, 322, 417-27.
- (5) Avnir, D.; Braun, S.; Lev, O.; Ottolenghi, M. *Chem. Mater.* **1994**, 6, 1605-14.
- (6) Avnir, D. *Acc. Chem. Res.* **1995**, 28, 328-34.

- (7) Huang, M. H.; Dunn, B. S.; Zink, J. I. *J. Am. Chem. Soc.* **2000**, *122*, 3739-45.
- (8) Jung, J. H.; Ono, Y.; Hanabusa, K.; Shinkai, S. *J. Am. Chem. Soc.* **2000**, *122*, 5008-9.
- (9) Sanchez, C.; Ribot, F.; Lebeau, B. *J. Mater. Chem.* **1999**, *9*, 35-44.
- (10) Lan, E. H.; Dave, B. C.; Fukuto, J. M.; Dunn, B.; Zink, J. I.; Valentine, J. S. *J. Mater. Chem.* **1999**, *9*, 45-53.
- (11) Gelman, F.; Avnir, D.; Schumann, H.; Blum, J. *J. Mol. Catal. A: Chem.* **1999**, *146*, 123-8.
- (12) Blum, J.; Rosenfeld, A.; Gelman, F.; Schumann, H.; Avnir, D. *J. Mol. Catal. A: Chem.* **1999**, *146*, 117-22.
- (13) Husing, N.; Schubert, U. *Angew. Chem., Int. Ed.* **1998**, *37*, 22-45.
- (14) Loy, D. A.; Shea, K. J. *Chem. Rev. (Washington, D. C.)* **1995**, *95*, 1431-42.
- (15) Spange, S.; Zimmermann, Y.; Graeser, A. *Chem. Mater.* **1999**, *11*, 3245-51.
- (16) Rottman, C.; Grader, G.; Hazan, Y. D.; Melchior, S.; Avnir, D. *J. Am. Chem. Soc.* **1999**, *121*, 8533-43.
- (17) Rao, M. S.; Dave, B. C. *J. Am. Chem. Soc.* **1998**, *120*, 13270-1.
- (18) Dunn, B.; Zink, J. I. *Chem. Mater.* **1997**, *9*, 2280-91.
- (19) Ueda, M.; Kim, H.-B.; Ichimura, K. *Chem. Mater.* **1994**, *6*, 1771-5.
- (20) Badjić, J. D.; Kostić, N. M. *J. Mater. Chem.* **2001**, *11*, 408-18
- (21) Badjić, J. D.; Kostić, N. M. *Chem. Mater.* **1999**, *11*, 3671-9.
- (22) Shen, C.; Kostić, N. M. *J. Electroanal. Chem.* **1997**, *438*, 61-5.
- (23) Shen, C.; Kostić, N. M. *J. Am. Chem. Soc.* **1997**, *119*, 1304-12.

- (24) Yamanaka, S. A.; Nishida, F.; Ellerby, L. M.; Nishida, C. R.; Dunn, B.; Valentine, J. S.; Zink, J. I. *Chem. Mater.* **1992**, *4*, 495-7.
- (25) Pearson, D. E.; Bruton, J. D. *J. Org. Chem.* **1954**, *19*, 957.
- (26) Suzuki, H. *Bull. Chem. Soc. Jap.* **1969**, *42*, 2618-23.
- (27) Tietze, L. F.; Eicher, T. *Reactions and Syntheses in an Organic-Chemical Practical Course. 2nd Ed.* 1995.
- (28) Boden, R. M. *Synthesis* **1975**, 784.
- (29) Ringwald, S. C.; Pemberton, J. E. *Environ. Sci. Technol.* **2000**, *34*, 259-65.
- (30) Ruetten, S. A. *J. Phys. Chem. B* **1999**, *103*, 9285-94.
- (31) Ruetten, S. A.; Thomas, J. K. *J. Phys. Chem. B* **1999**, *103*, 1278-86.
- (32) Ruetten, S. A.; Thomas, J. K. *J. Phys. Chem. B* **1998**, *102*, 598-606.
- (33) Suzuki, T.; Tamon, H.; Okazaki, M. *Chem. Lett.* **1994**, 2151-4.
- (34) Hench, L. L.; West, J. K. *Chem. Rev.* **1990**, *90*, 33-72.
- (35) Lide, D. R.; Frederikse, H. P. R. *CRC Handbook of Chemistry and Physics, 78th Edition*, 1997.
- (36) Du, C. M.; Valko, K.; Bevan, C.; Reynolds, D.; Abraham, M. H. *Anal. Chem.* **1998**, *70*, 4228-34.
- (37) Abraham, M. H.; Green, C. E.; Acree, J. W. E.; Hernandez, C. E.; Roy, L. E. *J. Chem. Soc., Perkin Trans. 2* **1998**, 2677-82.
- (38) Abraham, M. H.; Chadha, H. S.; Leitao, R. A. E.; Mitchell, R. C.; Lambert, W. J.; Kaliszan, R.; Nasal, A.; Haber, P. *J. Chromatogr., A* **1997**, *766*, 35-47.
- (39) Feller, D. *J. Phys. Chem. A* **1999**, *103*, 7558-61.

- (40) Gruenloh, C. J.; Hagemester, F. C.; Carney, J. R.; Zwier, T. S. *J. Phys. Chem. A* **1999**, *103*, 503-13.
- (41) Cabarcos, O. M.; Weinheimer, C. J.; Lisy, J. M. *J. Chem. Phys.* **1998**, *108*, 5151-4.
- (42) Rodham, D. A.; Suzuki, S.; Suenram, R. D.; Lovas, F. J.; Dasgupta, S.; Goddard, W. A., III; Blake, G. A. *Nature (London)* **1993**, *362*, 735-7.
- (43) Suzuki, S.; Green, P. G.; Bumgarner, R. E.; Dasgupta, S.; Goddard, W. A., III; Blake, G. A. *Science (Washington, D. C., 1883-)* **1992**, *257*, 942-5.
- (44) Atwood, J. L.; Hamada, F.; Robinson, K. D.; Orr, G. W.; Vincent, R. L. *Nature (London)* **1991**, *349*, 683-4.
- (45) Levitt, M.; Perutz, M. F. *J. Mol. Biol.* **1988**, *201*, 751-4.
- (46) Engdahl, A.; Nelander, B. *J. Phys. Chem.* **1985**, *89*, 2860-4.
- (47) Kamlet, M. J.; Taft, R. W. *J. Am. Chem. Soc.* **1976**, *98*, 377-83.
- (48) Kamlet, M. J.; Abboud, J. L. M.; Abraham, M. H.; Taft, R. W. *J. Org. Chem.* **1983**, *48*, 2877-87.
- (49) Kamlet, M. J.; Abboud, J. L.; Taft, R. W. *J. Am. Chem. Soc.* **1977**, *99*, 6027-38.
- (50) Reichardt, C. *Solvents and Solvent Effects in Organic Chemistry*. 2nd Ed, 1988.
- (51) Branton, P. J.; Reynolds, P. A.; Studer, A.; Sing, K. S. W.; White, J. W. *Adsorption* **1999**, *5*, 91-6.
- (52) Solymosi, F.; Rasko, J. *J. Catal.* **1995**, *155*, 74-81.
- (53) Lakowicz, J. R. *Principles of Fluorescence Spectroscopy*; Second Edition ed.; Kluwer Academic / Plenum Publishers:, 1999.
- (54) Sugiyama, K.; Esumi, K. *Langmuir* **1996**, *12*, 2613-15.

- (55) Itoh, H.; Ishido, S.; Nomura, M.; Hayakawa, T.; Mitaku, S. *J. Phys. Chem.* **1996**, *100*, 9047-53.
- (56) Karpovich, D. S.; Blanchard, G. J. *J. Phys. Chem.* **1995**, *99*, 3951-8.
- (57) Kalyanasundaram, K.; Thomas, J. K. *J. Am. Chem. Soc.* **1977**, *99*, 2039-44.
- (58) Dong, D. C.; Winnik, M. A. *Can. J. Chem.* **1984**, *62*, 2560-5.
- (59) Matsui, K.; Nakazawa, T. *Bull. Chem. Soc. Jpn.* **1990**, *63*, 11-6.
- (60) Wong, A. L.; Hunnicutt, M. L.; Harris, J. M. *Anal. Chem.* **1991**, *63*, 1076-81.
- (61) Zana, R.; Frasc, J.; Soulard, M.; Lebeau, B.; Patarin, J. *Langmuir* **1999**, *15*, 2603-6.
- (62) Baker, G. A.; Pandey, S.; Maziarz, E. P., III; Bright, F. V. *J. Sol-Gel Sci. Technol.* **1999**, *15*, 37-48.
- (63) Papoutsis, D.; Bekiari, V.; Stathatos, E.; Lianos, P.; Laschewsky, A. *Langmuir* **1995**, *11*, 4355-60.
- (64) Suib, S. L.; Kostapapas, A. *J. Am. Chem. Soc.* **1984**, *106*, 7705-10.

**Scheme 1.** Synthesis of stilbene derivatives.

group	a	b	c
R <sub>1</sub>	H	Me	F
R <sub>2</sub>	Me	Me	F
R <sub>3</sub>	H	Me	F



**Table 1.** Partitioning at equilibrium of halo derivatives of benzene between hexane solution and monolith of porous sol-gel silica glass at 25 °C.

guest	polarizability ( $10^{-24} \text{ cm}^3$ )	dipole moment (D)	uptake coefficient <sup>a</sup>
fluorobenzene	10.3	1.5	$1.3 \pm 0.2$
1,2-difluorobenzene	10.4	2.4	$1.4 \pm 0.1$
1,4-difluorobenzene	10.2	0	$1.4 \pm 0.2$
1,2,3- trifluorobenzene	10.4	3.0	$1.7 \pm 0.2$
1,3,5-trifluorobenzene	10.2	0	$1.3 \pm 0.1$
chlorobenzene	14.1	1.6	$1.3 \pm 0.1$
1,2-dichlorobenzene	14.2	2.2	$1.3 \pm 0.1$
1,4-dichlorobenzene	14.4	0	$1.3 \pm 0.1$
1,2,3-trichlorobenzene		2.4	$1.9 \pm 0.1$
1,3,5-trichlorobenzene	16.1	0	$1.0 \pm 0.1$
bromobenzene	14.7	1.7	$1.3 \pm 0.1$
1,2-dibromobenzene	16.3	2.0	$1.3 \pm 0.1$
1,4-dibromobenzene	13.5	0	$1.3 \pm 0.1$
1,2,3-tribromobenzene			$1.8 \pm 0.1$
1,3,5-tribromobenzene		0	$1.1 \pm 0.1$
iodobenzene	15.5		$1.5 \pm 0.1$
1,2-diiodobenzene	20.0	1.7	$1.7 \pm 0.1$
1,4-diiodobenzene		0	$1.7 \pm 0.1$

<sup>a</sup> Ratio of concentrations in glass and the surrounding solution.

**Table 2.** Uptake coefficients for partitioning of polynuclear and conjugated aromatic hydrocarbons between various solvents and monolith of porous sol-gel silica glass at 25 °C.

guest	solvent		
	hexane	dichloromethane	carbon tetrachloride
naphthalene	$3.0 \pm 0.2$	$1.00 \pm 0.02$	$0.94 \pm 0.08$
2,7-di- <i>tert</i> -butylnaphthalene	$3.0 \pm 0.1$	$0.85 \pm 0.03$	$0.95 \pm 0.02$
azulene	$3.6 \pm 0.1$	$0.99 \pm 0.03$	$1.35 \pm 0.02$
anthracene	$3.6 \pm 0.3$	$0.82 \pm 0.03$	$1.39 \pm 0.08$
pyrene	$3.7 \pm 0.5$	$0.88 \pm 0.02$	$1.30 \pm 0.03$
<i>trans</i> -stilbene	$4.6 \pm 0.2$	$0.95 \pm 0.02$	$1.24 \pm 0.08$

**Table 3.** Relative intensity of the bands III and I in the fluorescence spectra of pyrene when dissolved in four solvents and when taken up from these solutions into monolith of porous sol-gel silica glass at 25 °C.

solvent	III/I quotient		uptake coefficient
	solution	silica	
acetonitrile	0.55 ± 0.01	0.55 ± 0.05	0.93 ± 0.04
dichloromethane	0.71 ± 0.01	0.70 ± 0.03	0.88 ± 0.02
cyclohexyl chloride	0.93 ± 0.01	0.94 ± 0.03	0.88 ± 0.02
hexane	1.68 ± 0.01	0.75 ± 0.04	3.7 ± 0.5

**Table 4.** Uptake coefficients for partitioning of stilbene and its derivatives between solvent and monolith of porous sol-gel silica glass at 25 °C.

guest	isomer	solvent	
		hexane	dichloromethane
stilbene	<i>trans</i>	4.6 ± 0.2	0.95 ± 0.02
	<i>cis</i>	4.4 ± 0.1	1.14 ± 0.01
3,4,5-trifluoro 4'-methyl stilbene	<i>trans</i>	3.5 ± 0.1	0.95 ± 0.08
	<i>cis</i>	3.3 ± 0.1	0.95 ± 0.02
3,4,5-trifluoro 3',4',5'- trimethyl stilbene	<i>trans</i>	4.4 ± 0.1	1.16 ± 0.01
	<i>cis</i>	3.4 ± 0.1	1.14 ± 0.01
3,3',4,4',5,5'-hexafluoro stilbene	<i>trans</i>	4.9 ± 0.1	0.90 ± 0.01
	<i>cis</i>	4.0 ± 0.2	1.25 ± 0.09

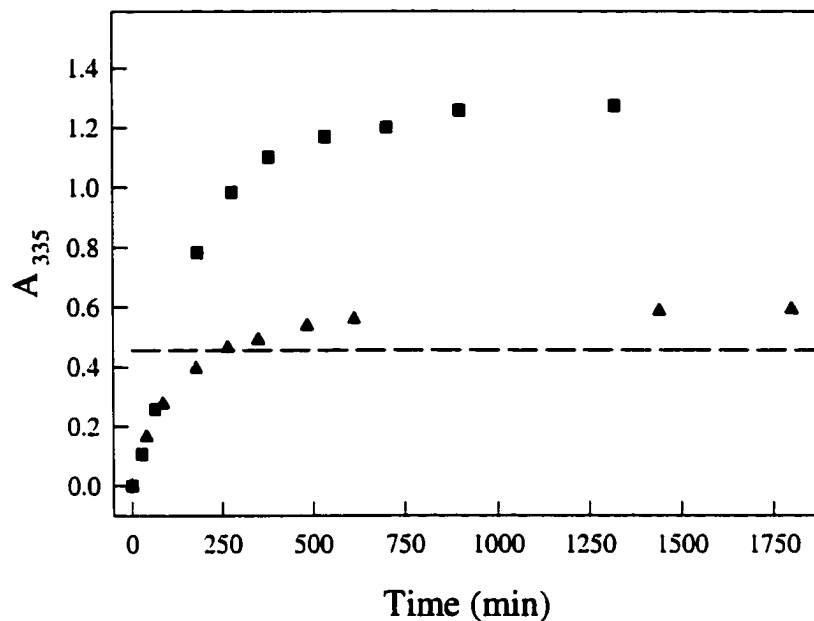


**Figure 1.** Uptake of pyrene by monoliths of porous sol-gel silica glass sized 8 x 8 x 27 mm soaked in 50.0 mL of  $1.8 \cdot 10^{-5}$  M solutions of pyrene in carbon tetrachloride (▲) and hexane (■). As pyrene enters, its absorbance in the glass increases. The dashed line marks the absorbance of the external solution. Uptake is nearly balanced in carbon tetrachloride and excessive in hexane.

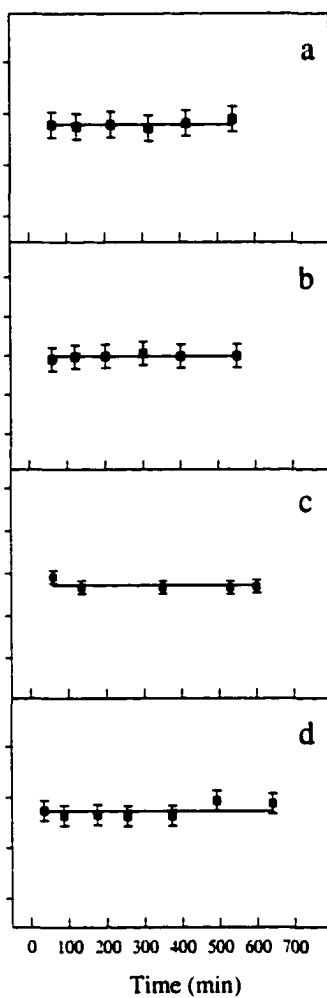


**Figure 2.** Relative intensity of the bands III and I in the fluorescence spectra of pyrene taken up by monoliths of porous sol-gel silica glass sized 8 x 8 x 27 mm from 50.0 mL of  $1.0 \cdot 10^{-5}$  M solutions of pyrene in: (a) acetonitrile, (b) dichloromethane, (c) cyclohexyl chloride, and (d) hexane.

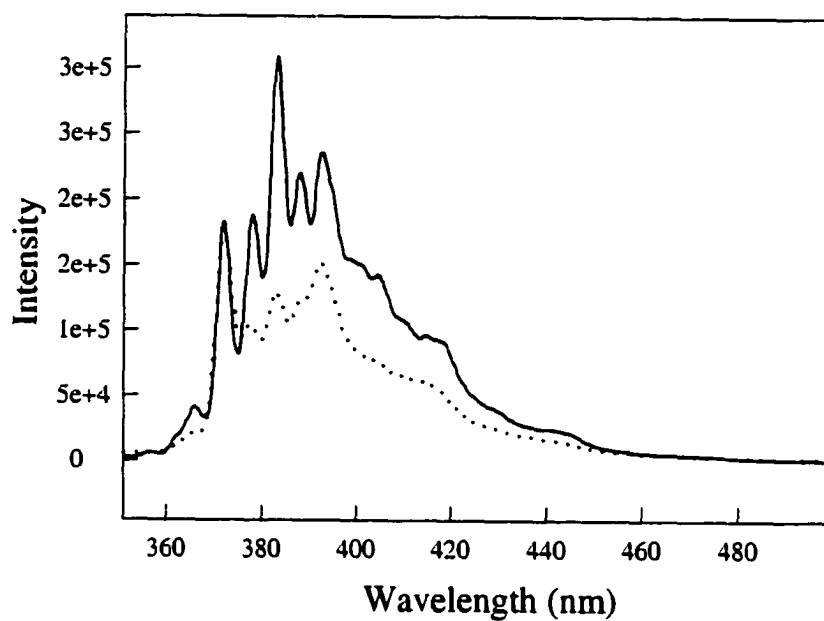


**Figure 3.** Fluorescence spectra of  $1.0 \cdot 10^{-5}$  M pyrene in hexane (solid line,  $I_{385}/I_{370} = 1.68 \pm 0.01$ ) and taken up from the hexane solution by monolith of porous sol-gel silica glass sized  $8 \times 8 \times 27$  mm (dotted line,  $I_{385}/I_{370} = 0.75 \pm 0.04$ ). The last point in Figure 2d is based on the dotted-line spectrum here.

**CHAPTER 5. REACTIVITY OF ORGANIC COMPOUNDS INSIDE  
MICELLES EMBEDDED IN SOL-GEL GLASS. KINETICS OF  
ISOMERIZATION OF AZOBENZENE INSIDE CTAB AND SDS  
MICELLES EMBEDDED IN SILICA MATRIX**

A paper submitted to *Journal of Physical Chemistry B*

Jovica D. Badjić and Nenad M. Kostić

***Abstract***

The sol-gel method allows preparation of composite materials consisting of surfactant micelles embedded in glasses. Moreover, this method allows doping of the embedded micelles with various compounds. In this study the four dopants are pyrene and azobenzene and its 3,3'-dimethyl and 3,3'-diacetyl derivatives. The relative intensities of the fluorescence bands of pyrene proved that cetyltrimethylammonium bromide (CTAB) and sodium dodecylsulfate (SDS) form micelles inside silica glass and that SDS does not hydrolyze during its encapsulation within silica. We studied the interactions of silica with the positively-charged CTAB micelles and with the negatively-charged SDS micelles and the kinetics of thermal (cis-to-trans) isomerization of the three azo dopants within micelles embedded in glass. The three isomerization reactions within the CTAB micelles embedded in silica and with water as the external liquid are monophasic; their rate constants are similar to those determined for the micelles in the absence of silica. The isomerization reactions within the SDS micelles embedded in silica and with water as the external liquid are multiphasic;



they are faster than the corresponding reactions within the SDS micelles in the absence of silica. Azobenzene isomerization within the CTAB micelles dissolved in aqueous solution is pH-independent and monophasic in the entire range 6.9 - 2.3. Azobenzene isomerization within the SDS micelles dissolved in aqueous solution is pH-independent and monophasic in the interval 6.9 - 3.9, but it becomes pH-dependent and multiphasic below pH 3.9.

Azobenzene isomerization within SDS micelles embedded in silica, in solution buffered at pH 6.9, remains multiphasic, and is faster than the isomerization within the SDS micelles dissolved in the same buffer but in the absence of silica. Azobenzene stayed within the CTAB/silica glass, but it leaked from the SDS/silica glass into the surrounding water. This leakage from the latter glass was suppressed by replacing water with a 1.50 M aqueous solution of NaCl. The isomerizations then became a monophasic reaction, with rate constants similar to those within the micelles in the absence of silica. Because partitioning of the dopant between the micelle/silica glass and the external liquid influences the reactivity of dopant molecules, control of the partitioning is necessary for the design and successful application of chemical sensors, optical devices, and drug-delivery systems.

### ***Introduction***

Various oxide glasses may be prepared at room temperature by the sol-gel method, that is, by condensation-polymerization of suitable alkoxides.<sup>1-4</sup> The most studied sol-gel material is silica. Mild reaction conditions during its preparation allow encapsulation of enzymes, catalytic antibodies, other proteins, and organic and organometallic catalysts.<sup>5-15</sup> Properties of silica affect the activity of enzymes<sup>16,17</sup> and reactivity of other

compounds<sup>3,18,19</sup> encapsulated in it. These properties of the glass can be controlled through chemical modification of precursors used in the sol-gel method<sup>20-22</sup> and by entrapment in the glasses of surface-active agents together with the compounds of interest.<sup>23-27</sup>

Surfactants are used as templates in the assembly of various ordered mesoporous silica materials, such as M41S,<sup>28-31</sup> which are applied in separations and selective catalysis and as sorbents and sensors.<sup>32-35</sup>

Micelles embedded in silica<sup>36-39</sup> depending on their charge,<sup>40,41</sup> may attract or repel this negatively-charged matrix. As a consequence of these electrostatic interactions, molecules entrapped within the micelles may undergo changes in reactivity, mobility, conformation, pKa, and other important properties. Effects of micelles on some properties of the sol-gel silica and on the co-entrapped acid-base indicators have begun to be studied.<sup>37-39</sup> Although little is known about these effects generally, it is clear that the function of the micelle/silica composites in various applications depends on the mobility and chemical reactivity of the dopant within these composites.

In this study, we examine the interplay of differently-charged micelles and surrounding silica matrix and their joint effects on the reactivity of compounds entrapped in the micelles. To elucidate these effects, we chose a reaction whose kinetics and mechanism are well understood, namely a thermal cis-to-trans isomerization of the azobenzene chromophore. Comparison of its kinetics inside monoliths of surfactant/silica glass and in solution revealed interesting properties of the composite glass.

### ***Experimental Procedures***

**Instrumentation.** Ultraviolet (UV) absorption spectra were recorded with a Perkin-Elmer Lambda 18 spectrophotometer whose cuvette holder was connected to the thermostated circulator bath model 9500 from Fisher Scientific Co. Emission spectra were recorded with a Jobin Yvon Fluoromax-2 fluorimeter. Photochemical reactions were studied with a Rayonet 100 reactor, which has six fluorescent tubes designated 3500 Å. An incubator model 655 D from Fisher Scientific Co. was used for keeping temperature at  $50 \pm 1$  °C.

**Chemicals.** Tetramethyl orthosilicate, methanol, and sodium dodecylsulfate (SDS) were purchased from Fisher Chemical Co.; cetyltrimethylammonium bromide (CTAB) and pyrene, from Fluka Chem. Co.; 1-dodecanol, from Acros Organics; azobenzene (designated A), from Aldrich Chemical Co.; and 3,3'-dimethyl azobenzene (designated B), from Trade TCI Mark; 3,3-diacetyl azobenzene (designated C) was prepared by a published procedure.<sup>19</sup> Distilled water was further demineralized to a resistivity greater than 17 MΩ cm. Concentration (40 mM) of the buffers, not their ionic strength, is stated throughout the article.

**General Procedure for the Preparation of the Micelle/Silica Monoliths.** Stock solutions of the two surfactants for the preparation of the micelle/silica monoliths were obtained by dissolving 2.54 g of SDS in 50.0 mL of a 40 mM phosphate buffer at pH 5.93 and by dissolving 0.65 g of CTAB in 50.0 mL of water (at pH 5.50). For the preparation of doped monoliths, to these solutions of the surfactants was added 26.0 μmol of the trans isomer of the azo-compound A, B, or C. For the preparation of non-doped monoliths, of

course, the azo-compounds were not added to the stock solutions. In both cases, the stock solutions were kept for 2 h in an ultrasonic bath at 50 °C, and for an additional 24 h in an incubator at 50 °C, before being used in preparation of the glasses.

A mixture of 17.10 g of methanol, 15.50 g of tetramethyl orthosilicate, and 14.70 g of the surfactant stock solution was kept in an ultrasonic bath at room temperature for 10 min. The resulting sol was poured into polystyrene cuvettes sized 10 x 10 x 45 mm to the height of 33 mm, and the cuvettes were capped, covered with an aluminum foil, and left in the dark at room temperature for five days. The SDS monoliths were exposed to air (in uncapped cuvettes) at room temperature for an additional seven days. The CTAB monoliths were exposed to air (in uncapped cuvettes) in an incubator at 50 °C for an additional two days. The resulting transparent SDS/silica monoliths sized 5.6 x 5.6 x 17.0 mm and CTAB/silica monoliths sized 4.8 x 4.8 x 16.2 mm were soaked in a 40 mM phosphate buffer at pH 5.93 and water (at pH 5.50), respectively, and stored for further use at room temperature in the dark.

**General Procedure for the Fluorescence Measurements.** Steady-state fluorescence spectra of pyrene were recorded both in solution and in the micelle/silica monoliths. The excitation was done at 330 nm, and each spectrum was an average of three scans. The ratio of emission intensities at 383.2 nm (band III) and 371.8 nm (band I) is termed the III/I quotient.

A stock solution in water that was  $1.00 \cdot 10^{-5}$  M in pyrene, and also 50.0 mM in SDS or 10.0 mM in CTAB, in a 500.0-mL volumetric flask was first ultrasonicated under a weak vacuum (created by a water aspirator) and then purged with nitrogen for 10 min. In

experiments with 1-dodecanol, a 40.0 mM phosphate buffer at pH 6.90 was used instead of water, and the  $1.00 \cdot 10^{-5}$  M pyrene solutions were made to be 47.50, 45.00, 41.50, 38.00, and 32.00 mM in SDS and, respectively, 2.50, 5.00, 8.50, 12.00, and 18.00 mM in 1-dodecanol, so that the sum of the concentrations of SDS and 1-dodecanol was always 50.0 mM. A 2.50-mL aliquot of the solution containing pyrene and surfactant (and sometimes also 1-dodecanol) was transferred to a 10-mm fluorescence cuvette, which was capped and put in the fluorimeter.

The glass monoliths sized 5.6 x 5.6 x 17.0 mm (50.0 mM, containing SDS) and 4.8 x 4.8 x 16.2 mm (10.0 mM, containing CTAB) were all  $1.70 \cdot 10^{-5}$  M in pyrene. Each monolith was soaked in 100.0 mL of water in a capped 500-mL Erlenmeyer flask, which was left overnight in the incubator at 50 °C. Water surrounding the glass monolith was purged with nitrogen for 15 min, while the monolith was kept upright in the cuvette by a shallow square holder made of glass, whose inner dimensions fitted the monolith. The holder and the monolith, together with ca. 2.0 mL of the deaerated water, were transferred to a 10-mm fluorescence cuvette, which was capped and put in the fluorimeter.

**Physical Characterization of the Micelle/Silica Monoliths.** A silica monolith containing SDS and another monolith containing CTAB, prepared as described above, were crushed, pulverized with mortar in a pestle, and kept in an oven at 100 °C for 24 h. The resulting xerogels were subjected to nitrogen-sorption measurements that gave the BET surface areas and the BJH mean pore diameters and cumulative pore volumes.

**General Procedure for the Isomerization of Azobenzene and Its Derivatives Within Micelles in Solution.** To a quartz cuvette sized 10 x 10 x 40 mm and having all walls

transparent (so-called fluorescence cuvette) was fused a ground-glass joint. When closed, the joint prevented evaporation of the solvent from the cuvette during the isomerization experiments. The following procedure was used with azobenzene (A) and its two derivatives (B and C).

A solution that was  $5.00 \cdot 10^{-5}$  M in the trans isomer of an azo-compound and also 50.0 mM in SDS or 10.0 mM in CTAB was prepared in a 500.0-mL volumetric flask and kept for 24 h in an incubator at 50 °C. In experiments with 1-dodecanol, the solution was prepared as above, except that it was made 5.0 mM in this alcohol and 45.0 mM in SDS. The solvents were water (at pH 5.50) and the following buffers: 40 mM phosphate buffer at pH values of 2.35, 2.90, 5.93, and 6.90; 40 mM formate buffer at pH 3.34; 40 mM acetate buffer at pH 3.92; and 40 mM cacodylate buffer at pH 5.06. The final solution was degassed in an ultrasonic bath under a weak vacuum (created by a water aspirator) and purged with nitrogen for 10 min. A 3.00-mL aliquot was transferred to a 10-mm fluorescence cuvette made of quartz, which was then capped and irradiated in a photo reactor. Ultraviolet spectra of the solution were taken occasionally. When they ceased changing, this was a sign that the photostationary state (pss) was reached. The cuvette was then transferred to a cuvette holder at 50.0 °C in the spectrophotometer, and the thermal cis-to-trans isomerization was followed by recording UV spectra as a function of time.

Ultraviolet bands of azobenzene and its two derivatives have maxima at different wavelengths. The maximum absorbance was converted to the concentration of the trans isomer according to eqs 1 and 2, in which A is absorbance,  $\epsilon$  is absorptivity, the subscript o denotes initial time, and lack of a subscript denotes the time of measurement. The change of

concentration in time was fitted by the linear-least-squares method to eq 3, in which  $k_2$  is the first-order rate constant for thermal isomerization.<sup>19</sup>

$$[\text{cis}] = \frac{1 - \frac{A}{A_0}}{1 - \frac{\epsilon_{\text{cis}}}{\epsilon_{\text{trans}}}} [\text{trans}]_0 \quad (1)$$

$$[\text{trans}] = [\text{trans}]_0 - [\text{cis}] \quad (2)$$

$$\ln \frac{[\text{trans}]_0 - [\text{trans}]_{\text{pss}}}{[\text{trans}]_0 - [\text{trans}]} = k_2 \cdot t \quad (3)$$

**General Procedure for Isomerization of Azobenzene and Its Derivatives as Dopants in the Micelle/Silica Monoliths.** A pair of doped glass monoliths sized 5.6 x 5.6 x 17.0 mm (containing SDS) and another pair of doped glass monoliths sized 4.8 x 4.8 x 16.2 mm (containing CTAB) were soaked in 100.0 mL of the solution in which the isomerization reaction was to be studied: Water (at pH 5.50), 40 mM phosphate buffer at pH 6.90, 40 mM phosphate buffer at pH 6.90 that was also 1.50 M in sodium chloride, and a 1.50 M solution of sodium chloride in water (at pH 5.50). A solution together with the two monoliths in a capped 500-mL Erlenmeyer flask was kept for 24 h in an incubator at 50 °C. The solution was purged with nitrogen for 15 minutes. The monolith was fixed into the square holder and transferred to a 10-mm quartz cuvette together with ca. 2.0 mL of the external solution. The capped cuvette was irradiated in the photo reactor until the photostationary state (pss) was reached. The cuvette was treated, and kinetic calculations done, as described in the preceding subsection.

**Azobenzene Partitioning between the Micelle/Silica Monolith and the External Solution.**

Undoped glass monoliths sized 5.6 x 5.6 x 17.0 mm (containing SDS) or 4.8 x 4.8 x 16.2 mm (containing CTAB) were soaked in 2.80 mL of water and in 2.80 mL of a 1.50 M aqueous solution of sodium chloride in polystyrene cuvettes sized 10 x 10 x 40 mm. There were a total of 16 monoliths each in a separate cuvette: four monoliths for each combinations of the type of micelle in the glass and the surrounding liquid. The cuvettes were capped and kept for 24 h in an incubator at 50 °C. A soaking liquid surrounding the monolith was drawn with a syringe and passed through a 0.22- $\mu$ m filter into a quartz cuvette sized 10 x 10 x 40 mm, and the UV spectrum of the solution was recorded. Each reported result for the partitioning is an average of four measurements, for the samples with the same micelle/liquid combination.

***Results and Discussion***

**Objective of This Study.** The presence of a surfactant in the silica glass allows doping of hydrophilic (inorganic) matrix with hydrophobic (organic) molecules.<sup>36-39</sup> Chemical reactivity and mobility of the dopant molecules may change not only owing to the interactions of the dopant with silica and with micelles but also owing to the interactions between the silica matrix and the micelles embedded in it. We examined the interplay of these interactions and their effects on the kinetics of well-behaved reactions, namely thermal isomerization of azobenzene and its two derivatives. We studied these reactions in anionic (SDS) and cationic (CTAB) micelles when these micelles were free in aqueous solution and when they were embedded in the negatively-charged silica matrix.

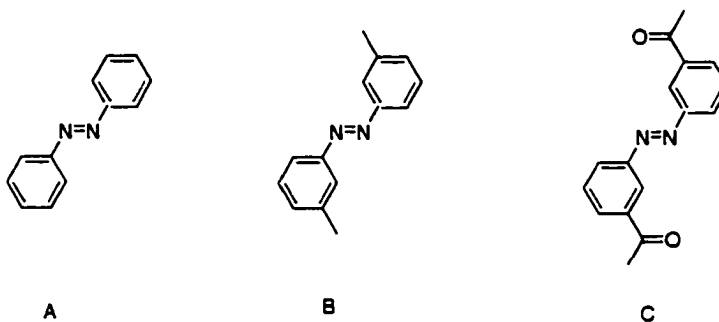


**Kinetics of Azobenzene Isomerization.** Isomerization of azobenzenes has reliably been used to explore microstructure and rigidity of solid polymers.<sup>19,42-45</sup> Although this isomerization has been studied within micelles in dissolved liquid,<sup>46</sup> to our knowledge it has not been studied within micelles embedded in sol-gel glass. Interconversion of geometric (trans and cis) isomers of azobenzene is shown in eq 4. It is a simple reaction, amounting to motion of molecular parts.



Initially the azobenzene and its two derivatives exist in the trans configuration. The so-called forward reaction ( $k_1$ ) is effected by UV light, and it is fast. When the photostationary mixture of the two isomers is obtained, the UV light is turned off, and the so-called back reaction ( $k_2$ ), thermal process, occurs spontaneously. We studied it at 50 °C, in the dark. The rate and the kinetic order of the back reaction may be influenced by the rigidity of the matrix environment, pH, and interactions between the azobenzene and its environment.<sup>19,46-52</sup>

**Azobenzene and Its Derivatives.** Azobenzene (designated A) and 3,3'-dimethyl azobenzene (B) were purchased, while 3,3'-diacetyl azobenzene (C) was synthesized by the published procedure;<sup>19</sup> the trans configuration is the more stable one. The volume required for isomerization of these three dopants increases in the order  $A < B < C$ . Because the methyl and acetyl groups, respectively, donate and withdraw electron density, these compounds differ also in their electron delocalization, and therefore in their propensity for intermolecular interactions such as van der Waals interactions and hydrogen bonding.



**Physical Characterization of the Micelle/Silica Monoliths.** We prepared doped and undoped CTAB/silica monoliths using water as a solvent. We prepared doped and undoped SDS/silica monoliths in two ways, using water or phosphate buffer as a solvent.

Results of the nitrogen sorption measurements for the xerogels are given in Table 1. Properties of the silica glass depend on both the solvent and the surfactant used in the glass preparation. The SDS/silica composites made in water have pore sizes from less than 20 to 35 Å and may be classified as either microporous or mesoporous materials. The other two micelle/silica composites are mesoporous materials. Pore sizes in them are more uniform, centered at ca. 48 Å and at ca. 35 Å, respectively, for SDS/silica made in the buffer at pH 5.93 and for CTAB/silica made in water at pH 5.50.

**Detection of Micelles Embedded in Silica.** To check whether CTAB and SDS actually form micelles when embedded in silica, we encapsulated pyrene with each of these surfactants. The so-called  $I_{337}/I_{325}$  quotient in the emission spectrum of pyrene depends on the polarity of the environment. These quotients for the pyrene molecules residing inside and outside the micelle differ so much<sup>53-55</sup> that their fluorescence can be used to determine critical micelle concentration.<sup>36,53,56,57</sup> The results in Table 2 show that CTAB and SDS do form micelles within the silica matrix. We are reassured that a recent study reached the

same conclusion.<sup>36,39</sup> Clearly, we will be able to compare micelles free in aqueous solvents and micelles encapsulated in silica as microreactors for azobenzene isomerization.

**Isomerization of Azobenzene and Its Derivatives Within the CTAB Micelles.** In these experiments the solvent was water. Azobenzene (A) and its two derivatives (B and C) were studied separately within CTAB micelles dissolved in water and within CTAB micelles embedded in the silica monoliths immersed in water. Thermal isomerizations of all three dopants in both dissolved and embedded micelles are monophasic reactions, i.e., they obey the first-order law. The slopes of the plots in Figure 1 are given in Table 3. Evidently, the positively-charged CTAB micelles, and the isomerization reaction taking place within them, are not detectably affected by the negatively-charged silica matrix surrounding the micelles.

**Isomerization of Azobenzene and Its Derivatives Within the SDS Micelles.** In these experiments, too, the solvent was water. As Figure 2 shows, the reactions of all three compounds within the SDS micelles dissolved in water are monophasic (i.e., they obey the first-order rate law), whereas these reactions within the SDS micelles embedded in silica are multiphasic (i.e., they disobey first-order rate law). The first-order rate constants, the slopes of the linear plots in Figure 2, are given in Table 4. We refrained from fitting the curved plots in Figure 2 to multiple exponentials, and thus do not report the rate constants for the reactions within the SDS micelles embedded in silica. It is clear, however, from inspection of the slopes in Figure 2 that the silica matrix enhances the rate of isomerization of the dopant within the SDS micelles.

**Consideration of Hydrolysis of SDS as a Possible Cause of the Multiphasic Isomerization Kinetics.** At pH less than 4.0 SDS hydrolyses to 1-dodecanol.<sup>61,62</sup> It is

conceivable that silica, being acidic, may catalyze hydrolysis of SDS during the preparation of the composite glass. This hydrolysis, if it occurred, would lead to formation of mixed SDS/dodecanol micelles<sup>63</sup> inside the silica matrix, and consequently the isomerization kinetics within those altered micelles might be changed. We tested this hypothesis by preparing micelles containing mostly SDS and some 1-dodecanol. As the last entry in Table 5 shows, the kinetics of azobenzene isomerization in these mixed micelles stayed the same as in the pure SDS micelles. This control experiment proved that even if SDS hydrolyzed during the preparation of the micelle/silica composites, this side reaction would not cause the kinetics of azobenzene isomerization to become multiphasic.

To check whether this side actually occurs, i.e., whether silica actually promotes hydrolysis of SDS, we prepared a series of solutions containing different proportions, but the same total concentration, of SDS and 1-dodecanol. The growing fraction of 1-dodecanol was a model of the hydrolysis occurring to various extents. The III/I quotient of pyrene engulfed by these micelles, in Table 2, shows that admixture of 1-dodecanol raises this quotient above that recorded in the pure SDS micelles. Evidently, admixture of the electroneutral surfactant lowers the polarity of the anionic micelle. However, Table 2 shows that these quotients determined in the SDS micelles dissolved in the buffer and those embedded in silica are the same, 0.905. This equality proves that SDS does not hydrolyze during the preparation of composite micelle/silica glasses. Once again, experiments ruled out this side reaction as a cause of the multiphasic kinetics.

#### **Effects of pH on Isomerization of Azobenzene Within the CTAB and SDS**

**Micelles.** In the composite glass the micelles are surrounded by silica,<sup>19,64</sup> which is acidic

and may change the local pH near the micelles.<sup>37-39</sup> Because azobenzene isomerization in water is pH-dependent at pH values less than ca. 2.0,<sup>47</sup> we examined possible pH-dependence of this reaction within micelles in aqueous solution (in the absence of silica).

As Table 5 shows, the isomerization within the CTAB micelles is independent of pH, and also monophasic, in the entire range examined. The same isomerization within the SDS micelles is independent of pH in the interval 6.9 - 3.9, but becomes dependent in the interval 3.9 - 3.3 and remains dependent as the pH is lowered further, to 2.3. Because of this pH-dependence, the reaction within the SDS micelles becomes multiphasic as the pH decreases.

One is tempted to attribute this difference between the two surfactants to their opposite charges; see Scheme 1. The Stern layer in the CTAB micelles does not,<sup>65-67</sup> whereas that in the SDS micelles does,<sup>66,67</sup> accumulate  $H^+$  ions from the external solution. Perhaps the azobenzene molecules located in the micelle palisade layer feel the increased local acidity, and the rate constant  $k_2$  for their isomerization increases. This local increase would then manifest itself as a new, faster phase in the reaction.

This hypothesis was refuted by the experiments in which the silica monoliths containing SDS micelles doped with the compounds A, B, and C were soaked in the phosphate buffer (at pH 6.90) instead of water (at pH 5.50). As the curved plots in Figure 2 show, the isomerization remained multiphasic, i.e., it still deviated from the first-order kinetic law. Although the buffer, unlike water, prevented the accumulation of the  $H^+$  ions in the Stern layer, the special effect of the silica matrix on the isomerization remained. We conclude that this special effect is not due to the accumulation of the  $H^+$  ions.

**Azobenzene Isomerization Within the SDS Micelles Embedded in Silica, at High Ionic Strength.** Micelles may interact with the polymer matrix, and the degree of this interaction depends on their characteristics.<sup>68,69</sup> In view of its negative charge at pH ca. 7, silica matrix is expected to attract the CTAB micelles and repel the SDS micelles.<sup>40,41,70</sup> After we suppressed these interactions by raising the ionic strength to 1.50 M, the isomerization of all three substrates (designated A, B, and C) obeyed the first-order rate law; see Figure 2. As Table 4 shows, the rate constants determined within the SDS micelles embedded in silica became the same as those within the SDS micelles in solution.

**Isomerization of the Azobenzene Derivatives in Different Environments.** Tables 3 and 4 consistently show that the isomerization is faster in solution than within micelles but is little affected by the environment surrounding the micelle - solvent or silica. Both probes B and C obey this trend. The ratio of the rate constants for the probes B and C remains approximately the same in all three environments. A given probe isomerizes at virtually equal rates within CTAB and SDS micelles. All three probes (A, B, and C) show this near-equality.

Because free solvent obviously does not impose steric constraint, these results show that neither do micelles, whether dissolved in liquid or embedded in silica. That the reaction remains monophasic under all these three conditions is further evidence that the dopant molecules everywhere within a micelle “feel” practically the same environment. This is true about each of the three dopants, regardless of their different molecular volumes. Within the micelles, as well as in solution, the intrinsic rate of isomerization of the azo-group is governed by the electronic effects of the substituents.<sup>48,58-60</sup>

### **Azobenzene Partitioning Between the Micelle/Silica Glass and the External**

**Solution.** High salt concentration stabilizes SDS micelles by lowering the critical concentration for their formation (cmc).<sup>70,71</sup> According to the familiar principles of extraction and partition chromatography,<sup>72,73</sup> the high salt concentration may also change the partitioning of the organic dopant between the hydrophobic micelles (embedded in glass) and the aqueous external solution. Since the partition coefficient for azobenzene between octanol and water is high (6600),<sup>74</sup> azobenzene is expected to accumulate inside the micelles, but a small fraction of it is expected to be found in the external solution. Indeed, organic molecules can leak from the surfactant/silica films into water.<sup>75</sup> We tested this partitioning of azobenzene between the micelles embedded in the silica glass and the liquid surrounding the glass.

In the case of CTAB micelles, azobenzene was barely detectable in the external water but undetectable in the external 1.50 M NaCl solution. In the case of SDS micelles, azobenzene was readily detectable in water but undetectable in the 1.50 M NaCl solution. In the absence of salt, leakage from the CTAB/silica glass is too slight to affect the observed kinetics of isomerization – the traces in Figure 1 are linear - but leakage from the SDS/silica glass is extensive enough to cause the curved plots in Figure 2. The curvature is probably caused by simultaneous isomerization of azobenzene in different environments, at different rates. The presence of salt, i. e., the high ionic strength, suppresses leakage from the micelle/silica glass into the external liquid and renders the isomerization a monophasic reaction, which obeys the first-order kinetic law. Ability to control, and if necessary suppress, partitioning of dopant between the composite glass and the surrounding liquid is

required in the successful design and application of chemical sensors, optical switches, optical-storage systems, and drug-delivery systems.

### ***Conclusion***

Mobility and chemical reactivity of dopants co-entrapped with surfactants inside silica depends on the concentration of the surfactant (that is, the existence of micelles) and the interactions among the dopants, the micelle, and silica. Doping causes relatively small changes in the macroscopic properties of the micelle/silica composites. Because catalytic activity depends on macroscopic properties of the glass, this finding bodes well for doping of the composite glasses with catalysts. The control of reactivity of dopants within the composite glass made of surfactant and silica is required for the design and application of new biosensors, immobilized catalysts, and various composite materials.

***Acknowledgment.*** We thank Professor Glenn L. Schrader and Thomas Paskach of the Chemical Engineering department for the nitrogen sorption measurements and Professor Victor Shang-Yi Lin of this department for permission to use the fluorimeter. This work was supported by the U.S. National Science Foundation.

### ***References***

- (1) Hench, L. L.; West, J. K. *Chem. Rev.* **1990**, *90*, 33-72.
- (2) Avnir, D. *Acc. Chem. Res.* **1995**, *28*, 328-34.
- (3) Dunn, B.; Zink, J. I. *Chem. Mater.* **1997**, *9*, 2280-91.



- (4) Husing, N.; Schubert, U. *Angew. Chem., Int. Ed.* **1998**, *37*, 22-45.
- (5) Avnir, D.; Braun, S.; Lev, O.; Ottolenghi, M. *Chem. Mater.* **1994**, *6*, 1605-14.
- (6) Shen, C.; Kostić, N. M. *J. Am. Chem. Soc.* **1997**, *119*, 1304-12.
- (7) Shen, C.; Kostić, N. M. *J. Electroanal. Chem.* **1997**, *438*, 61-5.
- (8) Bronshtein, A.; Aharonson, N.; Avnir, D.; Turniansky, A.; Altstein, M. *Chem. Mater.* **1997**, *9*, 2632-9.
- (9) Shabat, D.; Grynszpan, F.; Saphier, S.; Turniansky, A.; Avnir, D.; Keinan, E. *Chem. Mater.* **1997**, *9*, 2258-60.
- (10) Gill, I.; Ballesteros, A. *J. Am. Chem. Soc.* **1998**, *120*, 8587-98.
- (11) Badjić, J. D.; Kostić, N. M. *Chem. Mater.* **1999**, *11*, 3671-9.
- (12) Gelman, F.; Avnir, D.; Schumann, H.; Blum, J. *J. Mol. Catal. A: Chem.* **1999**, *146*, 123-8.
- (13) Hirai, T.; Okubo, H.; Komasaawa, I. *J. Phys. Chem. B* **1999**, *103*, 4228-30.
- (14) Lan, E. H.; Dave, B. C.; Fukuto, J. M.; Dunn, B.; Zink, J. I.; Valentine, J. S. *J. Mater. Chem.* **1999**, *9*, 45-53.
- (15) Wang, B.; Zhang, J.; Cheng, G.; Dong, S. *Chem. Commun. (Cambridge)* **2000**, 2123-4.
- (16) Reetz, M. T.; Zonta, A.; Simpelkamp, J. *Biotechnol. Bioeng.* **1996**, *49*, 527-34.
- (17) Reetz, M. T.; Wenkel, R.; Avnir, D. *Synthesis* **2000**, 781-3.
- (18) Badjić, J. D.; Kostić, N. M. *J. Phys. Chem. B* **2000**, *104*, 11081-7.
- (19) Badjić, J. D.; Kostić, N. M. *J. Mater. Chem.* **2001**, *11*, 408-18.
- (20) Loy, D. A.; Shea, K. J. *Chem. Rev. (Washington, D. C.)* **1995**, *95*, 1431-42.
- (21) Reetz, M.; Zonta, A.; Simpelkamp, J. *Angew. Chem., Int. Ed. Engl.* **1995**, *34*, 301-3.

- (22) Feng, Q.; Xu, J.; Dong, H.; Li, S.; Wei, Y. *J. Mater. Chem.* **2000**, *10*, 2490-4.
- (23) Lebeau, B.; Fowler, C. E.; Mann, S.; Farcet, C.; Charleux, B.; Sanchez, C. *J. Mater. Chem.* **2000**, *10*, 2105-8.
- (24) Anderson, M. T.; Martin, J. E.; Odinek, J. G.; Newcomer, P. P. *Chem. Mater.* **1998**, *10*, 1490-500.
- (25) Bekiari, V.; Ferrer, M.-L.; Lianos, P. *J. Phys. Chem. B* **1999**, *103*, 9085-9.
- (26) Dai, S.; Burleigh, M. C.; Shin, Y.; Morrow, C. C.; Barnes, C. E.; Xue, Z. *Angew. Chem., Int. Ed.* **1999**, *38*, 1235-9.
- (27) Lu, Y.; Ganguli, R.; Drewien, C. A.; Anderson, M. T.; Brinker, C. J.; Gong, W.; Guo, Y.; Soyez, H.; Dunn, B.; Huang, M. H.; Zink, J. I. *Nature (London)* **1997**, *389*, 364-8.
- (28) Ying, J. Y.; Mehnert, C. P.; Wong, M. S. *Angew. Chem., Int. Ed.* **1999**, *38*, 56-77.
- (29) Ogawa, M. *J. Am. Chem. Soc.* **1994**, *116*, 7941-2.
- (30) Huo, Q.; Margolese, D. I.; Ciesla, U.; Feng, P.; Gier, T. E.; Sieger, P.; Leon, R.; Petroff, P. M.; Schueth, F.; Stucky, G. D. *Nature (London)* **1994**, *368*, 317-21.
- (31) Huo, Q.; Leon, R.; Petroff, P. M.; Stucky, G. D. *Science (Washington, D. C.)* **1995**, *268*, 1324-7.
- (32) Vallet-Regi, M.; Ramila, A.; Real, R. P. d.; Perez-Pariente, J. *Chem. Mater.* **2001**, *13*, 308-11.
- (33) Wei, Y.; Feng, Q.; Xu, J.; Dong, H.; Qiu, K.-Y.; Jansen, S. A.; Yin, R.; Ong, K. K. *Adv. Mater. (Weinheim, Ger.)* **2000**, *12*, 1448-50.
- (34) Sellinger, A.; Weiss, P. M.; Anh, N.; Lu, Y.; Assink, R. A.; Gong, W.; Brinker, C. J. *Nature (London)* **1998**, *394*, 256-60.

- (35) Kresge, C. T.; Leonowicz, M. E.; Roth, W. J.; Vartuli, J. C.; Beck, J. S. *Nature (London)* **1992**, *359*, 710-12.
- (36) Matsui, K.; Nakazawa, T.; Morisaki, H. *J. Phys. Chem.* **1991**, *95*, 976-9.
- (37) Rottman, C.; Ottolenghi, M.; Zusman, R.; Lev, O.; Smith, M.; Gong, G.; Kagan, M. L.; Avnir, D. *Mater. Lett.* **1992**, *13*, 293-8.
- (38) Rottman, C.; Turniansky, A.; Avnir, D. *J. Sol-Gel Sci. Technol.* **1998**, *13*, 17-25.
- (39) Rottman, C.; Grader, G.; Hazan, Y. D.; Melchior, S.; Avnir, D. *J. Am. Chem. Soc.* **1999**, *121*, 8533-43.
- (40) Huang, Z.; Gu, T. *Colloids Surf.* **1987**, *28*, 159-68.
- (41) Huang, Z.; Yan, Z.; Gu, T. *Colloids Surf.* **1989**, *36*, 353-8.
- (42) Paik, C. S.; Morawetz, H. *Macromolecules* **1972**, *5*, 171-7.
- (43) Ueda, M.; Kim, H.-B.; Ichimura, K. *Chem. Mater.* **1994**, *6*, 1771-5.
- (44) Grebenkin, S. Y.; Bol'shakov, B. V. *J. Photochem. Photobiol., A* **1999**, *122*, 205-9.
- (45) Grebenkin, S. Y.; Bol'shakov, B. V. *Chem. Phys.* **1998**, *234*, 239-48.
- (46) Miyagishi, S.; Matsumura, S.; Asakawa, T.; Nishida, M. *J. Colloid Interface Sci.* **1988**, *125*, 237-45.
- (47) Ciccone, S.; Halpern, J. *Can. J. Chem.* **1959**, *37*, 1903-10.
- (48) Nishimura, N.; Sueyoshi, T.; Yamanaka, H.; Imai, E.; Yamamoto, S.; Hasegawa, S. *Bull. Chem. Soc. Jpn.* **1976**, *49*, 1381-7.
- (49) Sanchez, A. M.; Rossi, R. H. *J. Org. Chem.* **1995**, *60*, 2974-6.
- (50) Sanchez, A. M.; de Rossi, R. H. *J. Org. Chem.* **1996**, *61*, 3446-51.
- (51) Sanchez, A. M.; Barra, M.; de Rossi, R. H. *J. Org. Chem.* **1999**, *64*, 1604-9.

- (52) Gille, K.; Knoll, H.; Rittig, F.; Fleischer, G.; Kaerger, J. *Langmuir* **1999**, *15*, 1059-66.
- (53) Kalyanasundaram, K.; Thomas, J. K. *J. Am. Chem. Soc.* **1977**, *99*, 2039-44.
- (54) Dong, D. C.; Winnik, M. A. *Can. J. Chem.* **1984**, *62*, 2560-5.
- (55) Ferrer, M.; Lianos, P. *Langmuir* **1996**, *12*, 5620-4.
- (56) Itoh, H.; Ishido, S.; Nomura, M.; Hayakawa, T.; Mitaku, S. *J. Phys. Chem.* **1996**, *100*, 9047-53.
- (57) Zana, R.; Frasc, J.; Soulard, M.; Lebeau, B.; Patarin, J. *Langmuir* **1999**, *15*, 2603-6.
- (58) Cimiraglia, R.; Asano, T.; Hofmann, H.-J. *Gazz. Chim. Ital.* **1996**, *126*, 679-84.
- (59) Asano, T.; Okada, T. *J. Org. Chem.* **1986**, *51*, 4454-8.
- (60) Asano, T.; Okada, T. *J. Org. Chem.* **1984**, *49*, 4387-91.
- (61) Nakagaki, M.; Yokoyama, S. *J. Pharm. Sci.* **1985**, *74*, 1047-52.
- (62) Nakagaki, M.; Yokoyama, S. *Bull. Chem. Soc. Jpn.* **1986**, *59*, 935-6.
- (63) Abe, M.; Ogino, K. *J. Colloid Interface Sci.* **1981**, *80*, 146-52.
- (64) Spange, S.; Zimmermann, Y.; Graeser, A. *Chem. Mater.* **1999**, *11*, 3245-51.
- (65) Bunton, C. A.; Ohmenzetter, K.; Sepulveda, L. *J. Phys. Chem.* **1977**, *81*, 2000-4.
- (66) Fanghaenel, E.; Ortmann, W.; Hennig, A. *J. Prakt. Chem.* **1988**, *330*, 27-34.
- (67) Dugas, H.; Editor *Bioorganic Chemistry: A Chemical Approach to Enzyme Action*, 1995.
- (68) Goddard, E. D.; Ananthapadmanabhan, K. P.; Editors *Interactions of Surfactants with Polymers and Proteins*; CRC Press:, 1993.
- (69) Goddard, E. D. *Interact. Surfactants Polym. Proteins* **1993**, 171-201.

- (70) Jonsson, B.; Lindman, B.; Holmberg, K.; Kronberg, B. *Surfactants and Polymers in Aqueous Solution*, 1998.
- (71) van OS, N. M.; Haak, J. R.; Rupert, L. A. M. *Physico-Chemical Properties of Selected Anionic, Cationic and Nonionic Surfactants*; Elsevier:, 1993.
- (72) Abraham, M. H.; Chadha, H. S.; Leitao, R. A. E.; Mitchell, R. C.; Lambert, W. J.; Kaliszan, R.; Nasal, A.; Haber, P. *J. Chromatogr., A* **1997**, 766, 35-47.
- (73) Abraham, M. H.; Green, C. E.; Acree, J. W. E.; Hernandez, C. E.; Roy, L. E. *J. Chem. Soc., Perkin Trans. 2* **1998**, 2677-82.
- (74) Howard, P. H.; Meylan, W. M.; Editors *Handbook of Physical Properties of Organic Chemicals*, 1997.
- (75) Ferrer, M.-L.; Bekiari, V.; Lianos, P.; Tsiourvas, D. *Chem. Mater.* **1997**, 9, 2652-8.

**Table 1.** Surface Area (in m<sup>2</sup>/g), Mean Pore Diameters (in Å), and Cumulative Pore Volumes (in cm<sup>3</sup>/g) Obtained from the Nitrogen Sorption Measurements for Micelle/Silica Xerogels Prepared by the Sol-Gel Method Without and With a Dopant

micelle <sup>a</sup> , solvent	dopant			
	none	azobenzene (A)	3,3'-dimethyl azobenzene (B)	3,3'-diacetyl azobenzene (C)
<b>SDS, water at pH 5.50</b>				
area	639	555	412	530
diameter	< 20	27	< 20	34
volume	0.14	0.19	0.18	0.14
<b>SDS, buffer at pH 5.93</b>				
area	523	593	521	585
diameter	62	48	49	45
volume	0.76	0.63	0.58	0.62
<b>CTAB, water at pH 5.50</b>				
area	626	635	618	696
diameter	35	35	36	35
volume	0.40	0.31	0.44	0.30

<sup>a</sup>SDS is sodium dodecylsulfate and CTAB is cetyltrimethylammonium bromide.

**Table 2.** Relative Intensity of the Bands III and I in the Fluorescence Spectra of Pyrene Within Micelles Embedded in Monoliths of Sol-Gel Silica and Within Micelles Dissolved in Aqueous Media

micelle composition				III/I quotient	
surfactant(s) <sup>a</sup>	surfactant concentration (mM)	1-dodecanol concentration (mM)	pH <sup>b</sup>	micelles in silica	micelles in solution
CTAB	10.0	0	5.50	0.781 ± 0.005	0.755 ± 0.003
SDS	50.0	0	5.50	0.905 ± 0.009	0.875 ± 0.007
SDS	50.0	0	6.90		0.905 ± 0.003
SDS and 1-dodecanol	47.5	2.5	6.90		0.914 ± 0.005
SDS and 1-dodecanol	45.0	5.0	6.90		0.926 ± 0.007
SDS and 1-dodecanol	41.5	8.5	6.90		0.948 ± 0.007
SDS and 1-dodecanol	38.0	12.0	6.90		0.965 ± 0.007
SDS and 1-dodecanol	32.0	18.0	6.90		0.995 ± 0.005

<sup>a</sup>SDS is sodium dodecylsulfate and CTAB is cetyltrimethylammonium bromide.

<sup>b</sup>Water at pH 5.50; 40.0 mM phosphate buffer at pH 6.90.

**Table 3.** First-Order Rate Constants at pH 5.50 for Thermal (Cis-to-Trans) Isomerization (Eq 4) of Azobenzene and Its Two Derivatives in Solution and Within Cetyltrimethylammonium bromide (CTAB) Micelles That are Dissolved in Water at pH 5.50 and That are Embedded in Sol-Gel Silica Soaked in Water at pH 5.50

dopant	$10^4 k_2$ (min <sup>-1</sup> )		
	in solution <sup>a</sup>	in dissolved micelles	in embedded micelles
azobenzene (A)		11.2 ± 0.1	14.7 ± 0.1
3,3'-dimethyl azobenzene (B)	30.2 ± 0.2	13.0 ± 0.1	19.1 ± 0.1
3,3'-diacetyl azobenzene (C)	12.1 ± 0.1	3.9 ± 0.2	2.8 ± 0.1

<sup>a</sup>From Ref. 19. Solvent is a 9 : 1 mixture by volume of CCl<sub>4</sub> and DMF.



**Table 4.** First-Order Rate Constants for Thermal (Cis-to-Trans) Isomerization (Eq 4) of Azobenzene and Its Two Derivatives Within Sodium dodecylsulfate (SDS) Micelles that are Dissolved in Water at pH 5.50 ( $k_2$ ) and that are Embedded in Silica Monoliths Soaked in 40.0 mM Phosphate Buffer at pH 6.90 that is 1.50 M in NaCl ( $k'_2$ )

dopant	$10^4 k_2$ ( $\text{min}^{-1}$ )		
	in solution <sup>a</sup>	in dissolved micelles	in embedded micelles
azobenzene (A)		$9.5 \pm 0.4$	$15.1 \pm 0.1$
3,3'-dimethyl azobenzene (B)	$30.2 \pm 0.2$	$12.4 \pm 0.1$	$16.4 \pm 0.1$
3,3'-diacetyl azobenzene (C)	$12.1 \pm 0.1$	$4.3 \pm 0.1$	$5.7 \pm 0.1$

<sup>a</sup>From Ref. 19. Solvent is a 9 : 1 mixture by volume of  $\text{CCl}_4$  and DMF.

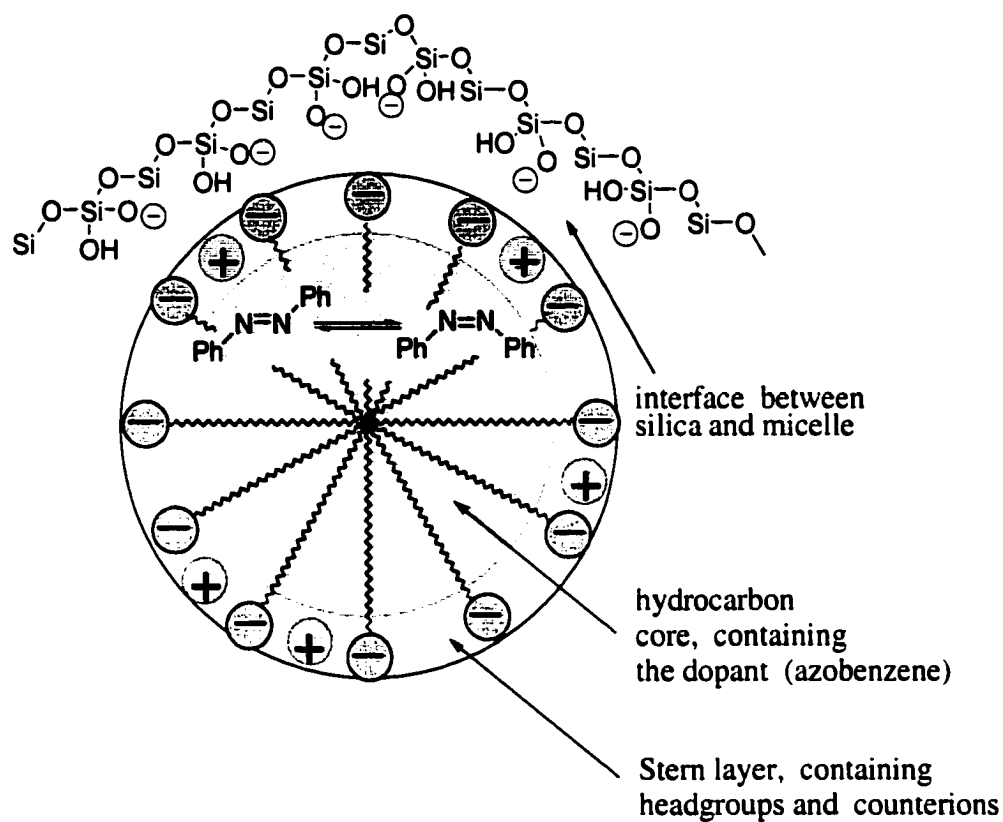
**Table 5.** Effects and Noneffects of pH on First-Order Rate Constants  $k_2$  for Thermal (Cis-to-Trans) Isomerization (Eq 4) of Azobenzene (Designated A) Within Cationic (CTAB) and Anionic (SDS) Micelles Dissolved in Aqueous Buffers

pH	buffer	CTAB <sup>a</sup>	SDS <sup>b</sup>	
		$k_2$ (min <sup>-1</sup> )	$k_2$ (min <sup>-1</sup> )	
2.35	phosphate	$9.8 \pm 0.2 \cdot 10^{-4}$	$1.61 \pm 0.05 \cdot 10^{-1}$	$3.16 \pm 0.04 \cdot 10^{-3}$
2.90	phosphate	$1.3 \pm 0.1 \cdot 10^{-3}$	$1.51 \pm 0.04 \cdot 10^{-1}$	$1.75 \pm 0.05 \cdot 10^{-3}$
3.34	formate		$3.03 \pm 0.06 \cdot 10^{-1}$	$8.2 \pm 0.1 \cdot 10^{-4}$
3.92	acetate	$9.3 \pm 0.1 \cdot 10^{-4}$		$7.9 \pm 0.1 \cdot 10^{-4}$
5.06	cacodylate	$9.0 \pm 0.1 \cdot 10^{-4}$		$8.8 \pm 0.1 \cdot 10^{-4}$
5.93	phosphate	$1.0 \pm 0.1 \cdot 10^{-3}$		$9.4 \pm 0.2 \cdot 10^{-4}$
6.90	phosphate	$1.1 \pm 0.1 \cdot 10^{-3}$		$7.9 \pm 0.1 \cdot 10^{-4}$
6.90 <sup>c</sup>	phosphate			$8.0 \pm 0.1 \cdot 10^{-4}$

<sup>a</sup> Cetyltrimethylammonium bromide; 10.0 mM.

<sup>b</sup> Sodium dodecylsulfate; 50.0 mM.

<sup>c</sup> 45.0 mM in sodium dodecylsulfate and 5.0 mM in 1-dodecanol.



**Scheme 1.** Isomerization of azobenzene entrapped in a sodium dodecylsulfate (SDS) micelle embedded in sol-gel silica glass. For a cetyltrimethylammonium bromide (CTAB) micelle the charges in the Stern layer would be reversed.

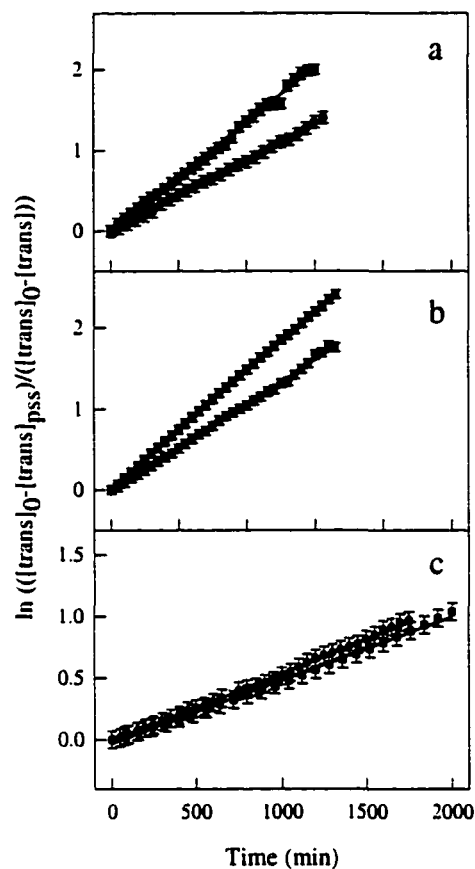


**Figure 1.** Kinetics of thermal (cis-to-trans) isomerization of (a) azobenzene, designated A, (b) 3,3'-dimethyl azobenzene, designated B, and (c) 3,3'-diacetyl azobenzene, designated C, in cetyltrimethylammonium bromide (CTAB) micelles dissolved in water (●) and within CTAB micelles embedded in monoliths of sol-gel silica immersed in water (■). Solid lines are fittings to the first-order rate law.

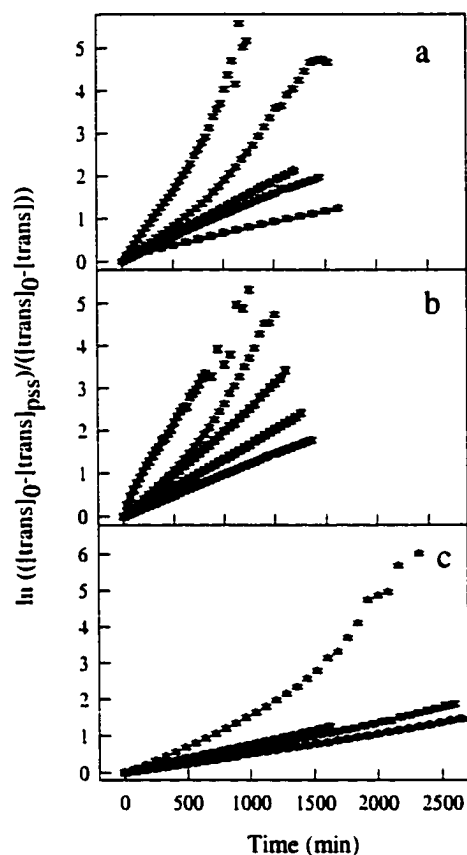


**Figure 2.** Kinetics of thermal (cis-to-trans) isomerization of (a) azobenzene, designated A, (b) 3,3'-dimethyl azobenzene, designated B, and (c) 3,3'-diacetyl azobenzene, designated C, in sodium dodecyl sulfate (SDS) micelles dissolved in water (●) and within SDS micelles embedded in monoliths of sol-gel silica in water at pH 5.50 (■), in 40.0 mM phosphate buffer at pH 6.90 (▲), in aqueous 1.5 M NaCl at pH 5.50 (◆), and in 40.0 mM phosphate buffer at pH 6.90 that is 1.50 M in NaCl (▼). Solid lines are fittings to the first-order rate law.

## CHAPTER 6. CONCLUSIONS

We studied the effects of sol-gel silica glass on activity and conformational stability of the encapsulated bovine carbonic anhydrase. A porous silica monolith limits access of an ester substrate to the enzyme embedded in the silica, which lowers the rate of the enzymatic reaction catalyzed by the entrapped enzyme. The conformational stability of the enzyme seems to be retained upon the encapsulation, which demonstrates importance of silica inorganic matrix in immobilizing biomolecules.

Interactions at the molecular level between host silica matrix and guest molecules govern mobility and chemical reactivity of guests. We showed that the classical hydrogen bonding interactions between silica glass and different organic compounds diffused into the glass modulate mobility and chemical reactivity of these compounds. Hydrogen bonding, also, causes immense accumulation of organic molecules from their solution into the silica matrix. Unexpectedly, hydrophobic aromatic hydrocarbons get accumulated into hydrophilic sol-gel silica matrix due to the hydrogen bonding between their aromatic  $\pi$  system and hydroxyl groups on the silica surface. We achieved full control over these interactions by using organic solvents with different hydrogen bonding propensity. The results of these studies help in better understanding of chemistry inside sol-gel glasses, which is essential in rational design of various molecular devices based on the sol-gel silica materials.

In study of chemical reactivities of azo-compounds inside micelle/silica composites, we discovered that these compounds partition between SDS/silica composite and a surrounding solution and that modulates their reactivity. Upon the ionic strength adjustment,

the partitioning can be suppressed and the reactivity normalized. The partitioning of azo-compounds was not observed in case of CTAB/micelle composite.

## **ACKNOWLEDGMENT**

I would like to thank Nenad for great support, useful suggestions, and guidance throughout all research projects that we successfully finished. Also, my special thanks to all groupies present and past, particularly Maja, Milan, Nebojsa, and Katya for useful discussions and suggestions.